In this lecture we cover some experimental aspects of diffraction, emphasizing the way measurements can be visualized in reciprocal space. We also give an account of the types of imperfections present in real crystals.

Every diffraction experiment has the following key components:

- An incident X-ray or neutron beam with a wave vector $\mathbf{k}_\mathrm{i}$ which is often fixed, but not always.
- A sample stage that incorporates an environment to control a variety of physical or chemical parameters (gas flow, temperature, pressure, magnetic field, electric field...). In the case of single crystal diffraction, the sample stage also allows precise motorised control of the crystal orientation.
- A detector, mounted on a separate arm to the sample stage, allowing the diffracted radiation to be measured as a function of the angle of deflection 2θ from the incident beam.

6.1 The Ewald sphere

The key result is the Laue diffraction condition, $\mathbf{Q} = \mathbf{G}$, where $\mathbf{Q} = \mathbf{k}_\mathrm{i} - \mathbf{k}_\mathrm{f}$ is the **scattering vector**, and $\mathbf{G}$ is a reciprocal lattice vector.[1] We are dealing with elastic scattering, so $|\mathbf{k}_\mathrm{i}| = |\mathbf{k}_\mathrm{f}| = 2\pi/\lambda$. Hence, the locus of possible scattering vectors maps out the surface of a sphere with radius $|\mathbf{k}_\mathrm{i}| = 2\pi/\lambda$. This sphere is known as the **Ewald sphere**, Fig. 1. Any $\mathbf{G}$ vector that lies on the surface of the Ewald sphere satisfies the Laue condition, and the associated Bragg reflection can be measured by a suitably placed detector.

To visualize the scattering geometry, it is helpful to draw the intersection of the Ewald sphere with the two-dimensional plane of the reciprocal lattice that contains the wavevectors $\mathbf{k}_\mathrm{i}$ and $\mathbf{k}_\mathrm{f}$. This plane is called the **scattering plane**. The origin of the reciprocal lattice is chosen to be at the beginning of $\mathbf{k}_\mathrm{i}$. Diffraction occurs if a reciprocal lattice point lies on the perimeter of the circle. This can be achieved by turning the sample (and hence the reciprocal lattice) relative to $\mathbf{k}_\mathrm{i}$. Equivalently, one can keep the reciprocal lattice fixed and rotate the circle around the origin.

[1] In crystallography literature, the scattering vector is often defined as $\mathbf{Q} = \mathbf{k}_\mathrm{f} - \mathbf{k}_\mathrm{i}$. Here I use $\mathbf{Q} = \mathbf{k}_\mathrm{i} - \mathbf{k}_\mathrm{f}$ to be consistent with the use in spectroscopy. I am certain that students will have the mental agility to reverse the signs as and when required.

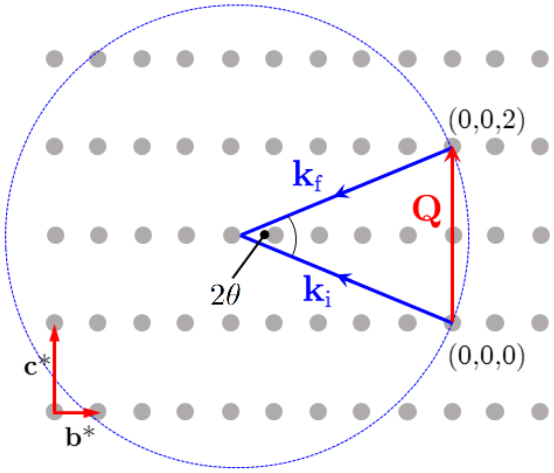
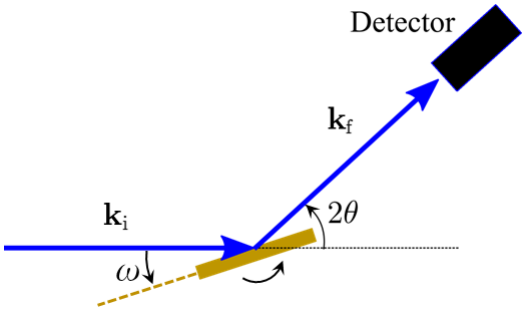


Figure 1: Section through the reciprocal lattice containing $\mathbf{k}_\mathrm{i}$ and $\mathbf{k}_\mathrm{f}$ (the scattering plane). The $\mathbf{a}^*$ direction points out of the plane. The circle is the intersection of the Ewald sphere with the scattering plane, and $\mathbf{Q}$ is set up to coincide with the $(0, 0, 2)$ reciprocal lattice point.

6.2 Single crystal diffraction



In a single crystal diffraction experiment, individual Bragg diffraction peaks with chosen (h, k, l) are 'scanned'. Scans are performed by either (a) rotating the sample by an angle ω about an axis perpendicular to the scattering plane, with the detector at fixed 2θ, where θ is the Bragg angle, (b) scanning the detector angle 2θ while keeping the sample fixed, or (c) by a coupled ω–2θ scan, in which both the detector and the sample rotate, but the detector rotates at twice the rate of the sample. In an ω–2θ scan $\mathbf{Q}$ moves radially from the origin of reciprocal space. These three scan types are shown in reciprocal space in Figs. 2(a), (b) and (c).

The above scan types can be used to measure all accessible reciprocal lattice points in the diffraction plane within a circle radius $|\mathbf{Q}|_{\max} = 2|\mathbf{k}_i|$, as shown in Fig. 3 (left). If the crystal is sufficiently thick or absorbing that the incident beam cannot transmit through the sample then the accessible area of reciprocal space is more restricted, and imposes two further constraints on ω to avoid transmission of the incident or scattered beam through the sample. Firstly, ω cannot be negative, as this would require the incident beam to hit the back of the sample and pass through it to reach the detector. Second, ω cannot be larger than 2θ, as this would result in x-rays being diffracted into the sample. The restriction to the 'reflection geometry' just described is common in X-ray diffraction because the penetration depth of X-rays is relatively small. The accessible region of reciprocal space in the diffraction plane for reflection geometry is shown in Figure 3 (right).

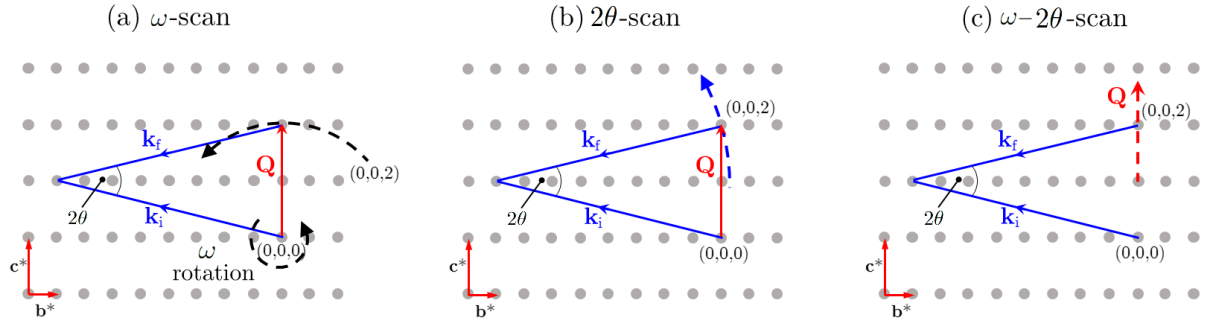


Figure 2: (a) An ω scan, performed by rotating the sample. (b) A 2θ scan, performed by rotating the detector. (c) An $\omega - 2\theta$ scan, performed by rotating both the sample and the detector. The detector rotates at twice the rate as the sample.

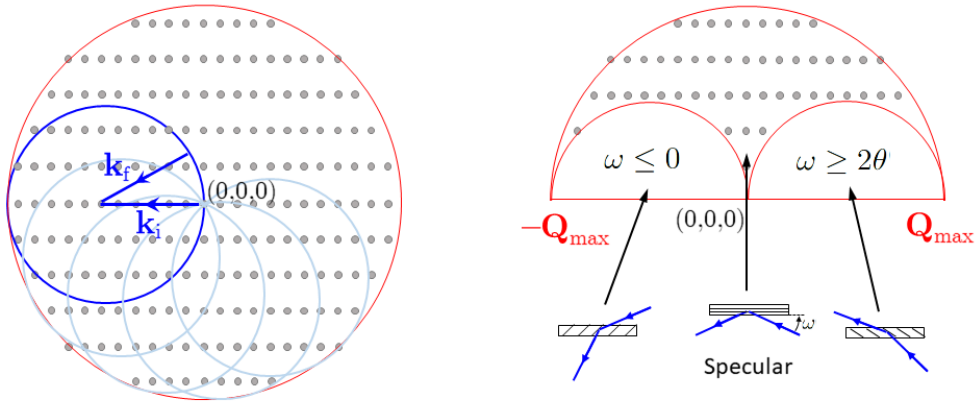


Figure 3: The accessible region of reciprocal space within the diffraction plane for single crystal diffraction. Left: the case when the radiation can be transmitted through the crystal. Right: for absorbing crystals from which only reflection is possible ($\omega \leq 0$ corresponds to the incident beam hitting the back of the sample, and $\omega \geq 0$ corresponds to a scattered beam below the surface of the sample).

6.3 Powder diffraction

A powder sample is a collection of randomly oriented small single crystals of sufficient number that, to a good approximation, every crystal orientation occurs within the sample. In the single crystal experiment the detector and sample must be positioned correctly in order to achieve a given diffraction condition. Owing to the random orientation of crystals in a powder, the sample orientation is no longer relevant — so long as the detector is set at the correct value of 2θ, diffraction will occur. As such, we are only concerned with the value of $|\mathbf{Q}|$, as illustrated in Fig. 4.

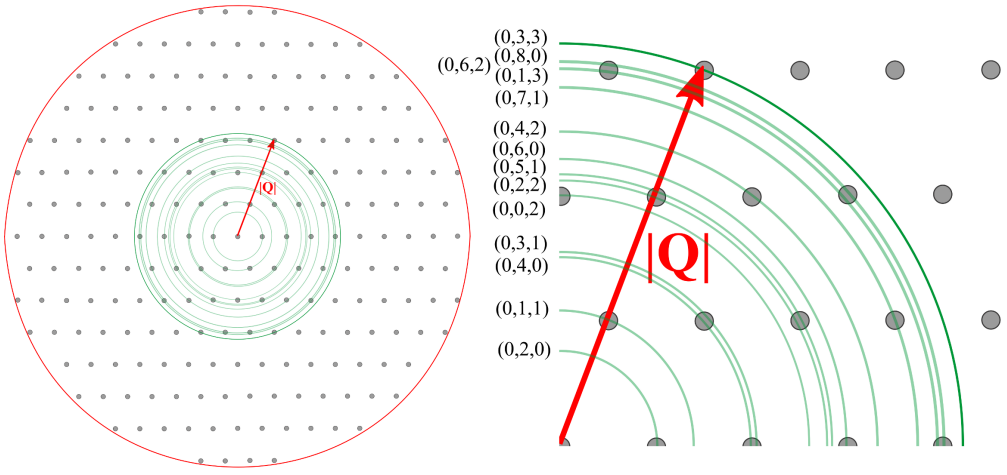
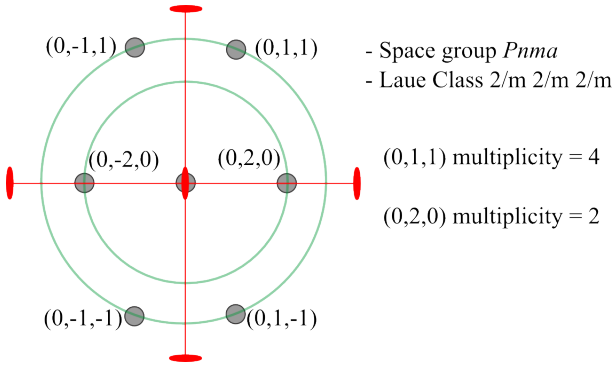


Figure 4: For a powder sample, the Bragg planes are in random orientations, so the corresponding reciprocal lattice points are spread around spheres (left). The Laue condition is satisfied when $|\mathbf{Q}| = |\mathbf{G}|$ (right).

All symmetry-equivalent reciprocal lattice points contribute to the same Debye–Scherrer cone. When calculating the powder diffraction intensity we can consider single diffraction peaks, and then multiply the structure factor squared (or the intensity) by the **multiplicity** of the peak, which is derived from the Laue Class. The figure below illustrates the multiplicity of reflections for a crystal with space group *Pnma*.



Sometimes, powder diffraction peaks are accidentally degenerate beyond symmetry equivalence. For example, in the case of the tetragonal crystal system $|\mathbf{Q}| = 2\pi\sqrt{(h^2+k^2)/a^2 + l^2/c^2}$, hence the $(4,3,0)$ and $(5,0,0)$ Bragg peaks are degenerate in $|\mathbf{Q}|$, despite being inequivalent by symmetry.

The 2θ angle is fixed for a given diffraction condition. For a randomly oriented powder, the locus of all possible scattered beams is a cone around the direction of the incident beam. These cones are known as **Debye–Scherrer cones** (see Fig. 5). The intensity around the cones is integrated over the width of the detector, producing 1D data of diffracted intensity as a function of $|\mathbf{Q}|$. As the detector has finite width the fraction of the cone measured is angle dependent, with a maximum at $2\theta = 0°$ and 180°, and a minimum at $2\theta = 90°$. A correction is always applied to the diffraction data — similar to that used for single crystal diffraction. The exact form of the correction is non-examinable.

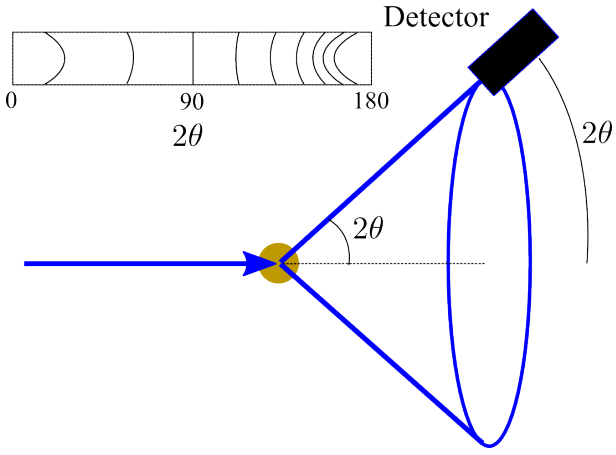


Figure 5: The Debye-Scherrer cone

6.4 Physical imperfections in crystals

Up to now, we have considered crystals to be ideal. That is, perfect periodic structures that extend indefinitely in all directions without blemish. This picture is only approximately correct. Even the very purest materials, such as silicon wafers used as supports for miniature integrated circuits, contain a low concentration of chemical impurities and physical defects. Here we are going to introduce some of the physical imperfections commonly found in real-world crystals.

Many physical phenomena originate from defects in crystal. The low temperature resistance of metals is usually caused by the scattering of electrons from physical imperfections. Indeed, the quantum mechanical description of waves in periodic potentials implies that in a perfect crystal electronic quasiparticles would be perfectly coherent and would propagate without resistance at absolute zero.[2] The colour of many minerals, such as diamonds, is due to transitions between the energy levels of electrons trapped in local defects. Metals typical become harder when they are mechanically deformed, called work hardening. And so on...

We shall give a brief account of four types of physical defects in crystalline solids:

1. Vacancies
2. Dislocations
3. Twinning
4. Site disorder

1 Vacancies

Atoms are mobile, and given enough energy they can move off their crystallographic sites and diffuse through the crystal (Fig. 6). One possibility is that the atom re-locates to a position in the crystal which is not a crystallographic site, called an **interstitial site**. This type of imperfection is called a **Frenkel defect**. Another possibility is that a pair of atoms of opposite charge diffuse out of the crystal entirely. This is called a **Schottky defect**. These defects can form by radiation damage or by thermal activation over an energy barrier. If the energy to form a vacancy is ϵ_v, and the number of atoms of one type in the crystal is N, then the number of thermally excited vacancies $n_\mathrm{v}(T)$ will be

$$n_\mathrm{v}(T) \sim N\exp(-\epsilon_\mathrm{v}/k_\mathrm{B}T).$$

Typically $\epsilon_\mathrm{v} = 1\,\mathrm{eV}$, giving $n/N \sim 10^{-17}$ at $T = 300\,\mathrm{K}$ and $\sim 10^{-5}$ at $T = 1000\,\mathrm{K}$.

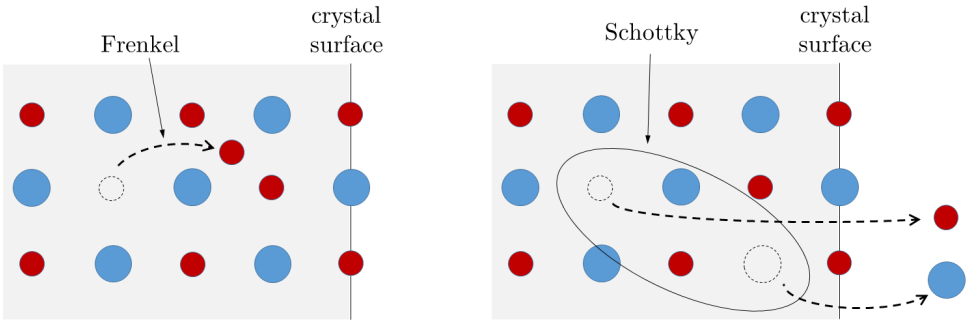


Figure 6: Vacancies in a crystal associated with Frenkel and Schottky defects.

[2]This is not the same as superconductivity, which involves the formation of coherent electron pairs due to some kind of attractive electron–electron interaction.

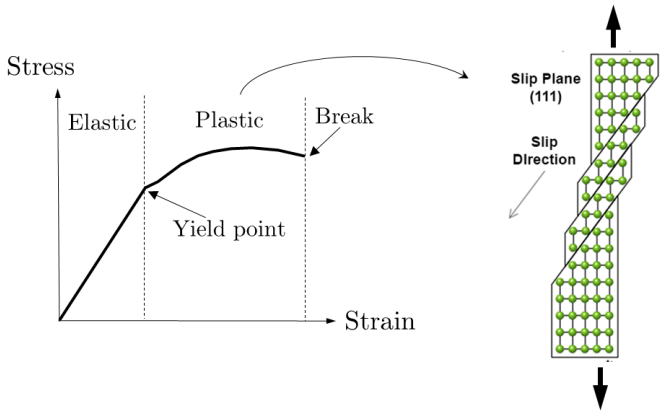


Figure 7: Typical stress–strain curve for a metal.

2 Dislocations

Figure 7 shows the stress–strain curve for a wire stretched under a tensile force. When the force is small, the extension of the wire (strain) is proportional to the applied force (stress) in accordance with Hooke's law for a spring. If the force is removed the wire returns to its original length. This regime of behaviour is call **elastic**. Eventually, a point is reached when the linear relationship breaks down. This is called the **yield point**. Beyond the yield point the wire is permanently changed, so that if the force is removed the wire does not return to its original length. This regime is called **plastic**. What is happening here is that the force is so large that entire planes of atoms are slipping over one another, as shown in Figure 7.

The process by which two planes of atoms slip is subtle. If all the atoms in a plane were to slip simultaneously it would require the breaking of very large numbers of bonds, which would cost a huge amount of energy. However, slip can take place with relatively little energy is the atoms slip one at a time. The process is analogous to making a ruck in a carpet, as shown at the top of Fig. 8. When the ruck propagates from one end of the carpet to the other, it has the same effect as sliding the carpet sideways, but no friction is involved once the ruck has initially formed. The lower diagram Fig. 8 shows the same process in a crystal. The shearing force causes one bond to break and an atom slips sideways, leaving a broken bond called a **dislocation**. Once formed, the dislocation can move along the slip plane relatively easily, because each time a bond is broken another is formed. Each time a dislocation moves from one side of the crystal to the other the crystal slips by one lattice spacing.

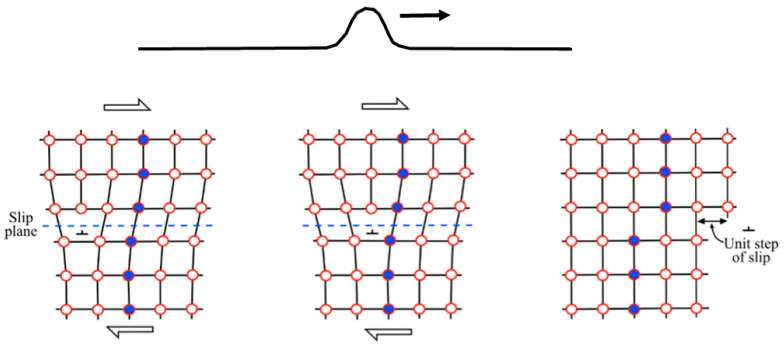


Figure 8: The upper drawing represents a 'ruck' in a carpet. The lower figure shows an edge dislocation propagating through a crystal under shear strain.

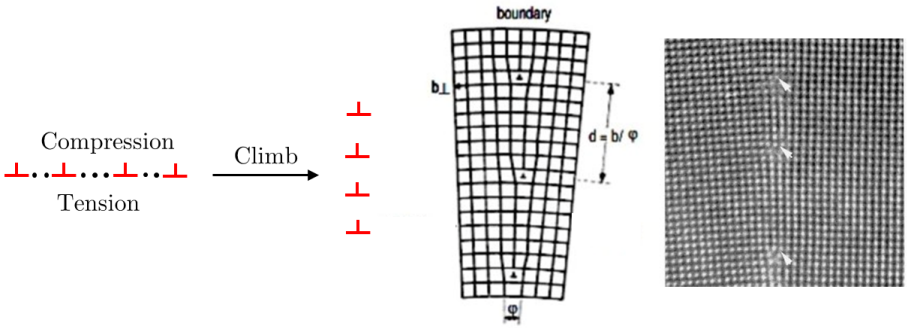


Figure 9: Dislocations on a slip plane rearrange themselves by climbing into a wall, leading to a low-angle boundary between two crystal grains. On the right is an electron microscope image on a low-angle grain boundary in $SrTiO_3$. (After Zhang *et al.*, Phys. Rev. B **66**, (2002) 214112.)

Above the slip plane the atoms are being forced together, giving a compressive stress, while below the plane there is a tensile stress. These stresses can be relieved if several dislocations move out of the plane and build up one above another. This process is called **climb**, and the end result is a wall of dislocations which separates two crystal **grains** within which the crystal planes are slightly tilted relative to one another, as shown in Fig. 9. This wall is called a **low-angle grain boundary**.

Real crystals are typically formed from large numbers of individual grains, whose size can vary from nanometres to millimetres. Usually the grains have a statistical distribution of crystallographic orientations, and the effect on diffraction is that the Bragg peaks exhibit an intrinsic width due to the variation in Bragg angle from grain to grain.

3 Twinning

Twinning is another process which causes crystals to sub-divide into grains, or crystallites. **Twins** are structurally identical regions of a crystal related to one another by reflection, and joined on the mirror plane, as illustrated in Fig. 10. Twins are formed during the growth of the crystal. Usually the angle between the twins is large, so diffraction from each twin domain occurs at widely different positions in reciprocal space. This can complicate the interpretation of diffraction data because it can be difficult to identify diffraction peaks belonging to the same twin. The problem is exacerbated if there are more than two twins.

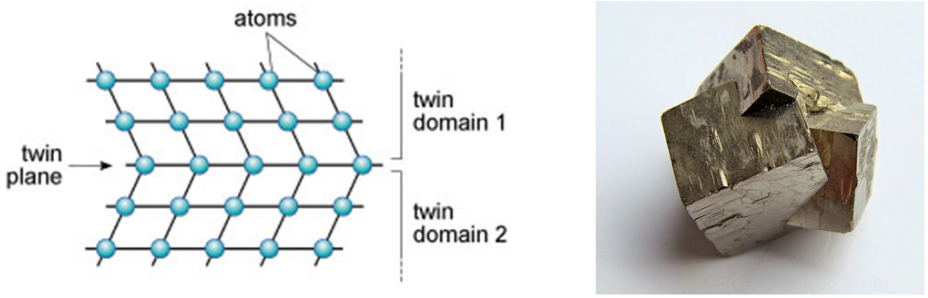


Figure 10: Illustration of twinning between two regions of a crystal related by reflection in the twin plane. Right: macroscopic twins of pyrite (FeS_2). (image credit: `http://www.geologyin.com/2014/07/crystal-twinning.html`.)

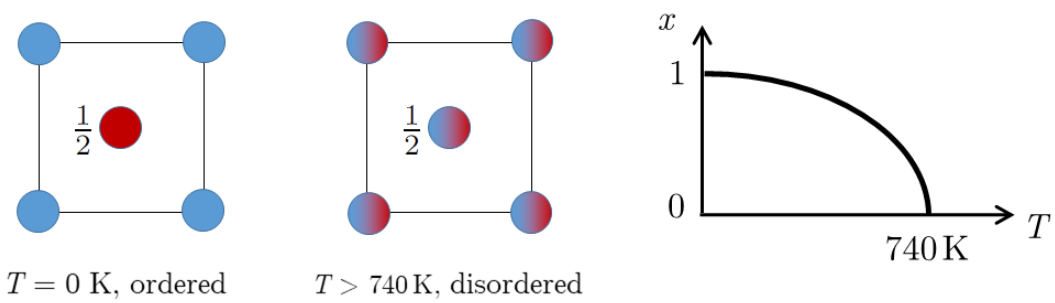


Figure 11: The ordered and disordered phases of β-brass. Right: the order parameter x, defined as the fraction of Cu atoms on the Cu site minus the fraction of Cu atoms on the Zn site, or *vice versa*.

4 Site disorder

Ideal crystals are perfectly periodic, but if a crystal contains different atoms or ions which are of similar size and valence state, and two or more chemically similar crystallographic sites, then it is possible for some of the atoms to become lodged on the 'wrong' sites. This phenomenon is called **site disorder**, or **site mixing**.

Suppose, for example, a crystal contains atoms of type A and atoms of type B (different from A), one might find a fraction x of the A atoms on the A site and a fraction $1-x$ of the B atoms on the A site, and *vice versa*, where for an ideal crystal $x = 1$.

An extreme example of site mixing is the order–disorder phase transition in β-brass. Brass is an alloy of copper (Cu) and zinc (Zn). β-brass is a structural phase which forms when the composition is around 50% Cu and 50% Zn. At low temperatures, the atoms crystallize into a primitive cubic structure, with a two-atom basis comprising Cu at $0, 0, 0$ and Zn at $\frac{1}{2}, \frac{1}{2}, \frac{1}{2}$ (or *vice versa*): See Fig. 11.

Cu and Zn are adjacent to one another in the periodic table, and they have nearly the same atomic radius. Therefore, the energy change if a Cu and a Zn atom were to swap places is rather small. As temperature increases, it becomes entropically advantageous for site disordering to take place, and eventually, at a temperature of around 740 K, the structure becomes completely disordered, with an equal probability of finding Cu or Zn on any given site, see Fig. 11. The crystallographic sites are now no longer inequivalent, and so the average structure becomes body-centred-cubic. One can distinguish between the two phases by diffraction, because when indexed on the cubic cell all reflections are allowed in the primitive cubic structure, whereas in the bcc structure allowed reflections must satisfy the selection rule $h + k + l = 2n$.

By *bulk properties*, I mean physical characteristics that arise when very large numbers of atoms come together. Examples of bulk properties are: resistivity, relative permittivity, refractive index, magnetic susceptibility, thermal conductivity, heat capacity, Young's modulus, and so on. Although these are not properties associated with individual atoms, they do depend on the way the atoms are arranged in the material. In this lecture I shall explore how crystal symmetry affects bulk physical properties, especially how tensors can be deployed to great advantage in making the link between crystal symmetry and anisotropic properties.

7.1 Neumann's Principle

In simple terms, Neumann's principle[1] states that **any bulk physical property exhibits at least the symmetry of the crystal structure.** In most cases of interest, the measurement of bulk properties occurs on a length scale that effectively averages over the translational symmetry of the crystal (diffraction is an exception). Therefore, we can be more specific and state the principle as: **the symmetry of any bulk physical property of a crystal must include the point symmetries of the crystal.**

One caveat is that if a bulk crystal contains twins then a physical measurement will be an average over the different orientation of the twins. Another is that if the material orders magnetically, then the symmetry of the magnetic structure may need to be taken into consideration as well as the crystal symmetry.

7.2 Tensor properties of crystals

Consider first an *isotropic material*, such as a liquid, polycrystalline solid, or (as we shall see) a crystal with cubic symmetry. In such cases, physical properties are the same in all directions, for example

$$\mathbf{D} = \varepsilon_0 \varepsilon_\mathrm{r} \mathbf{E}.$$

In an isotropic material, $\mathbf{D}$ and $\mathbf{E}$ are parallel vectors, and ε_r is a scalar. If an electric field is applied to an *anisotropic material* then $\mathbf{D}$ is not necessarily parallel to $\mathbf{E}$. We can extend the relation to describe this case by expressing ε_r as a 3×3 matrix.

Whenever two properties are linked by a linear relationship of the form

$$g = Tf, \tag{1}$$

where g describes an 'effect' brought about by a 'cause' f, the quantities f, g and T are **tensors**. Such a relation is shorthand for a set of simultaneous equations that link together the sets of coefficients which are needed to describe f and g. In the case of relative permittivity, the tensor is a matrix containing 9 coefficients, which relates two vectors, each of which contains 3 coefficients.

The **rank, r** of a tensor is related to the number of coefficients contained in the tensor. In d dimensions, the number of coefficients in an r-rank tensor is d^r. In general,

$$(\text{rank of } T) = (\text{rank of } f) + (\text{rank of } g).$$

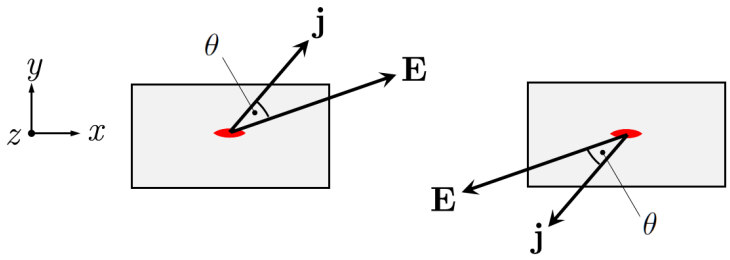
Here are some tensors of different ranks in three dimensions ($d = 3$) and examples of physical properties described by the tensor:

Rank	Object	Examples
0	scalar	temperature (T), heat capacity (C_p), charge (Q)
1	vector	electric field ($\mathbf{E}$), magnetic field ($\mathbf{H}$,) temperature gradient (∇T)
2	matrix	relative permittivity ($\boldsymbol{\varepsilon}_\mathrm{r}$), electrical conductivity ($\boldsymbol{\sigma}$)

[1] Named after Franz Neumann, who was born in 1798, fought against Napoleon, and died at the age of 96.

7.3 Tensors and symmetry transformations

Suppose a crystal has two-fold rotational symmetry about the z-axis. We apply an electric field $\mathbf{E}$ in an arbitrary direction within the plane perpendicular to z, which induces an electric current density $\mathbf{j}$ at an angle θ to $\mathbf{E}$, given by $\mathbf{j} = \boldsymbol{\sigma}\mathbf{E}$:



We now rotate $\mathbf{E}$ by 180° around the z-axis. Because of the 2-fold symmetry the new direction of $\mathbf{E}$ is entirely equivalent to the old one, so we expect the relationship between $\mathbf{j}$ and $\mathbf{E}$ to be exactly the same as before. There is no physical difference between directions which are related by the 2_z symmetry operation. The tensor $\boldsymbol{\sigma}$ must be the same in both cases. In other words, $\boldsymbol{\sigma}$ is invariant under a two-fold rotation of the axes about z.

This simple example illustrates an important requirement of tensors that link together two physical observables. Applying Neumann's principle, we can say that **the tensor is invariant under the point symmetries of the crystal**.

7.4 How do you transform tensor components?

In this section I shall prove that the components of tensors transform in the same way as the corresponding products of Cartesian coordinates.

As presented in Lecture 1, a transformation of Cartesian coordinates $(q_1, q_2, q_3) \equiv (x, y, z)$ under a symmetry operation R can be written

$$q'_i = \sum_j a_{ij} q_j, \tag{2}$$

where a_{ij} is the matrix that represents R. For the rotation and roto-inversion operations with which we are concerned here the a_{ij} matrix is orthogonal, i.e. $a_{ij}^{-1} = a_{ji}$, and the inverse transformation may be written

$$\begin{aligned} q_i &= \sum_j a_{ij}^{-1} q'_j \\ &= \sum_j a_{ji} q'_j. \end{aligned} \tag{3}$$

We can transform products of coordinates as follows:

$$\begin{aligned} q'_i q'_j &= \Big(\sum_k a_{ik} q_k\Big)\Big(\sum_l a_{jl} q_l\Big) \\ &= \Big(\sum_{kl} a_{ik} a_{jl}\Big) q_k q_l. \end{aligned} \tag{4}$$

Turning to tensors, a **scalar** (rank 0 tensor) is a pure number and is invariant under a transformation of coordinates. A **vector** contains the components of a quantity along the Cartesian axes, and so a vector $\mathbf{g}$

transforms in the same way as the coordinates. From (2),

$$g'_i = \sum_j a_{ij} g_j. \tag{5}$$

We now establish the transformation rule for the components of a matrix T that links two vectors $\mathbf{f}$ and $\mathbf{g}$,

$$g_i = \sum_j T_{ij} f_j. \tag{6}$$

Applying R to $\mathbf{g}$, we have from eq. (5)

$$\begin{aligned} g'_i &= \sum_k a_{ik} g_k \\ &= \sum_k a_{ik} \sum_l T_{kl} f_l \qquad [\text{from (6)}] \\ &= \sum_k a_{ik} \sum_l T_{kl} \sum_j a_{jl} f'_j \qquad [\text{from (3)}] \\ &= \sum_j \Big(\sum_{kl} a_{ik} a_{jl} T_{kl} \Big) f'_j \\ &= \sum_j T'_{ij} f'_j, \end{aligned} \tag{7}$$

where,

$$T'_{ij} = \Big(\sum_{kl} a_{ik} a_{jl} \Big) T_{kl}. \tag{8}$$

Comparing (8) and (4) we see that the **components of a matrix transform under a symmetry operation in the same way as the corresponding bilinear products of coordinates**.

The procedure may be extended to higher rank tensors. If T is an r-rank tensor then an individual component of T is labelled with r suffices, and

$$T'_{ijk\ldots} = \Big(\sum_{\alpha\beta\gamma\ldots} a_{i\alpha} a_{j\beta} a_{k\gamma} \ldots \Big) T_{\alpha\beta\gamma\ldots}. \tag{9}$$

This result is known as the **tensor transformation law**.

Example

As the working above has been rather abstract, it might be helpful to work through a simple example. Consider the relation between current density and electric field

$$\mathbf{j} = \boldsymbol{\sigma} \mathbf{E},$$

where $\boldsymbol{\sigma}$ is the electrical conductivity tensor (matrix)

$$\boldsymbol{\sigma} = \begin{pmatrix} \sigma_{11} & \sigma_{12} & \sigma_{13} \\ \sigma_{21} & \sigma_{22} & \sigma_{23} \\ \sigma_{31} & \sigma_{32} & \sigma_{33} \end{pmatrix}. \tag{10}$$

Let us now rotate the coordinate axes clockwise through 90° about the z-axis. The rotation operation is described by the matrix

$$a_{ij} = 4_z = \begin{pmatrix} 0 & -1 & 0 \\ 1 & 0 & 0 \\ 0 & 0 & 1 \end{pmatrix}.$$

in other words,

$$x' = -y$$
$$y' = x$$
$$z' = z$$

and so

$$x'^2 = y^2$$
$$x'y' = -yx$$
$$x'z' = -yz$$
$$\text{etc.}$$

Therefore, applying the tensor transformation law,

$$\boldsymbol{\sigma}' = \begin{pmatrix} \sigma_{22} & -\sigma_{21} & -\sigma_{23} \\ -\sigma_{12} & \sigma_{11} & \sigma_{13} \\ -\sigma_{32} & \sigma_{31} & \sigma_{33} \end{pmatrix}. \tag{11}$$

7.5 Use of symmetry to simplify tensors

We now show how it is possible to simplify tensors by combining Neumann's principle with the tensor transformation law. We shall show (1) how to find which tensor components are constrained to vanish purely on symmetry grounds, and (2) how to determine the number of independent constants in a tensor.

We adopt the conductivity tensor as a concrete example. Suppose a crystal has tetragonal symmetry, in which case crystal point group contains the symmetry element 4_z. This imposes the requirement that the conductivity tensor must be invariant under the 4_z symmetry operation (see Section 7.3), i.e. the matrices in eqs. (10) and (11) must be equal. From the diagonal elements we see that

$$\sigma_{11} = \sigma_{22}.$$

For the off-diagonal elements, there are different constraints depending on whether the tensor is symmetric or antisymmetric. For a *symmetric tensor* (this applies in the absence of a magnetic field) $\sigma_{21} = \sigma_{12}$, etc, so comparing eqs. (10) and (11) we obtain the constraint $\sigma_{12} = -\sigma_{12}$ which can only be satisfied if

$$\sigma_{12} = \sigma_{21} = 0.$$

We also see that $\sigma_{13} = -\sigma_{23}$ and $\sigma_{23} = \sigma_{13}$. Together, these imply that

$$\sigma_{13} = \sigma_{31} = 0$$
$$\sigma_{23} = \sigma_{32} = 0.$$

Therefore, the conductivity tensor in zero field has two independent constants and has the general form

$$\boldsymbol{\sigma} = \begin{pmatrix} a & 0 & 0 \\ 0 & a & 0 \\ 0 & 0 & c \end{pmatrix}. \tag{12}$$

For an *antisymmetric tensor* (in the presence of a magnetic field applied along the z-axis), $\sigma_{21} = -\sigma_{12}$, etc. Comparing eqs. (10) and (11) we see that there is no constraint on σ_{12}, but $-\sigma_{23} = \sigma_{13} = -\sigma_{31}$ and $\sigma_{23} = \sigma_{13} = -\sigma_{31}$. Hence, $\sigma_{13} = \sigma_{23} = 0$, and the tensor in a z-axis field has three independent constants:

$$\boldsymbol{\sigma} = \begin{pmatrix} a & b & 0 \\ -b & a & 0 \\ 0 & 0 & c \end{pmatrix}. \tag{13}$$

The constant b is the Hall conductivity (see the Electronic Properties course).

7.6 Symmetry of physical properties

Once we have found the general form of a tensor consistent with the point symmetry of a crystal, we can determine what symmetry this imposes on the physical observable represented by the tensor.

In the case of the conductivity tensor, the direction of $\mathbf{j}$ for a given $\mathbf{E}$ is found simply by matrix multiplication: $\mathbf{j} = \boldsymbol{\sigma}\mathbf{E}$. From (12) it can be seen that the current density $\mathbf{j}$ will be parallel to $\mathbf{E}$ for any direction of $\mathbf{E} \perp z$. We say that the electrical conductivity is *isotropic* in the xy plane. $\mathbf{j}$ is also parallel to $\mathbf{E}$ for $\mathbf{E} \parallel z$, but not for any other direction of $\mathbf{E}$.

Representation surface for a second-rank tensor

There are many important physical properties described by second-rank tensors (3×3 matrices), which are particularly common. The **representation surface** is a way to visualize a 2^{nd} rank tensor geometrically, as well as to see what effect the anisotropy of the tensor has on the physical observables it relates.

Consider a 2^{nd} rank tensor $\mathbf{T}$ which relates two vectors $\mathbf{g}$ and $\mathbf{f}$, i.e. $\mathbf{g} = \mathbf{T}\mathbf{f}$. Now consider the equation

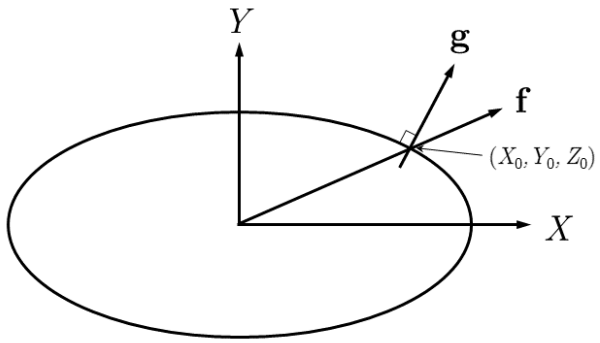
$$(x, y, z)\,\mathbf{T}\begin{pmatrix} x \\ y \\ z \end{pmatrix} = 1. \tag{14}$$

The left-hand side is a *quadric form*, and (14) is an equation which defines a quadric surface (ellipsoid, paraboloid or hyperboloid) in 3D space of the Cartesian coordinates x, y, z. This surface is the **representation surface** of the tensor. If $\mathbf{T}$ is symmetric then we can diagonalize it and transform eq. (14) into

$$T_1X^2 + T_2Y^2 + T_3Z^2 = 1, \tag{15}$$

where X, Y, Z are the principal axes (eigenvectors) of $\mathbf{T}$. If T_1, T_2, T_3 are all positive then (15) is the equation of an ellipsoid aligned with the principal axes.

A useful property of the representation surface is that is we draw a line parallel to $\mathbf{f}$ starting at the origin, then $\mathbf{g}$ is parallel to the normal to the representation surface at the point where $\mathbf{f}$ intersects the surface:



Proof: write (15) in the form $Z = f(X, Y)$, so that the surface is defined by $\mathbf{r} = (X, Y, f)$. The partial derivatives $\partial\mathbf{r}/\partial x$ and $\partial\mathbf{r}/\partial y$ are vectors which lie in the tangent plane, so the normal vector to the tangent

plane is given by the cross product

$$\begin{aligned}\mathbf{n} &= \frac{\partial \mathbf{r}}{\partial X} \times \frac{\partial \mathbf{r}}{\partial Y} \\ &= \begin{pmatrix} 1 \\ 0 \\ \frac{\partial f}{\partial X} \end{pmatrix} \times \begin{pmatrix} 0 \\ 1 \\ \frac{\partial f}{\partial Y} \end{pmatrix} \\ &= \begin{pmatrix} -\frac{\partial f}{\partial X} \\ -\frac{\partial f}{\partial Y} \\ 1 \end{pmatrix}\end{aligned}$$

Let (X_0, Y_0, Z_0) be the point where $\mathbf{f}$ intersects the representation surface. From (15),

$$\frac{\partial Z}{\partial X} = -\frac{T_1 X_0}{T_3 Z_0} \quad \text{and} \quad \frac{\partial Z}{\partial Y} = -\frac{T_2 Y_0}{T_3 Z_0}.$$

Therefore,

$$\begin{aligned}\mathbf{n} &= \frac{1}{T_3 Z_0} \begin{pmatrix} T_1 X_0 \\ T_2 Y_0 \\ T_3 Z_0 \end{pmatrix} \\ &= \frac{1}{T_3 Z_0} \begin{pmatrix} T_1 & 0 & 0 \\ 0 & T_2 & 0 \\ 0 & 0 & T_3 \end{pmatrix} \begin{pmatrix} X_0 \\ Y_0 \\ Z_0 \end{pmatrix}.\end{aligned}$$

The vector from the origin to the point (X_0, Y_0, Z_0) is parallel to $\mathbf{f}$, so

$$\begin{aligned} & \mathbf{n} \parallel \mathbf{Tf} \\ \rightarrow \quad & \mathbf{n} \parallel \mathbf{g}.\end{aligned}$$

Examples

1. *Tetragonal* crystal. The representation surface for the $\boldsymbol{\sigma}$ tensor given in (12) is defined by the equation

$$a(x^2 + y^2) + cz^2 = 1,$$

which for $a, c > 0$ is an ellipsoid of revolution about the z-axis. Therefore, $\boldsymbol{\sigma}$ is isotropic in the xy plane.

2. *Cubic* crystal. Application of the principal symmetry operations shows that the tensor is a diagonal matrix with only one independent constant a. The representation surface is a sphere described by

$$a(x^2 + y^2 + z^2) = 1,$$

which means that the conductivity is completely isotropic.

Earlier in the course we looked at the point group symmetry of isolated molecules in their ground state (i.e. assuming the atoms to be static). We now wish to consider dynamical properties. By measuring the vibrational modes of a molecule one can determine the strength and character of the bonds which hold the atom together, and hence calculate the molecule's properties at non-zero temperature. Furthermore, the vibrational spectrum of each molecule is unique, and can be used as a fingerprint for the presence of the molecule. I shall describe infra-red absorption and Raman spectroscopy, which are important techniques for measuring vibrational spectra and extensively used as analytical tools, for example in forensic science and blood alcohol content testing.

8.1 Vibrational normal modes of molecules

The coupled oscillations of the atoms in a molecule can be described by a set of **normal modes**, i.e. states of motion in which all the atoms vibrate at the same frequency (and therefore with a fixed relative phase). As such, normal modes are discrete resonant modes of the molecule. The validity of the normal mode picture depends on the **harmonic approximation**, which assumes that the interatomic potentials are quadratic. The harmonic approximation works best when the amplitudes of vibration are small. Normal modes are linearly independent (they form an orthonormal basis), and any general motion of the molecule can be expressed as a linear combination of normal modes.

The normal modes of a molecule can be obtained from the set of coupled linear equations of motion of the atoms, which can be expressed in matrix form as

$$\mathsf{D}\mathbf{x} = \omega^2\mathbf{x}, \tag{1}$$

where D is an Hermitian matrix called the **dynamical matrix**. The normal modes are obtained by diagonalizing D. The eigenvectors $\mathbf{x}$ of D give the amplitude and relative phase of each atom in a normal mode, and the eigenvalues give the normal mode angular frequencies ω.

For a molecule containing N atoms there are $3N$ equations of motion. D is then a $3N \times 3N$ matrix, and so there are $3N$ normal modes. Of these $3N$ modes, three will be centre-of-mass translations of the whole molecule along the x, y and z directions, and three will be rigid rotations of the molecule about the x, y and z axes (for a linear molecule like CO_2 there are only two rigid rotations). The remaining $3N - 6$ modes are **vibrational modes**, which we shall label q_i, $i = 1$ to $3N - 6$.

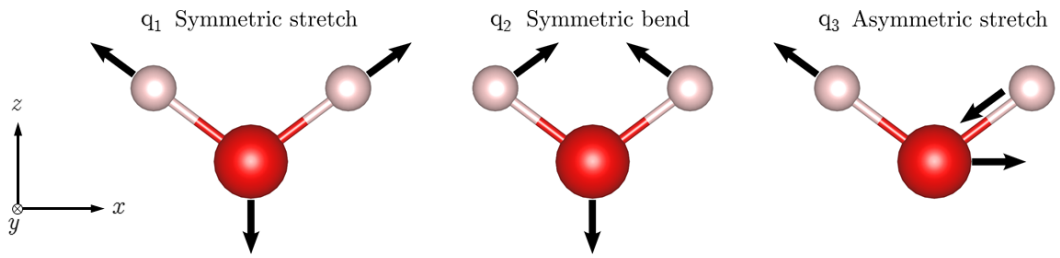
In this course we shall not be concerned with setting up or solving the eigenvalue problem, eq. (1). Instead, we shall focus on the symmetry properties of the normal modes of molecules, and on the consequences of symmetry for spectroscopic measurements.

8.2 Symmetry of molecular normal modes

The Hamiltonian $\mathcal{H}$ which represents the total energy of the molecule is invariant under the symmetry operations in the point group of the (static) molecule. Referring to the symmetry–degeneracy principle discussed in Lecture 4, we can consider two cases:

1. $Rq_i = \chi q_i$. In other words, a point symmetry operation R transforms the mode into the same mode multiplied by a scalar constant χ. In the harmonic approximation we can write $\mathcal{H} = \frac{1}{2}(\dot{q}^2 + q^2)$. If $\mathcal{H}$ is invariant under R then $R\mathcal{H} = \mathcal{H}$, i.e. $\frac{1}{2}\chi^2(\dot{q}^2 + q^2) = \frac{1}{2}(\dot{q}^2 + q^2)$. Hence, $\chi^2 = 1$, and so $\chi = \pm 1$.

2. $Rq_i = q_j$, $j \neq i$. In this case, modes q_i and q_j are distinct modes which are degenerate. In the general case Rq_i can be a linear combination of several modes all of which, therefore, are degenerate.



Let's look at a specific example, the water molecule. There are three atoms ($N = 3$), so nine modes in total, three of which are vibrational normal modes. These are shown in the figure above. The point group of the molecule is $mm2$, which contains the symmetry operations E, 2_z, m_x, m_y. Under 2_z, q_1 and q_2 remain invariant while q_3 changes sign. Similarly for m_x, while all modes are invariant under m_y. The table below lists the scalar constants χ (which are called **characters**) obtained from this symmetry analysis.

Mode	E	2_z	m_x	m_y
q_1	1	1	1	1
q_2	1	1	1	1
q_3	1	−1	−1	1

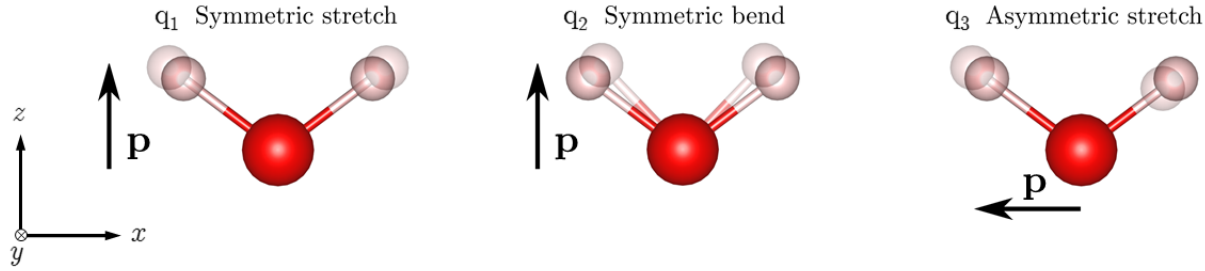
8.3 Infra-red absorption

At sufficiently low temperature a molecule will be in its vibrational ground state. Transitions to the normal mode excited states can be induced by absorption of electromagnetic radiation (usually in the infra-red) as long as certain selection rules are satisfied, as we explain now.

Infra-red (IR) absorption is a process in which single photons are completely absorbed and vibrational energy is created. The experiment usually measures the transmission of IR radiation through the material, from which the absorption is determined.

The absorption process is described classically by the dipole oscillator model, which implies that in order to absorb radiation a vibrational mode must generate an oscillating electric dipole. Furthermore, the absorption depends on the projection of the polarization of the radiation onto the molecule's oscillating electric dipole. If absorption is allowed, the vibrational mode is termed **infra-red active**. One can often determine whether a mode is IR active simply by looking to see whether the mode generates an oscillating dipole moment, and if it does, identifying the direction in which the dipole moment points.

Take the water molecule, for example:



From the direction of the oscillating electric dipole $\mathbf{p}$ it can be seen that the q_1 and q_2 modes will be IR active for incident polarization along z, and the q_3 mode will be IR active for incident polarization along x.

These selection rules are easy to see by inspection, but we can determine the selection rules more systematically from symmetry. The transition rate from the ground state q_0 to one of the excited normal mode states q_n is described by Fermi's Golden Rule, which depends on the matrix elements of the components p_j of the electric dipole operator $\mathbf{p}$ between initial and final states of the molecule:

$$M_j = \langle q_n | p_j | q_0 \rangle. \tag{2}$$

Now let's apply a symmetry operation from the point group of the molecule to this equation. For the case when the symmetry operations simply multiply each of q_0, q_n and p_j by a scalar χ, we can write

$$\chi(M_j) = \chi(q_n) \times \chi(p_j) \times \chi(q_0)$$

As M_j is a scalar it is invariant under any symmetry transformation, so $\chi(M_j) = 1$. Hence, a mode q_n is IR active if

$$1 = \chi(q_n) \times \chi(p_j) \times \chi(q_0) \tag{3}$$

for each and every symmetry operation in the point group.[1] If (3) is not satisfied for all symmetries in the point group then we must conclude that $\langle q_n | p_j | q_0 \rangle = 0$, and so the transition is forbidden for the component p_j.

The characters of q_0 are all $+1$ by definition, because the ground state of the molecule is invariant under all symmetry operations in the point group. Therefore, because the characters for the other modes are all either $+1$ or -1 we see that a mode q_n is IR active if the set of characters $\{\chi(q_n)\}$ for each of the symmetry operations is the same as $\{\chi(p_j)\}$, where p_α is one of the components of $\mathbf{p}$. If the condition $\{\chi(q_n)\} = \{\chi(p_j)\}$ is satisfied then the mode q_n is observable when the electric field of the incident photon has a component in the j direction.

The dipole moment $\mathbf{p}$ is a vector, so it transforms like the coordinates x, y, z (see Lecture 7). For the point group $mm2$ it has characters

$\mathbf{p}$	E	2_z	m_x	m_y
p_x	1	-1	-1	1
p_y	1	-1	1	-1
p_z	1	1	1	1

Consider the q_1 mode of the water molecule. The set of characters of q_1 is $\{\chi(q_1)\} = \{1, 1, 1, 1\}$ — see character table in Section 8.2 — which is the same as $\{\chi(p_z)\}$, therefore q_1 is IR active when the incident radiation has a component of polarization along the z direction. On the other hand, $\{\chi(q_1)\} \neq \{\chi(p_x)\}$ or $\{\chi(p_y)\}$, so q_1 would not be observed if the incident polarization was purely along x or y.

Similarly, for q_3 we see that $\{\chi(q_3)\} = \{\chi(p_x)\}$, and so q_3 is IR active for x polarization but not for y or z polarization.

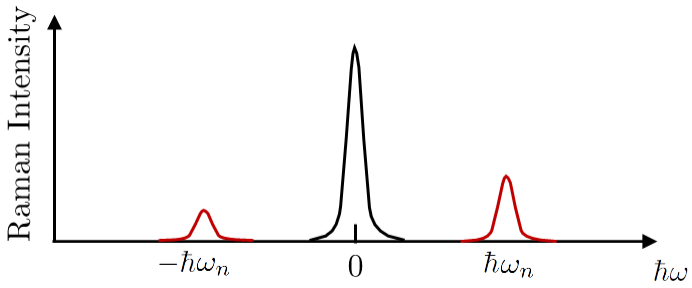
[1] The volume element $\mathrm{d}V$ contained in the matrix element integral is invariant under any point symmetry transformation.

8.4 Raman spectroscopy

Unlike infra-red (absorption) spectroscopy, Raman spectroscopy is based upon an inelastic scattering process in which a photon scatters from the molecule, and in doing so transfers energy $\hbar\omega$ to the molecule. As energy is conserved in this process, the initial and final energies of the photon are related by

$$\hbar\omega_\mathrm{i} - \hbar\omega_\mathrm{f} = \hbar\omega.$$

By measuring the intensity of the scattered photons as a function of $\hbar\omega$, one would expect to observe a strong elastic line at $\hbar\omega = 0$, and two inelastic side-bands, one corresponding to creation of a quantum of vibrational energy in a mode with angular frequency ω_n, and one corresponding to the removal of a quantum from the mode (which requires that the mode was previously populated, e.g. by thermal excitation). Qualitatively, the Raman spectrum looks like the sketch below.



In experiments, a high power laser operating in the visible part of the electromagnetic spectrum is typically used as the light source.

The Raman scattering process is more subtle than IR absorption. The electric field $E\cos\omega_\mathrm{i}t$ of the incident radiation provides a time-dependent perturbation at the incident angular frequency ω_i, which induces a time-varying electric dipole moment $p(t)$ on the molecule. However, owing to anharmonic effects, $p(t)$ has frequency components not only at ω_i, but also at sum and difference frequencies $\omega_\mathrm{i} \pm \omega_n$, where ω_n are frequencies of the vibrational modes of the molecule:

$$p(t) = p_0 \exp(\mathrm{i}\omega_\mathrm{i}t) + p_+ \exp\{\mathrm{i}(\omega_\mathrm{i} + \omega_n)t\} + p_- \exp\{\mathrm{i}(\omega_\mathrm{i} - \omega_n)t\}. \tag{4}$$

So the frequency of the emitted photon may be ω_i or $\omega_\mathrm{i} \pm \omega_n$.

The relation between the induced polarization and incident electric field can be expressed in terms of the polarizability α, which here is a time-dependent quantity. In isotropic media, α is a scalar, but in anisotropic systems such as molecules, α is a tensor of rank 2, that we represent as a 3×3 matrix:

$$p_i = \alpha_{ij} E_j,$$

where

$$\alpha_{ij} = \begin{pmatrix} \alpha_{11} & \alpha_{12} & \alpha_{13} \\ \alpha_{21} & \alpha_{22} & \alpha_{23} \\ \alpha_{31} & \alpha_{32} & \alpha_{33} \end{pmatrix}$$

In the quantum-mechanical treatment, the Raman process appears in second-order time-dependent perturbation theory, and the Raman scattering depends on the matrix element

$$M_{ij} = \langle q_n | \alpha_{ij} | q_0 \rangle. \tag{5}$$

This result is like the matrix element for IR absorption, eq. (2), except that α_{ij} replaces p_j. Hence, we can use the same symmetry arguments to determine whether or not a mode is Raman active. For this purpose

we need the character table for α_{ij}, which we can compile using the fact that the components of a 2^{nd}-rank tensor transform under point symmetry operations like the corresponding bilinear products of coordinates, x^2, y^2, z^2, xy, xz, yz. This was proved in the notes for Lecture 7.

The character table for α_{ij} for the point group $mm2$ of the water molecule is found to be (the tensor is symmetric, $\alpha_{ij} = \alpha_{ji}$)

α_{ij}	E	2_z	m_x	m_y
α_{11}	1	1	1	1
α_{22}	1	1	1	1
α_{33}	1	1	1	1
α_{12}	1	1	−1	−1
α_{13}	1	−1	−1	1
α_{23}	1	−1	1	−1

Comparing the characters for q_n and α_{ij} we immediately see that the q_1 and q_2 modes of water are Raman active through the α_{11}, α_{22} and α_{33} tensor components, i.e. for light polarized in the x, y or z directions which does not change its polarization on scattering ($x \to x$, $y \to y$ or $z \to z$). However, the q_1 and q_2 modes are not Raman active for any of the rotated polarization channels (i.e. $x \to y$, $x \to z$, etc.).

On the other hand, the q_3 mode is only active through the α_{13} tensor component, corresponding to incident light polarized along x and scattered light polarized along z, or *vice versa*.

8.5 Final remarks

The symmetry analysis method to determine IR and Raman selection rules, as described above, applies when the vibrational modes are **singly degenerate**, and is a special case of **group representation theory**. When there are degenerate modes the method needs to be generalized. The general method also involves characters, but the characters are not restricted to ± 1.

Group representation theory is incredibly interesting and powerful, but is beyond the scope of the present course. It is taught in Oxford as a graduate-level course.

In Lecture 8 we found that infra-red and Raman spectroscopy could be used to measure the vibrational modes of simple molecules. These techniques can also be used to probe vibrational modes of crystals (phonons), but a major limitation is that they can only access regions of reciprocal (momentum) space very close to the origin, i.e. they are limited to phonon frequencies in the limit $|\mathbf{k}| \to 0$. This is because the momentum of visible or infra-red photons is several orders of magnitude smaller than the dimensions of the first Brillouin zone.

Neutrons and X-rays have typical wavelengths which are comparable to inter-atomic spacings, giving them a momentum that is well matched to phonon wavevectors in crystals. Both neutrons and X-rays can be used to measure phonon dispersion relations in crystals, but the neutron scattering technique is more straightforward and better established.[1] Unlike X-rays, one can produce neutron beams that have an energy comparable to typical phonons (less than ∼100 meV), and for this reason they are usually the probe of choice for studying phonon dispersion relations.

9.1. Neutron scattering

The neutron interacts with the nucleus of the atom via the strong nuclear force — a process known as **nuclear scattering**.[2] The scattering amplitude is dependent upon the element, isotope, and the relative orientation of the neutron and nuclear spin (if present). Different isotopes are expected to be distributed randomly throughout a crystal, and the relative orientation of neutron and nuclear spins is random in both space and time. This leads to two types of scattering: (i) coherent scattering, which depends on the average scattering amplitude of the nuclei and gives information on the relative positions of atoms through interference effects; (ii) incoherent scattering, which arises from random deviations from the average scattering length and does not give information on the relative positions of the atoms. In the study of structure and dynamics we are usually only interested in coherent scattering, and we strive to minimise incoherent backgrounds (see Fig. 1 for an illustration of coherent and incoherent scattering in the context of neutron powder diffraction).

The nucleus is point-like on the scale of the wavelength of the neutron. The neutron scattering amplitude therefore carries no form factor (it is independent of $\mathbf{Q}$) and is expressed by a single number, known as the scattering length, b. When it is averaged over the random distribution of isotopes and nuclear spin orientations it is called the coherent (or mean) scattering length $\overline{b}$. The scattering length can be positive or

[1] Many textbooks imply that X-rays are unsuitable for measuring phonon dispersion relations, but thanks to the development of very high resolution X-ray scattering spectrometers at synchrotron radiation facilities in the last two decades the measurement of phonon spectra with X-rays has become fairly routine.

[2] Neutrons also interact with electrons via the magnetic dipole interaction, hence **magnetic neutron scattering** can occur when the atoms have unpaired electrons and a dipole moment. Magnetic neutron scattering is discussed in the magnetism part of the C3 course

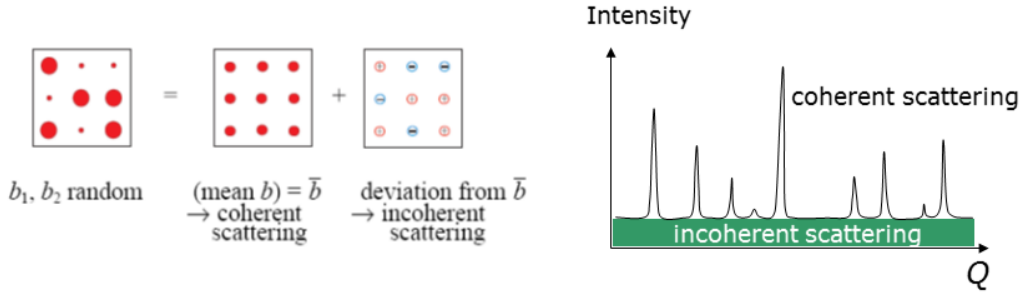


Figure 1: Coherent and incoherent elastic neutron scattering from a powder sample.

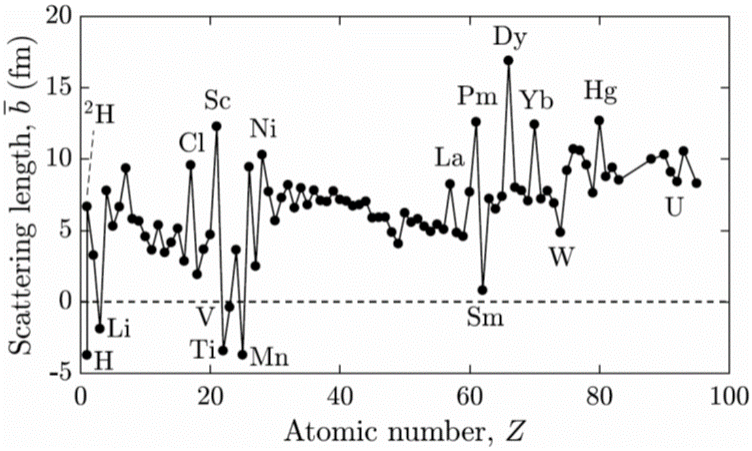


Figure 2: Variation of the neutron scattering length across the periodic table. (Image source: A. T. Boothroyd, *Principles of Neutron Scattering from Condensed Matter*, OUP (2020).)

negative, depending on whether or not the interaction with the neutron is attractive or repulsive. Unlike the atomic form factor in X-ray scattering, the neutron scattering length does not vary systematically across the periodic table (see Fig. 2). This can be an advantage over X-ray scattering as it is possible to achieve contrast between elements of similar atomic number, or even contrast between different isotopes of the same element. It also makes neutrons sensitive to light elements such as hydrogen in the presence of heavy elements.

9.2. Inelastic neutron scattering

The inelastic neutron scattering process is as follows. A neutron of initial wavevector $\mathbf{k}_\mathrm{i}$ and energy E_i is scattered through an angle ϕ into a final state with wavevector $\mathbf{k}_\mathrm{f}$ and energy E_f. As in any scattering process, energy and momentum must be conserved. Because the phonon dispersion relation is periodic in the reciprocal lattice, the wavevector of a phonon can be written $\mathbf{k}_\mathrm{ph} + \mathbf{G}$, where $\mathbf{k}_\mathrm{ph}$ is a phonon wavevector in the first Brillouin zone and $\mathbf{G}$ is a reciprocal lattice vector. If the corresponding angular frequency of the phonon is ω_ph then the conservation laws may be written

$$\begin{aligned} \mathbf{Q} &= \mathbf{k}_\mathrm{i} - \mathbf{k}_\mathrm{f} \\ &= \mathbf{k}_\mathrm{ph} + \mathbf{G} \qquad \text{(momentum)} \end{aligned} \tag{1}$$

$$\begin{aligned} \hbar\omega &= E_\mathrm{i} - E_\mathrm{f} \\ &= \hbar\omega_\mathrm{ph} \qquad \text{(energy)}. \end{aligned} \tag{2}$$

Here, $\hbar\mathbf{Q}$ is the amount of momentum transferred from the neutron to the sample and is called the **momentum transfer**, and $\hbar\omega$, the amount energy transferred to the sample, is called the **energy transfer**.

When a neutron scattering event creates a phonon, converting the system to an excited state which is higher in energy than the initial state, momentum and energy are transferred from the neutron to the system. We call this a **neutron energy-loss** process. The corresponding **neutron energy-gain** process is when a pre-existing phonon excitation is annihilated in the scattering event, thus transferring momentum and energy from the system to the neutron. A significant thermal population of phonons is required for measurable energy gain scattering, which means that $k_\mathrm{B}T \gtrsim \hbar\omega_\mathrm{ph}$, where T is the temperature.

The neutron energy-loss and energy-gain processes can be represented by **scattering triangles**, as shown

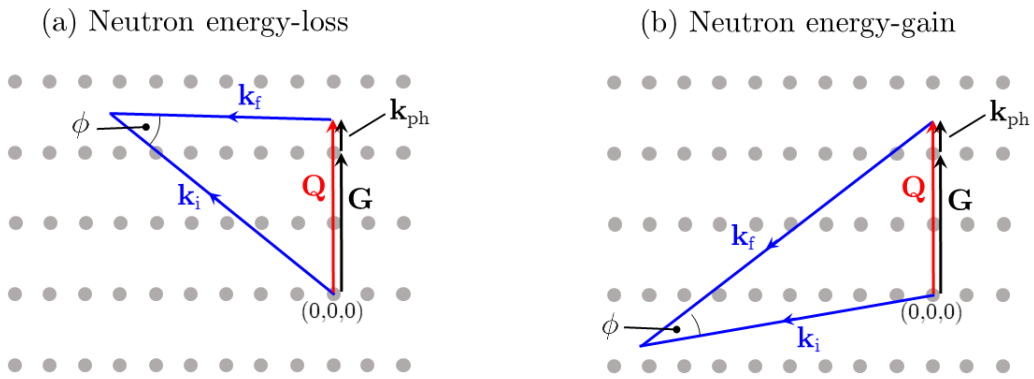


Figure 3: Scattering triangles for (a) neutron energy-loss and (b) energy-gain processes with the same $\mathbf{Q}$, superimposed on a reciprocal lattice. Both configurations are set up to measure a phonon with wavevector $\mathbf{k}_\mathrm{ph}$ relative to a reciprocal lattice vector $\mathbf{G}$.

in Fig. 3. The kinematics are governed by eqs. (1) and (2), together with the non-relativistic kinetic energy relation

$$E = \frac{\hbar^2|\mathbf{k}|^2}{2m_\mathrm{n}}. \tag{3}$$

From the cosine rule as applied to the scattering triangle, we find

$$Q^2 = k_\mathrm{i}^2 + k_\mathrm{f}^2 - 2k_\mathrm{i}k_\mathrm{f}\cos\phi \tag{4}$$

$$= \frac{2m_\mathrm{n}}{\hbar^2}\left\{E_\mathrm{i} + E_\mathrm{f} - 2(E_\mathrm{i}E_\mathrm{f})^{\frac{1}{2}}\cos\phi\right\}, \tag{5}$$

where $Q = |\mathbf{Q}|$, etc, and $m_\mathrm{n} = 1.675 \times 10^{-27}$ kg is the mass of the neutron.

9.3. Triple-axis neutron spectroscopy

The traditional instrument used to measure phonon dispersion relations is the **triple-axis neutron spectrometer** (Fig. 4) installed at a continuous source of neutrons (usually a nuclear reactor).

A monochromatic incident beam of neutrons of energy E_i strikes the sample, and the neutrons that are scattered into a particular direction and with a chosen final energy E_f are recorded in the detector. The divergence of the incident and final beams can be constrained through the use of collimators. The incident neutrons are picked out from the broad spectrum of neutrons produced in the source by Bragg reflection from a crystal monochromator. Similarly, the detected neutrons are selected by Bragg reflection from a crystal analyser. The values of E_i and E_f are determined by the Bragg angles θ_M and θ_A at the monochromator and analyser, respectively. The three angles θ_M, θ_A, and ϕ (the scattering angle at the sample), which all have common (vertical) rotation axes, are what give the triple-axis spectrometer its name, and the ability to set these independently allows one to perform point-by-point measurements. Usually, measurements are restricted to a plane in reciprocal space, but by mounting the crystal in different orientations one can explore the entire Brillouin zone.

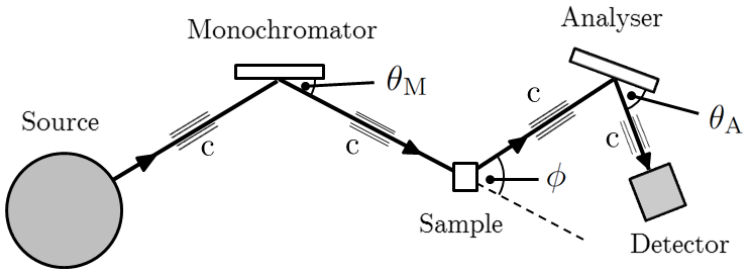
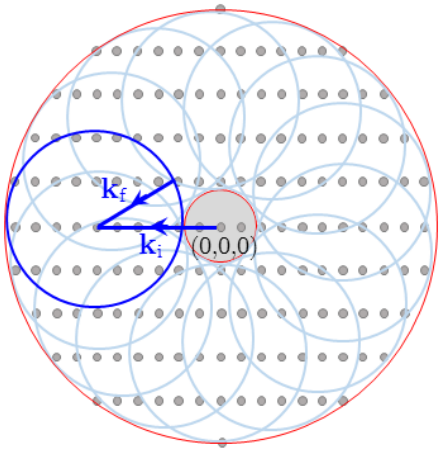
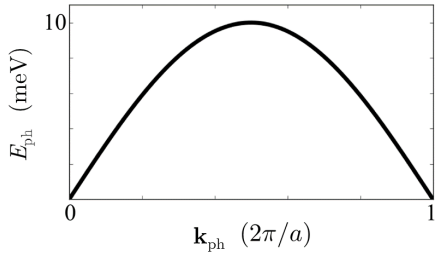


Figure 4: Diagram showing the components of a triple-axis neutron spectrometer. Collimators (c) can be placed at the positions indicated. [Image source: A. T. Boothroyd, *Principles of Neutron Scattering from Condensed Matter*, OUP (2020).]

Unlike elastic scattering (in transmission), it is not possible to access all regions of reciprocal space within a sphere of radius $|2\mathbf{k}_\mathrm{i}|$ (see Lecture 6 notes, Fig. 3). For inelastic scattering $|\mathbf{k}_\mathrm{i}| \neq |\mathbf{k}_\mathrm{f}|$, and so we can access the range $|\mathbf{k}_\mathrm{i}| - |\mathbf{k}_\mathrm{f}| \leq |\mathbf{Q}| \leq |\mathbf{k}_\mathrm{i}| + |\mathbf{k}_\mathrm{f}|$. The diagram below is for energy-loss scattering and shows the kinematically inaccessible region near $(0, 0, 0)$:



The constraints on $|\mathbf{Q}|$ mean that one may have to exploit the periodicity of the phonon dispersion relation in reciprocal space to measure the modes of interest in a Brillouin zone centred about a reciprocal lattice point with $\mathbf{G} \neq 0$.



Take, for example, the zone-boundary phonon $\mathbf{k}_\mathrm{ph} = (\frac{\pi}{a}, 0, 0)$ ($a = 0.5\,\mathrm{nm}$) with energy $E_\mathrm{ph} = 10$ meV on the acoustic dispersion relation shown above, to be measured by energy-loss inelastic neutron scattering. If the neutron beam has an incident energy of $E_\mathrm{i} = 25$ meV, we can determine which $\mathbf{k}_\mathrm{ph} + \mathbf{G}$ points are

accessible. From eqs. (2) and (3),

$$|\mathbf{k}_\mathrm{i}| = \sqrt{\frac{2m_\mathrm{n}E_\mathrm{i}}{\hbar^2}} = 34.7\,\mathrm{nm}^{-1} \quad \text{and} \quad |\mathbf{k}_\mathrm{f}| = \sqrt{\frac{2m_\mathrm{n}(E_\mathrm{i}-E_\mathrm{ph})}{\hbar^2}} = 26.9\,\mathrm{nm}^{-1}$$

therefore

$$|\mathbf{Q}|_\mathrm{min} = 34.7 - 26.9 = 7.8\,\mathrm{nm}^{-1} \quad \text{and} \quad |\mathbf{Q}|_\mathrm{max} = 34.7 + 26.9 = 61.6\,\mathrm{nm}^{-1}$$

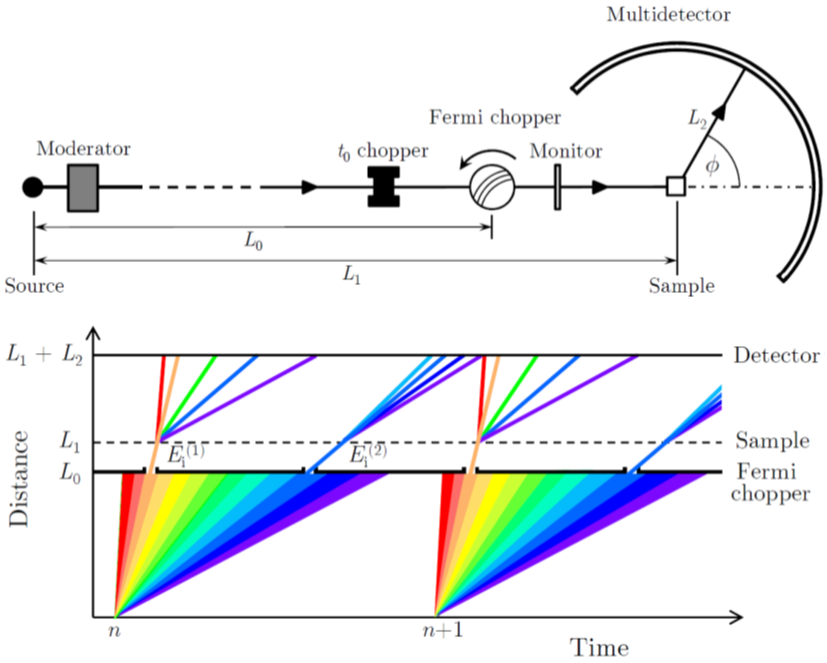
$|\mathbf{k}_\mathrm{ph}| = \pi/a = 6.3\,\mathrm{nm}^{-1}$, $|\mathbf{k}_\mathrm{ph} + (1,0,0)| = 3\pi/a = 18.8\,\mathrm{nm}^{-1}$, $|\mathbf{k}_\mathrm{ph} + (2,0,0)| = 5\pi/a = 31.4\,\mathrm{nm}^{-1}$, etc...

So the boundary of the first Brillouin Zone cannot be accessed, but equivalent points further out in reciprocal space can be accessed.

9.4. Time-of-flight spectroscopy

Triple-axis spectrometers are found on continuous reactor neutron source, such as the Institut Laue–Langevin in Grenoble. Some neutron sources are pulsed, for example the ISIS spallation source located on the Harwell Campus, near Oxford. With this type of source it is technically feasible to time the neutron pulse from the moment it is created to the moment it is detected. For example, a 10 meV neutron of mass $m_\mathrm{n} = 1.6750 \times 10^{-27}$ kg, with a 10 m flight path (neutron instruments are large!) has a flight time of 7 ms.

A schematic of a time-of-flight spectrometer is shown below together with a distance–time diagram of the neutron pulse in the spectrometer. In this instrument a device called a Fermi chopper is used to select a single incident energy. The Fermi chopper is a rotating cylinder containing curved channels that are phased to be open (transmitting) when neutrons with the desired energy arrive. In contrast with the triple-axis spectrometer, the time-of-flight spectrometer measures scattered neutrons with all energies by recording the time of detection, which is then converted into a value for the scattered neutron energy (neutrons that arrive later have transferred more energy to the sample than those that arrive earlier). Large detector arrays measure the scattering over a range of angles simultaneously so that large regions of reciprocal space can be mapped in one setting, making the process very efficient.



In this Lecture we shall consider structural phase transitions characterised by atomic displacements, which result in a low temperature structure that is distorted compared to a higher temperature, higher symmetry structure. Such **displacive** phase transitions are intimately linked to the breaking of symmetry, and hence they can be described in terms of space groups, and measured by diffraction techniques. Moreover, the static distortion that occurs below the phase transition is often associated with an optic phonon mode whose frequency decreases on cooling towards the transition from above. This vibrational mode is called a **soft mode**. The atomic displacements present after a displacive phase transition often produce an electric dipole moment, and if the dipole moment is the same in every unit cell then the crystal exhibits a macroscopic electric polarization. Materials which develop an electric polarization via a displacive phase transition include a large class of insulating crystals called **ferroelectrics**.

10.1 Ferroelectric phase transitions in $PbTiO_3$

At high temperature, lead titanate ($PbTiO_3$) crystallizes in the well known perovskite crystal structure. This structure, which is shown in Fig. 1, has a cubic unit cell with the Pb atoms at the corners, the Ti atoms at the body centre, and the O atoms at the face centres (see Figure 1). At $T_C = 766\,K$, $PbTiO_3$ undergoes a displacive structural phase transition. The O atoms move by a small amount along the z direction, and the Ti atoms move by a small amount in the opposite direction. These atomic displacements break the cubic symmetry of the high temperature phase, and the crystal system becomes tetragonal. The resulting strain causes the lattice to distort and become tetragonal, i.e. $a_c = b_c = c_c \longrightarrow a_t = b_t \neq c_t$, where subscripts c and t refer to the cubic and tetragonal crystal systems, respectively. Because O^{2-} and Ti^{4+} are oppositely charged, the unit cell acquires an electric dipole moment below T_C.

$PbTiO_3$ is an example of a **ferroelectric**. More specifically, a ferroelectric is a material which undergoes a displacive phase transition at T_C (called the Curie temperature) from a structure that does not have a macroscopic electric polarization (**non-polar**) to one that does (**polar**). Moreover, the polarization has the property that it can be reversed by the application of an external electric field. This second property distinguishes ferroelectrics from a class of materials called **pyroelectrics** which have a macroscopic polarization that cannot be reversed by an electric field. At a ferroelectric phase transition the atomic displacements are the same in every unit cell of the crystal, so they are the dielectric analogues of ferromagnets.

One can see by looking at Fig. 1 that the atomic displacements in $PbTiO_3$ generate a net microscopic dipole moment in the unit cell. The centre of mass of the negative charges (O^{2-}) is no longer coincident with the centre of mass of the positive charges (Pb^{2+}, Ti^{4+}). The bulk crystal will therefore exhibit a macroscopic electric polarization, as every unit cell is the same by the translational symmetry of the lattice. The electrical polarization appears spontaneously below T_C, and the material becomes ferroelectric.

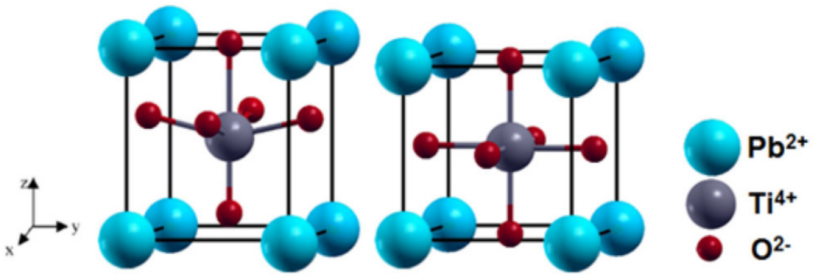


Figure 1: The crystal structure of $PbTiO_3$ above (right) and below (left) the ferroelectric displacive phase transition (n.b. distortions are not drawn to scale).

10.2 Symmetry requirement for ferroelectricity

There are two symmetry requirements in order for a crystal to be ferroelectric. First, the crystal structure must lack a centre of inversion symmetry. This is because if a crystal structure has inversion symmetry, then for any electric dipole moment P in the unit cell there is a moment $-P$ related by the inversion symmetry, giving a net moment of zero. The second requirement is that the crystal must have a one unique direction, in the sense that the direction is not equivalent by symmetry to any other direction.

We can deduce whether a crystal can support a spontaneous electric polarization from the space group of the distorted structure. The high-temperature space group of $PbTiO_3$ is cubic ($Pm3m$), and has 48 symmetry operators including the inversion. At the displacive phase transition 40 of the 48 symmetries are broken, and the crystal space group becomes tetragonal, $P4mm$. Firstly, $P4mm$ does not contain inversion symmetry. Therefore, by symmetry alone we know that it could support a macroscopic polar vector. Secondly, $P4mm$ has a unique axis, the four-fold axis. All other symmetry operators (1, m_x, m_y, m_{xy}, $m_{\bar{x}y}$) leave a polarization parallel to this axis invariant. It is inevitable, therefore, that the polarization will develop along the four-fold axis.

The absence of inversion symmetry is a necessary but not sufficient condition for a space group to allow a spontaneous polarization. For example, $P422$ does not have inversion symmetry, but it also does not have a unique rotation axis. A polarization P_z along the four-fold axis transforms into its inverse $-P_z$ by the two orthogonal two-fold axes, therefore $P_z = 0$ by symmetry.

By applying the two symmetry requirements, one finds a subset of the 32 crystallographic point groups which can support a macroscopic electric polarization. These are: 1, 2, m, $mm2$, 4, $4mm$, 3, $3m$, 6, and $6mm$.

10.3 Domains

In the cubic structure of $PbTiO_3$ there are three 4-fold axes parallel to x, y, and z. At the ferroelectric transition the atomic displacements can in principle occur along any of the three symmetry-equivalent directions, which means that the z axis of the tetragonal structure that forms when $T < T_C$ can be aligned along any one of the cubic x, y, or z axes. This leads to the formation of six domains (positive and negative displacements along x, y, or z).

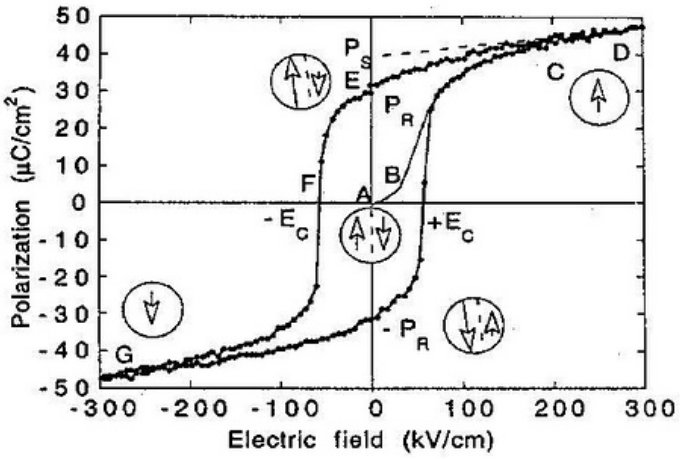


Figure 2: Ferroelectric hysteresis loop

The domains of the distorted structure are related by the symmetry operations that are broken at the phase transition. The number of domains can therefore be calculated by dividing the number of symmetry operators in the high temperature point group by the number of operators in the low temperature point group. For $PbTiO_3$ we get $48/8 = 6$, consistent with the discussion above.

As the atomic displacements are small they can be influenced by an externally applied electric field. In a ferroelectric, the effect of an electric field is to grow domains of one polarisation at the expense of domains of the other, giving rise to ferroelectric hysteresis (analogous to ferromagnetism), as shown in Fig. 2. Hysteresis occurs because energy is dissipated when ferroelectric domains grow or shrink, so the process is irreversible.

10.4 Antiferrodisplacive phase transitions

In a ferroelectric phase transition the atomic displacements in each unit cell are the same, hence the translational symmetry of the lattice is preserved below T_C. This situation is in fact rare. It is more usual for the atomic displacements that develop in one unit cell of the high temperature structure to be balanced by atomic displacements in different directions in neighbouring unit cells. The unit cell of the low temperature structure is then larger which gives rise to a new real-space periodicity, and hence a new direct lattice.

If the atomic displacements create an electric dipole moment which points in opposite directions in neighbouring unit cells then the phase transition is termed **antiferroelectric**. An antiferroelectric is the dielectric analogue of an antiferromagnet. In an antiferroelectric there is an exact cancellation of the electric polarization along opposite directions, so there is zero macroscopic polarization.

Like $PbTiO_3$, $SrTiO_3$ has the cubic perovskite crystal structure at high temperature. Unlike $PbTiO_3$, $SrTiO_3$ undergoes an antiferrodisplacive phase transition at 105 K, as illustrated in Fig. 3. The atomic displacements correspond to a rotation of the TiO_6 octahedra about the z axis, and the sense of rotation alternates in neighbouring unit cells within the xy plane (and also between adjacent unit cells along z). The low temperature crystallographic unit cell is tetragonal with a volume $\sqrt{2} \times \sqrt{2} \times 2$ times larger than the high temperature cubic cell. The basis vectors of the tetragonal cell are given by $[1, 1, 0]$, $[-1, 1, 0]$, and $[0, 0, 2]$ relative to the cubic axes (see Fig. 3). Accordingly, the reciprocal lattice unit cell is $\sqrt{2} \times \sqrt{2} \times 2$ times smaller than that for the undistorted structure.

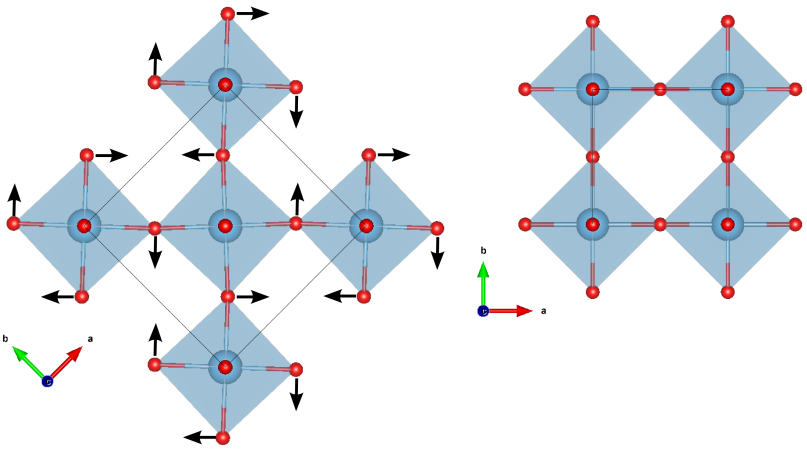


Figure 3: The crystal structure of $SrTiO_3$ below (left) and above (right) the antiferrodisplacive phase transition. Arrows indicate the direction of oxygen displacements compared to the high temperature phase. The Sr atoms are not shown.

At the displacive phase transition the space group symmetry of $SrTiO_3$ is lowered from cubic ($Pm3m$) to tetragonal $I4/mcm$, which has 16 symmetry operations in the primitive unit cell. We therefore expect 48/16 = 3 domains, corresponding to rotation of the TiO_6 octahedra along the x, y, or z axes of the cubic cell.

10.5 Diffraction

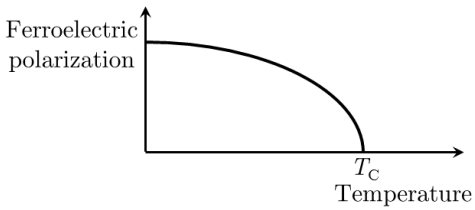
Displacive phase transitions can be observed by diffraction. Figure 4(a) shows the powder diffraction pattern for $SrTiO_3$ in the high temperature cubic phase. Figure 4(b) shows the same pattern but overlaid with the pattern for the low temperature tetragonal phase. The two patterns are similar, but there are two key differences which can be seen in the log intensity plot in Fig. 4(c). One can see that in the low temperature phase additional, well isolated, weak diffraction peaks have appeared, marked with an asterisk. These diffraction peaks arise due to the increase in the direct lattice periodicity, and the respective decrease in the reciprocal lattice periodicity. For example, there are twice as many reciprocal lattice points along the $\mathbf{c}^*$ direction for a crystal with a direct lattice of periodicity $2\mathbf{c}$, compared to a crystal with periodicity $\mathbf{c}$.

The second difference is illustrated in Fig. 5, which shows the 200 reflection above and below the phase transition. Below T_C, the 200 reflection splits into two peaks because the d-spacing of the (002) planes is slightly different from that of the (200) and 020) planes due to the distortion of the lattice from cubic to tetragonal. Moreover, in the cubic phase the multiplicity of the 200 reflection is 6, but in the tetragonal phase the multiplicities of the 200/020 and 002 reflections are 4 and 2, respectively. These multiplicities account for the observed intensity ratio of 2:1. In Fig. 5 the peak splitting has been calculated for a tetragonal lattice parameter ratio $a_t/c_t < 1$. If $a_t/c_t > 1$ then the positions of the split peaks would be reversed.

10.6 The order parameter

The order parameter of a phase transition is some physical quantity which quantifies the progress of the transition. In the case of displacive phase transitions we can use the magnitude of the individual atomic displacements as an order parameter. This is straightforward when the pattern of atomic displacements remains the same at all temperatures below the phase transition, so that all that changes is the magnitude of the displacements.

The order parameter can sometimes be represented as a macroscopic observable. For example, in $PbTiO_3$ the net ferroelectric polarization is directly proportional to the ferroelectric order parameter (see below). In other cases the order parameter can be represented microscopically, for example, the angle of rotation of the TiO_6 octahedra in $SrTiO_3$.



If upon warming out of the low temperature distorted phase the order parameter varies smoothly down to zero at the phase transition, then the transition is known as continuous, or **second order**. If, upon warming, the order parameter abruptly drops to zero at the phase transition, the transition is discontinuous, or **first order**. The names for the phase transitions come from thermodynamics. First and second-order phase transitions correspond to discontinuities in the first or second derivatives of the free energy as a function of temperature. Landau theory (see later in the C3 course) provides a useful phenomenological description of the general properties of first and second order phase transitions.

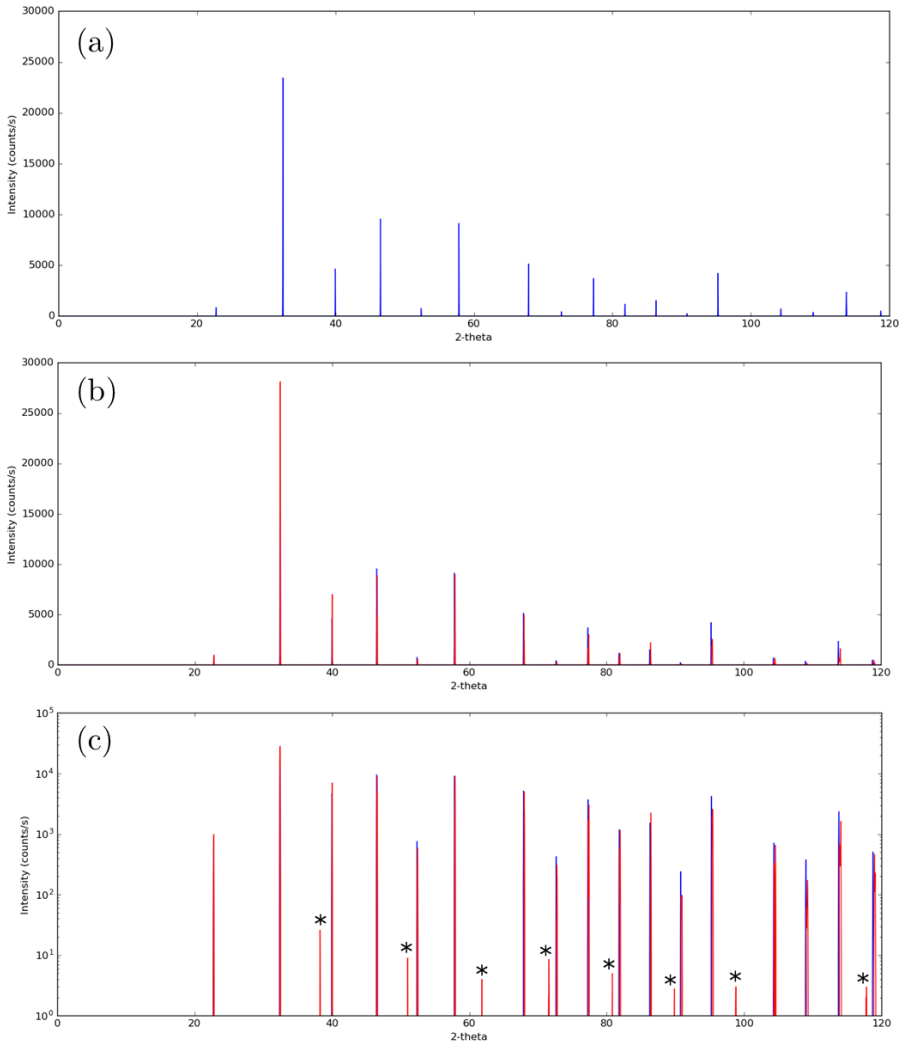


Figure 4: Simulated X-ray powder diffraction patterns for $SrTiO_3$. (a) Cubic phase. (b) Cubic phase (blue) overlaid with the tetragonal phase (red). (c) The same as (b) but plotted on a log scale.

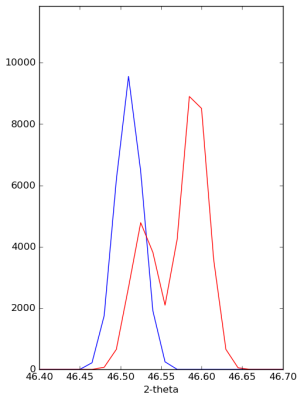
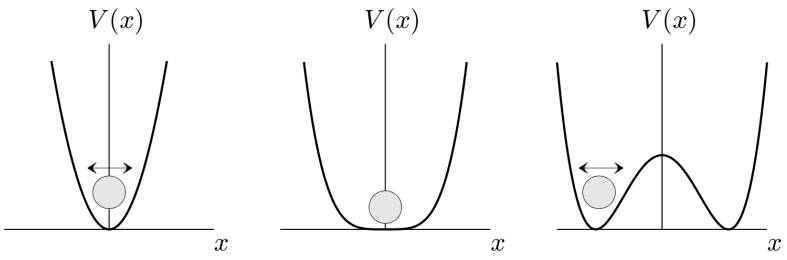


Figure 5: The {200} X-ray powder diffraction peaks of $SrTiO_3$ in cubic (blue) and tetragonal (red) phases.

10.7 Soft phonon modes

If a displacive phase transition occurs in a crystal, then the potential energy of an atom that becomes displaced must change as a function of temperature, as shown schematically below. Above the transition, the potential is symmetric about the equilibrium position of the undistorted structure. Then at the transition itself, the potential must flatten to allow the atom to shift off its initial position. Below the transition the potential has a minimum which is centred on the new position. In a ferroelectric, the electric polarization can be switched by application of an external field so the potential must have a double-well shape.



Now consider the vibrations of the atom about its equilibrium position. The angular frequency of vibration ω of an atom in a quadratic potential $V(x) = \frac{1}{2}\kappa x^2$ is proportional to $\sqrt{\kappa}$, where $\kappa = \mathrm{d}^2V/\mathrm{d}x^2$ is the curvature of the potential. As the sample is cooled towards the transition the curvature must decrease, until at the transition itself the curvature vanishes locally. Hence, ω must decrease on cooling towards T_C, and vanish exactly at T_C. For $T < T_C$, the frequency increases again, but now the atom vibrates about a different equilibrium position.

The structural distortion that appears below T_C corresponds to a frozen version of a vibrational mode of the high temperature crystal structure. The mode in question has the same pattern of atomic displacements as the distortion that appear below T_C. The frequency of this mode reduces, or *softens*, on cooling towards the transition, eventually vanishing at T_C. A mode with this behaviour is called a **soft mode**.

A *ferroelectric* phase transition can be described by the softening of an optic mode with a wavevector at the centre of the Brillouin zone. A wavevector at the zone centre means that the translational symmetry of the lattice is not broken at the phase transition — a phonon with zero momentum has the same periodicity as the lattice, and hence the respective atomic displacements are the same in every unit cell. The fact that the phonon is an optic mode tells us that it is associated with some atoms moving in opposite directions, which gives rise to a net electric dipole moment if the atoms/ions carry different charges.

The softening of a mode with non-zero wavevector will result in a change in the translational symmetry of the lattice below the displacive transition and an increase in the unit cell by an integer multiple of the high temperature cell. For example, the softening of a mode with wavevector $(\frac{1}{2}, 0, 0)$ will result in a doubling of the direct lattice periodicity along **a** (note that the wavevector of the soft mode corresponds exactly to the new set of diffraction peaks observed below the phase transition, discussed above).

The soft mode in $SrTiO_3$ has wavevector $(\frac{1}{2}, \frac{1}{2}, \frac{1}{2})$, which corresponds to the A-point of the tetragonal Brillouin zone (the R-point of the cubic Brillouin zone), which is on the zone boundary. Figure 6 shows the temperature dependence of the soft mode, and Fig. 7 shows the calculated phonon dispersion relations for $SrTiO_3$ at the displacive phase transition. One can see that the optic phonon modes at the A-point, which have moderately high frequencies elsewhere in the Brillouin zone, have softened. In fact, the calculation gives a negative frequency around the A-point, which is unphysical. This reflects the fact that the high temperature crystal structure is no longer stable at the phase transition.

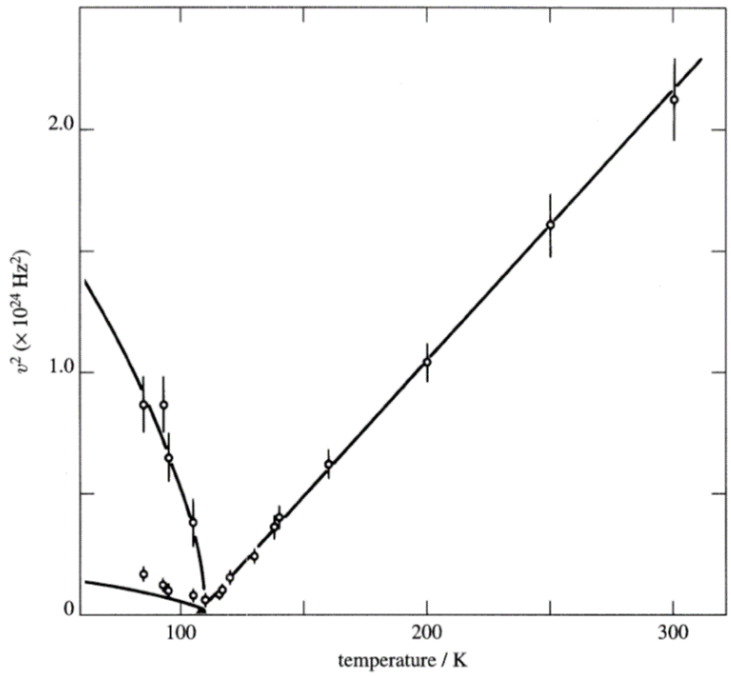


Figure 6: The temperature dependence of the frequencies of the soft mode at wave vector $(\frac{1}{2}, \frac{1}{2}, \frac{1}{2})$ in $SrTiO_3$, both above and below the antiferrodisplacive phase transition temperature 105 K. From R. A. Cowley *et al.*, Solid State Commun. **7**, 181 (1969).

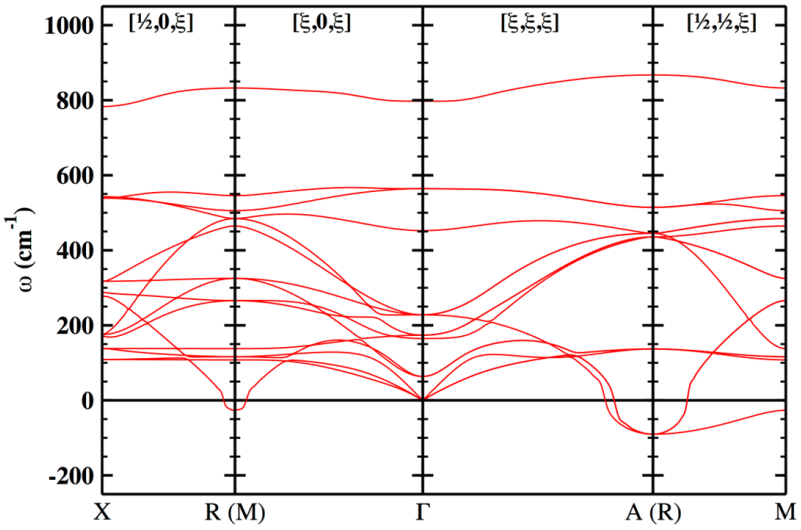


Figure 7: The calculated phonon dispersion for $SrTiO_3$ at the displacive phase transition, plotted along high symmetry directions of the tetragonal Brillouin zone (the corresponding points in the cubic Brillouin zone are shown in brackets). Brillouin diagrams showing the locations of the high symmetry points can be found in Fig. 2 of the lecture notes for Lecture 4.

Symmetry is a powerful concept in physics, providing both a means of classification as well as a tool for making predictions about physical properties without the need for a microscopic model. I begin with an introduction to the types of the symmetries possessed by isolated objects. These are called *point symmetries*. I shall define the *point group*, which provides a classification of an object according to its symmetry. Symmetry transformations will be described both geometrically and mathematically.

1.1 Point symmetry operations

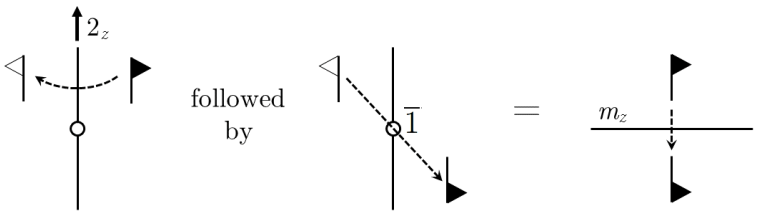
A **symmetry operation** is a transformation that leaves an object looking the same after it has been carried out. The transformation must preserve all attributes of the object. If the new object is indistinguishable from the old object, the object is said to be *invariant* under the symmetry transformation, or *symmetry invariant*.

A **point symmetry operation** is a symmetry operation that leaves at least one point stationary. The point symmetry operations we shall be concerned with are:

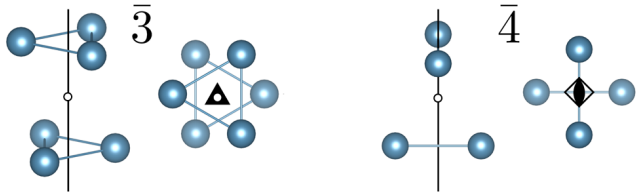
- Rotation (around an axis)
- Inversion (through a point), i.e. $\mathbf{r} \rightarrow -\mathbf{r}$ with the inversion point as the origin
- Rotoinversion (also known as an improper rotation) — a rotation followed by inversion through a point
- Reflection (in a mirror plane)

Each symmetry operation has a corresponding **symmetry element**, which is the axis, point or plane with respect to which the transformation is carried out.

A rotation through an angle of $360°/n$ is denoted by the symbol n (an n-fold rotation), a rotoinversion by the symbol $\overline{n}$, and a reflection by m. Sometimes we shall add a subscript to indicate the axis about which the rotation is made (e.g. 2_z is a rotation through 180° about the z axis), or the normal to a mirror plane (e.g. m_z is a reflection in a mirror plane perpendicular to the z-axis). The inversion ($\overline{1}$) and reflection (m or $\overline{2}$) operations are special cases of rotoinversions through 0° and 180°, respectively. The illustration below demonstrates the equivalence of m_z and $\overline{2}_z$:



Later in the course we shall extend our discussion to the symmetry of the atomic arrangement in crystals. This restricts the set of all point symmetry operations to those which are compatible with an infinite periodic lattice, i.e. those that describe the symmetry of objects that tessellate. In this case we may only have rotations of order 1, 2, 3, 4 or 6, and rotoinversions of order $\overline{1}$, $\overline{2}$, $\overline{3}$, $\overline{4}$ or $\overline{6}$. These 10 symmetry operators are summarised in Supplementary Table 1. The figure below illustrates two rotoinversion operations.



1.2 Transformation matrices

One can represent point symmetry operators as orthogonal matrices in a Cartesian basis. For example, an anticlockwise rotation operation by an angle θ about the z-axis is described by the rotation matrix

$$R_z(\theta) = \begin{pmatrix} \cos\theta & -\sin\theta & 0 \\ \sin\theta & \cos\theta & 0 \\ 0 & 0 & 1 \end{pmatrix}.$$

In other words, if the rotation moves a point P with coordinates (x, y, z) to the point P$'$ with coordinates (x', y', z'), then

$$\begin{pmatrix} x' \\ y' \\ z' \end{pmatrix} = \begin{pmatrix} \cos\theta & -\sin\theta & 0 \\ \sin\theta & \cos\theta & 0 \\ 0 & 0 & 1 \end{pmatrix} \begin{pmatrix} x \\ y \\ z \end{pmatrix},$$

or in suffix notation (summation over repeated indices)

$$q'_i = a_{ij} q_j,$$

where a_{ij} are the components of $R_z(\theta)$.

Alternatively, we can consider P to be a fixed point, and regard $R_z(\theta)$ as a clockwise rotation of the axes by an angle θ. This way, we can apply symmetry transformations to abstract functions:

$$R_z(\theta) f(x, y, z) = g(x', y', z'),$$

This expression means: *find x, y and z in terms of x′, y′ and z′ and substitute into f.*

Example Let R be a clockwise rotation of the coordinates by 45° about the z-axis. Inverting the $R_z(45°)$ matrix, we find

$$\begin{pmatrix} x \\ y \\ z \end{pmatrix} = \begin{pmatrix} \frac{1}{\sqrt{2}} & \frac{1}{\sqrt{2}} & 0 \\ -\frac{1}{\sqrt{2}} & \frac{1}{\sqrt{2}} & 0 \\ 0 & 0 & 1 \end{pmatrix} \begin{pmatrix} x' \\ y' \\ z' \end{pmatrix}.$$

(i) Suppose that

$$f(x, y, z) = (x - y)^2$$

then

$$\begin{aligned} Rf(x, y, z) &= \frac{1}{2}(x' + y' + x' - y')^2 \\ &= 2x'^2 \\ &= g(x', y', z'). \end{aligned}$$

(ii) Now suppose

$$\begin{aligned} f(x, y, z) &= x^2 + y^2 + z^2 \\ \rightarrow \quad Rf(x, y, z) &= x'^2 + y'^2 + z'^2 \\ &= f(x', y', z'). \end{aligned}$$

The transformed function is same as the original function, but of the rotated coordinates (physically, the reason is that $x^2 + y^2 + z^2$ is the distance from the origin to P, which is invariant under rotations). In such cases, we say that *f is invariant under R.*

1.3 More on the rotation and rotoinversion operations

The 10 rotation and rotoinversion operations relevant to crystal symmetry, and the symbols used to denote them on pictures, are listed in Supplementary Table 1. Here we give some further details.

The rotation 1 is known as **the identity**, and the operator is often given the symbol E. This operator maps the object onto itself. The identity operator is represented by the matrix

$$E = \begin{pmatrix} 1 & 0 & 0 \\ 0 & 1 & 0 \\ 0 & 0 & 1 \end{pmatrix}.$$

A rotation axis 2 is present if the object is invariant under a 180° rotation about the axis.

A rotation axis 3 is present if the object is invariant under consecutive 120° rotations about the axis. One must self-consistently define positive and negative rotations, which are labelled 3^+ and 3^-.

Rotation axes 4 and 6. Similarly, these are present if the object is invariant under consecutive 90° or 60° rotations, respectively. One must self-consistently define positive and negative rotations, which are labelled $4^+/4^-$ or $6^+/6^-$.

The rotoinversion point $\overline{1}$ is the point through which an object has inversion symmetry. This element is present if the object is invariant upon transforming every point (x, y, z) into its inverse $(-x, -y, -z)$ about the inversion point (here taken to be at the origin). The inversion operator with inversion point $(0, 0, 0)$ is represented by the matrix

$$\overline{1} = \begin{pmatrix} -1 & 0 & 0 \\ 0 & -1 & 0 \\ 0 & 0 & -1 \end{pmatrix}.$$

The rotoinversion plane $\overline{2}$ is known as the **mirror plane**. As shown earlier, the rotoinversion operation $\overline{2}$ is equivalent to reflection in a mirror plane, and is usually given the symbol m. The matrix representing, for example, $m_z$is

$$m_z = \overline{1} \circ 2_z = \begin{pmatrix} -1 & 0 & 0 \\ 0 & -1 & 0 \\ 0 & 0 & -1 \end{pmatrix} \begin{pmatrix} -1 & 0 & 0 \\ 0 & -1 & 0 \\ 0 & 0 & 1 \end{pmatrix} = \begin{pmatrix} 1 & 0 & 0 \\ 0 & 1 & 0 \\ 0 & 0 & -1 \end{pmatrix}.$$

A rotoinversion point $\overline{3}$ is present if the object is invariant under 120° rotation about an axis combined with inversion through the $\overline{3}$ point. One must self-consistently define positive and negative rotational components $\overline{3}^+$ and $\overline{3}^-$. If + is anticlockwise, then

$$\overline{3}_z^+ \circ \overline{3}_z^+ = \begin{pmatrix} \frac{1}{2} & \frac{\sqrt{3}}{2} & 0 \\ -\frac{\sqrt{3}}{2} & \frac{1}{2} & 0 \\ 0 & 0 & -1 \end{pmatrix} \begin{pmatrix} \frac{1}{2} & \frac{\sqrt{3}}{2} & 0 \\ -\frac{\sqrt{3}}{2} & \frac{1}{2} & 0 \\ 0 & 0 & -1 \end{pmatrix} = \begin{pmatrix} -\frac{1}{2} & \frac{\sqrt{3}}{2} & 0 \\ -\frac{\sqrt{3}}{2} & -\frac{1}{2} & 0 \\ 0 & 0 & 1 \end{pmatrix} = 3_z^-$$

and

$$\overline{3}\circ\overline{3}\circ\overline{3} = \begin{pmatrix} \frac{1}{2} & \frac{\sqrt{3}}{2} & 0 \\ -\frac{\sqrt{3}}{2} & \frac{1}{2} & 0 \\ 0 & 0 & -1 \end{pmatrix} \begin{pmatrix} \frac{1}{2} & \frac{\sqrt{3}}{2} & 0 \\ -\frac{\sqrt{3}}{2} & \frac{1}{2} & 0 \\ 0 & 0 & -1 \end{pmatrix} \begin{pmatrix} \frac{1}{2} & \frac{\sqrt{3}}{2} & 0 \\ -\frac{\sqrt{3}}{2} & \frac{1}{2} & 0 \\ 0 & 0 & -1 \end{pmatrix} = \begin{pmatrix} -1 & 0 & 0 \\ 0 & -1 & 0 \\ 0 & 0 & -1 \end{pmatrix} = \overline{1}.$$

A rotoinversion point $\overline{4}$ is present if the object is invariant under 90° rotation about an axis combined with inversion through the $\bar{4}$ point. Note that

$$\overline{4}_z^+ \circ \overline{4}_z^+ = \begin{pmatrix} 0 & 1 & 0 \\ -1 & 0 & 0 \\ 0 & 0 & -1 \end{pmatrix} \begin{pmatrix} 0 & 1 & 0 \\ -1 & 0 & 0 \\ 0 & 0 & -1 \end{pmatrix} = \begin{pmatrix} -1 & 0 & 0 \\ 0 & -1 & 0 \\ 0 & 0 & 1 \end{pmatrix} = 2_z$$

$$\overline{4}_z^- \circ \overline{4}_z^- = 2_z.$$

A rotoinversion point $\bar{6}$ is present if the object is invariant under 60° rotation about an axis combined with inversion through the $\bar{6}$ point. Note that

$$\overline{6}_z^+ \circ \overline{6}_z^+ = \begin{pmatrix} -\frac{1}{2} & \frac{\sqrt{3}}{2} & 0 \\ -\frac{\sqrt{3}}{2} & -\frac{1}{2} & 0 \\ 0 & 0 & -1 \end{pmatrix} \begin{pmatrix} -\frac{1}{2} & \frac{\sqrt{3}}{2} & 0 \\ -\frac{\sqrt{3}}{2} & -\frac{1}{2} & 0 \\ 0 & 0 & -1 \end{pmatrix} = \begin{pmatrix} -\frac{1}{2} & -\frac{\sqrt{3}}{2} & 0 \\ \frac{\sqrt{3}}{2} & -\frac{1}{2} & 0 \\ 0 & 0 & 1 \end{pmatrix} = 3_z^+$$

Another property of interest is that the combination of an even-order rotation axis and a perpendicular mirror plane produces an inversion point where the axis and plane intersect, e.g.

$$m_z \circ 2_z = \begin{pmatrix} 1 & 0 & 0 \\ 0 & 1 & 0 \\ 0 & 0 & -1 \end{pmatrix} \begin{pmatrix} -1 & 0 & 0 \\ 0 & -1 & 0 \\ 0 & 0 & 1 \end{pmatrix} = \begin{pmatrix} -1 & 0 & 0 \\ 0 & -1 & 0 \\ 0 & 0 & -1 \end{pmatrix} = \overline{1},$$

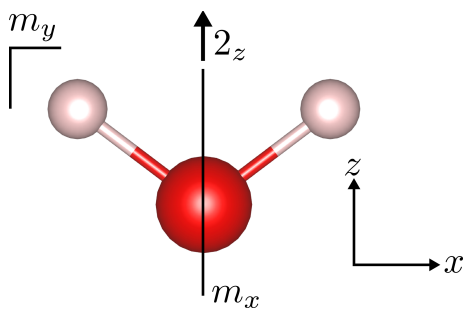
On the other hand, the combination of an odd-order rotation axis and a perpendicular mirror plane does not generate an inversion point, e.g.

$$m_z \circ 3_z^+ = \begin{pmatrix} 1 & 0 & 0 \\ 0 & 1 & 0 \\ 0 & 0 & -1 \end{pmatrix} \begin{pmatrix} -\frac{1}{2} & -\frac{\sqrt{3}}{2} & 0 \\ \frac{\sqrt{3}}{2} & -\frac{1}{2} & 0 \\ 0 & 0 & 1 \end{pmatrix} = \begin{pmatrix} -\frac{1}{2} & -\frac{\sqrt{3}}{2} & 0 \\ \frac{\sqrt{3}}{2} & -\frac{1}{2} & 0 \\ 0 & 0 & -1 \end{pmatrix} = \overline{6}_z^-$$

When both an even-order rotation axis and a perpendicular mirror plane are present this is indicated by the notation $2/m$, $4/m$ or $6/m$, and denoted pictorially by one of three additional symbols (see Supplementary Table 1).

1.4 Point symmetries of molecules

Let's take the water molecule (H_2O) as an example. We define a set of Cartesian axes with x and z in the plane of the molecule, and z parallel to the two-fold rotation axis. There are four symmetry elements, 1 (or E), 2_z, m_x and m_y, as shown below.



1.5 Point groups

We have seen that point symmetry operations can be represented by matrices, and that the process of combining two symmetry operations is equivalent to matrix multiplication. We can summarize all the binary combinations of symmetries of an object in a **multiplication table**. Taking the water molecule as an example, we obtain the following multiplication table:

mm2	E	m_x	m_y	2_z
E	E	m_x	m_y	2_z
m_x	m_x	E	2_z	m_y
m_y	m_y	2_z	E	m_x
2_z	2_z	m_y	m_x	E

Operations in the top row are performed first, and those in left-hand column are performed second. When symmetry elements are combined in this way they form a **point group**.

More generally, a **group** is an algebraic structure comprising a set of elements together with a binary operation which combines the elements in such a way that four **group axioms** are satisfied: *closure*, *associativity*, *identity* and *inverse*. A **point group** is simply a group of point symmetry operators. Binary combination of symmetries is called **composition**. Composition of any two symmetries f and g in the set generates a third symmetry h,

$$f \circ g = h.$$

The symbol $\circ$ is used to denote composition, and the operator to the right is always applied first. The following explains how the group axioms are satisfied:

- **Closure**. Closure means that composition of any two elements in the group always generates an element which is also in the group. This property is summarized in the multiplication table.
- **Associativity**. Composition (or matrix multiplication) has the property

  $$f \circ (g \circ h) = (f \circ g) \circ h,$$

  which is known as *associativity*.
- **Identity**. Every group contains the **identity operator**, E, such that for each operator g

  $$g \circ E = E \circ g = g.$$

- **Inverse**. Every operator g has an **inverse**, g^{-1}, which is also contained in the group:

  $$g \circ g^{-1} = g^{-1} \circ g = E.$$

Although there are an infinite number of point groups, the constraints imposed by periodicity restrict the total number of point groups in crystals to 32. These are the **crystallographic point groups**.

Two further definitions are worth mentioning:

i) A **subgroup** is a subset of elements of a group that is also a group (including, trivially, that the group is a subgroup of itself).

ii) Elements h' and h are **conjugate** if there exists an element g in the same group such that

$$h' = g \circ h \circ g^{-1}$$

Conjugate symmetry elements h and h' in a point group represent the same symmetry element but in different orientations. Hence, conjugation is analogous to a *similarity transformation* in linear algebra. For an element h of a group, its **conjugacy class** is the set of elements $\{h'\}$ that are conjugate to h.

1.6 Point group notation and stereographic projections

Students are expected to be able to represent points, directions and symmetry elements on a stereographic projection, but are not expected to memorize point group notation, assign crystals to point groups, or know the symmetry elements contained in a given point group. Any point group referred to in an examination question will be defined in full.

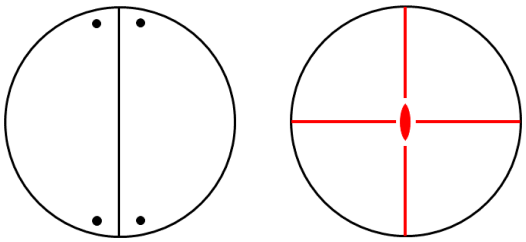
Two systems of notation are in common use to label crystallographic point groups, **Schönflies notation** and **International notation** (or Hermann–Mauguin notation). Here we shall describe the latter.

International point group notation comprises an abbreviated list of symmetry elements of the group. Symmetry elements that belong to the same class are not duplicated, and lower-order elements generated by composition of higher-order elements, for example $2 = 4 \circ 4$ (see above), are not shown explicitly. The ordering of symmetry elements in the point group symbol depends upon the crystal system (see Lecture 2 for the definition of the crystal system). For triclinic and monoclinic crystal systems there is no ambiguity. For the orthorhombic system, the symbols from left to right refer to the x,y,z axes, respectively (it is conventional to place the twofold axis parallel to z in $mm2$). For the tetragonal, trigonal, and hexagonal crystal systems, the highest symmetry axis (for example 4 or $\bar{4}$ in tetragonal) is taken to be parallel to the z axis and is given first, the second symbol, if present, is associated with the symmetry-equivalent x and y axes, and the third symbol, if present, is associated with the axes bisecting x and y. For the cubic case, the first symbol is associated with the symmetry-equivalent x, y, and z axes, the second symbol is associated with the body diagonal (3 or $\bar{3}$), and the third symbol is associated with the face diagonals.

Returning to the water molecule example, one can readily identify the point group as $mm2$. In more complex cases, one can refer to the decision tree given in the next section.

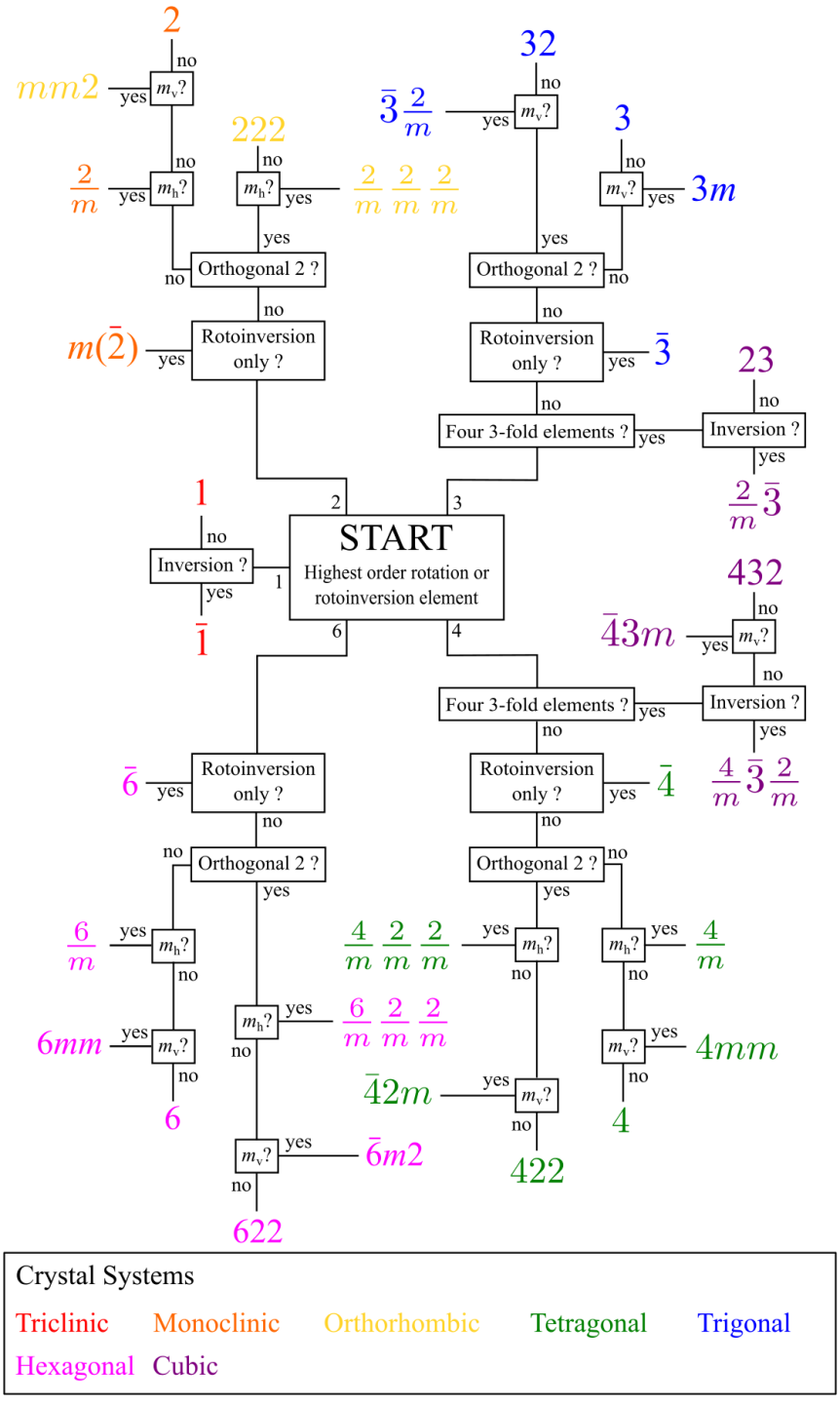
Each point group can be illustrated graphically using a **stereographic projection**. The projection is a mapping of a sphere onto the plane perpendicular to the z axis. The z axis passes through the centre of the projection. The circumference of the projection represents the xy plane. To represent a point on the surface of the sphere in the northern hemisphere, draw a line from the point to the south pole, and mark a filled circle where the line intercepts the equatorial plane. Similarly, points in the southern hemisphere are connected to the north pole and drawn as open circles.

To represent point groups, we construct two stereographic projections side-by-side. On the left, we draw symmetry-equivalent points, where solid and open circles represent points above and below the equatorial plane, respectively. The symmetry elements are drawn in red on the right projection, using the symbols presented in Supplementary Table 1. The stereographic projections for all 32 point groups are shown in Supplementary Table 2. Below we reproduce the stereographic projection of point group $mm2$.



1.7 Determining the point group of a molecule (non-examinable)

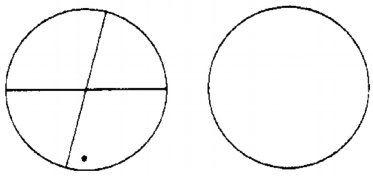
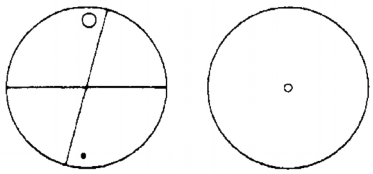
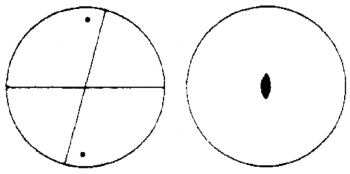
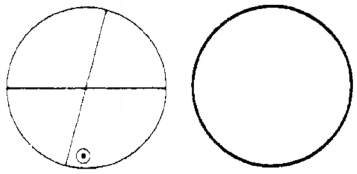
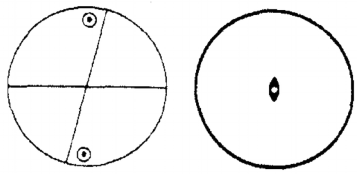
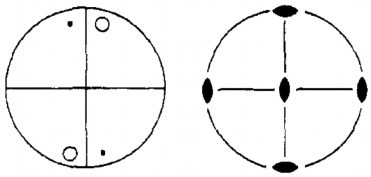
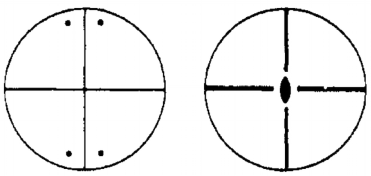
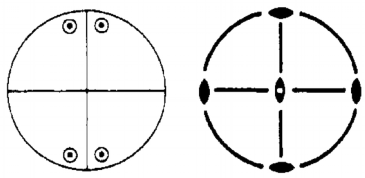
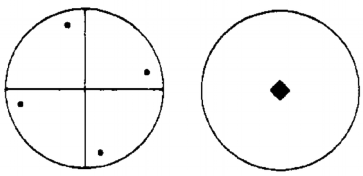
A decision tree for the 32 crystallographic point groups is given below. m_v refers to a mirror plane containing a primary rotation axis, and m_h refers to a mirror plane with a rotation axis normal to it.

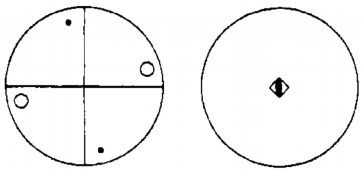
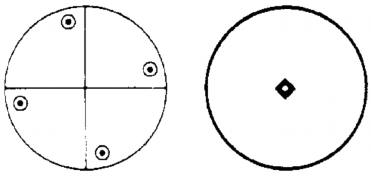
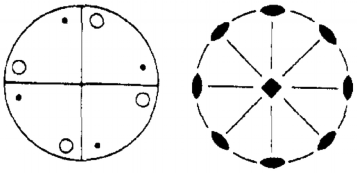
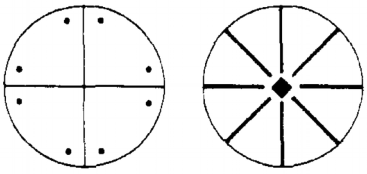
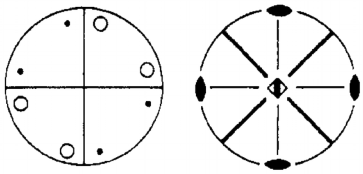
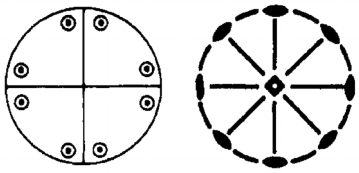
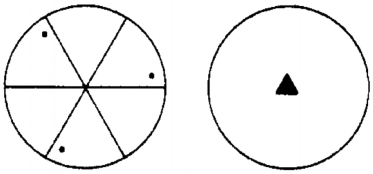
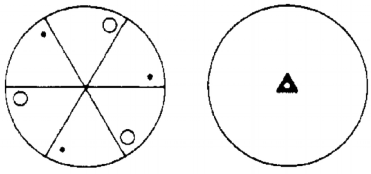
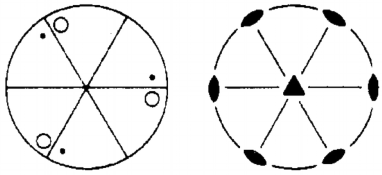


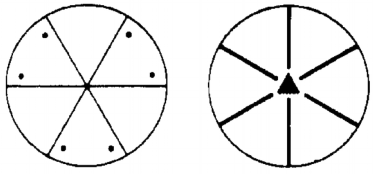
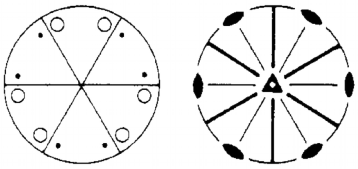
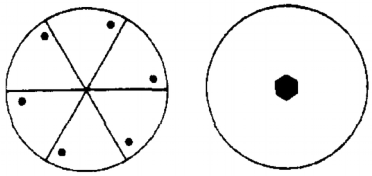
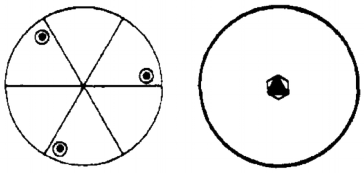
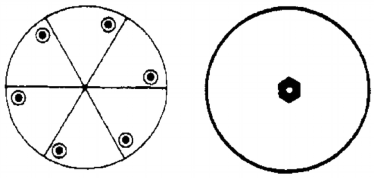
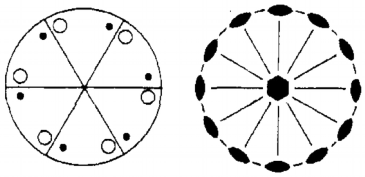
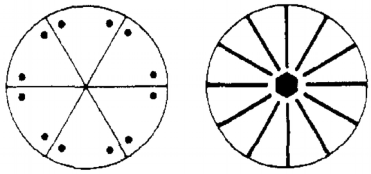
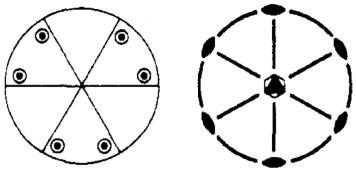
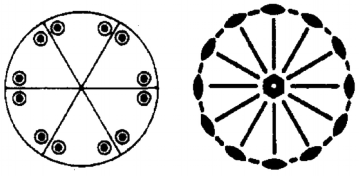
Supplementary Table 1. The 10 symmetry elements of the 32 crystallographic point groups.
Three additional symbols for the 2/m, 4/m, and 6/m symmetries are included, but as they are compositions of symmetry operations they are not given a matrix representation.

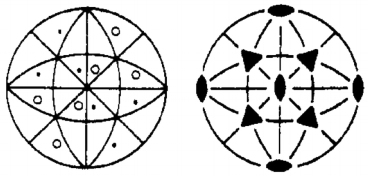
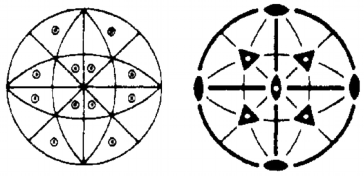
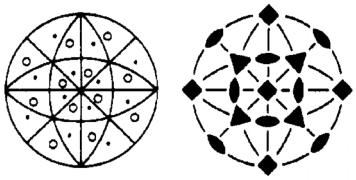
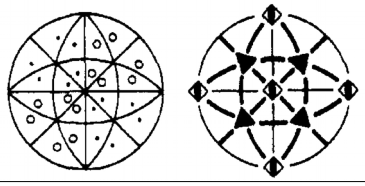
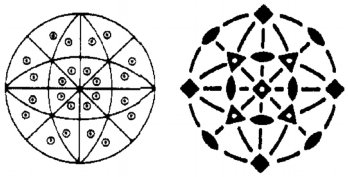
Symmetry element	**Notation**	**Symbol** (from above)	**Symbol** (from side)	**Symmetry operator (Cartesian Matrix)**
Identity	1	*None*	*None*	$\begin{pmatrix} 1 & 0 & 0 \\ 0 & 1 & 0 \\ 0 & 0 & 1 \end{pmatrix}$
Inversion point	$\bar{1}$			$\begin{pmatrix} \bar{1} & 0 & 0 \\ 0 & \bar{1} & 0 \\ 0 & 0 & \bar{1} \end{pmatrix}$
Twofold rotation axis	2			$\begin{pmatrix} \bar{1} & 0 & 0 \\ 0 & \bar{1} & 0 \\ 0 & 0 & 1 \end{pmatrix}$
Mirror plane	$m\ (\bar{2})$			$\begin{pmatrix} 1 & 0 & 0 \\ 0 & 1 & 0 \\ 0 & 0 & \bar{1} \end{pmatrix}$
Threefold rotation axis	3		*None*	$\begin{pmatrix} -0.5 & -\sqrt{3}/2 & 0 \\ \sqrt{3}/2 & -0.5 & 0 \\ 0 & 0 & 1 \end{pmatrix}$ or $\begin{pmatrix} -0.5 & \sqrt{3}/2 & 0 \\ -\sqrt{3}/2 & -0.5 & 0 \\ 0 & 0 & 1 \end{pmatrix}$
Threefold rotoinversion axis and point	$\bar{3}$		*None*	$\begin{pmatrix} 0.5 & \sqrt{3}/2 & 0 \\ -\sqrt{3}/2 & 0.5 & 0 \\ 0 & 0 & \bar{1} \end{pmatrix}$ or $\begin{pmatrix} 0.5 & -\sqrt{3}/2 & 0 \\ \sqrt{3}/2 & 0.5 & 0 \\ 0 & 0 & \bar{1} \end{pmatrix}$
Fourfold rotation axis	4			$\begin{pmatrix} 0 & \bar{1} & 0 \\ 1 & 0 & 0 \\ 0 & 0 & 1 \end{pmatrix}$ or $\begin{pmatrix} 0 & 1 & 0 \\ \bar{1} & 0 & 0 \\ 0 & 0 & 1 \end{pmatrix}$
Fourfold rotoinversion axis and point	$\bar{4}$			$\begin{pmatrix} 0 & 1 & 0 \\ \bar{1} & 0 & 0 \\ 0 & 0 & \bar{1} \end{pmatrix}$ or $\begin{pmatrix} 0 & \bar{1} & 0 \\ 1 & 0 & 0 \\ 0 & 0 & \bar{1} \end{pmatrix}$
Sixfold rotation axis	6		*None*	$\begin{pmatrix} 0.5 & -\sqrt{3}/2 & 0 \\ \sqrt{3}/2 & 0.5 & 0 \\ 0 & 0 & 1 \end{pmatrix}$ or $\begin{pmatrix} 0.5 & \sqrt{3}/2 & 0 \\ -\sqrt{3}/2 & 0.5 & 0 \\ 0 & 0 & 1 \end{pmatrix}$
Sixfold rotoinversion axis and point	$\bar{6}$		*None*	$\begin{pmatrix} -0.5 & \sqrt{3}/2 & 0 \\ -\sqrt{3}/2 & -0.5 & 0 \\ 0 & 0 & \bar{1} \end{pmatrix}$ or $\begin{pmatrix} -0.5 & -\sqrt{3}/2 & 0 \\ \sqrt{3}/2 & -0.5 & 0 \\ 0 & 0 & \bar{1} \end{pmatrix}$
Extra symbols:				
Twofold rotation axis with inversion centre	$2/m$		*None*	N/A
Fourfold rotation axis with inversion centre	$4/m$		*None*	N/A
Sixfold rotation axis with inversion centre	$6/m$		*None*	N/A

Supplementary Table 2. The 32 crystallographic point groups
The point groups have been listed according to their crystal system. In the left hand stereographic projection, the solid and open circles represent symmetry equivalent points that are above and below the pane, respectively.

Crystal system	Point group	Stereographic projection
Triclinic	1	
	$\bar{1}$	
Monoclinic	2	
	$m(\bar{2})$	
	$\frac{2}{m}$	
Orthorhombic	222	
	$mm2$	
	$\frac{2}{m}\frac{2}{m}\frac{2}{m}$	
Tetragonal	4	

Crystal system	Point group	Stereographic projection
Tetragonal cont.	$\bar{4}$	
	$\frac{4}{m}$	
	422	
	$4mm$	
	$\bar{4}2m$	
	$\frac{4}{m}\frac{2}{m}\frac{2}{m}$	
Trigonal	3	
	$\bar{3}$	
	32	

Crystal system	Point group	Stereographic projection
Trigonal cont.	$3m$	
	$\bar{3}\frac{2}{m}$	
Hexagonal	6	
	$\bar{6}$	
	$\frac{6}{m}$	
	622	
	$6mm$	
	$\bar{6}m2$	
	$\frac{6}{m}\frac{2}{m}\frac{2}{m}$	

Crystal system	Point group	Stereographic projection
Cubic	23	
	$\frac{2}{m}\bar{3}$	
	432	
	$\bar{4}3m$	
	$\frac{4}{m}\bar{3}\frac{2}{m}$	

In the last lecture I considered the symmetry of isolated objects, such as individual molecules. In this lecture, we turn our attention to three-dimensional crystals, i.e. materials with periodic arrangements of atoms. To describe the structure and symmetry of crystals we must introduce the concepts of *translational symmetry*.

2.1 The crystal lattice and basis

A crystal is a periodic structure built from a large number of identical units that stack together to fill space. The underlying periodicity, or *translational symmetry*, is represented by a **lattice**, which is a periodic array of points such that each point is in an identical environment. A lattice may be generated mathematically by

$$\mathbf{R} = n_1\mathbf{a}_1 + n_2\mathbf{a}_2 + n_3\mathbf{a}_3, \tag{1}$$

where $\mathbf{R}$ represents the position vector of a lattice point with respect to some arbitrarily-chosen origin which is also a lattice point; $\mathbf{a}_1$, $\mathbf{a}_2$ and $\mathbf{a}_3$ are three non-coplanar vectors known as *primitive lattice vectors* or *lattice translation vectors*; and n_1, n_2 and n_3 are integers.

The first correct enumeration of all possible types of lattice was presented by Bravais (Auguste Bravais, 1811–1863) in around 1848. He showed that there are only 14 distinct lattice types in three dimensions. These are known as the **Bravais lattices**. In two dimensions there are only 5 distinct lattice types. Details of the geometry of the Bravais lattices is given in Supplementary Material 1.

The arrangement of atoms associated with a lattice point is the fundamental repeating unit of the crystal and is known as the **basis** or **motif**. Since every lattice point is in an identical environment, a knowledge of the lattice type together with the basis specifies the crystal structure completely.

2.2 The unit cell

A **unit cell** is a fundamental building block of a crystal. When many identical unit cells are stacked together they fill space completely and generate the whole crystal. For a given crystal structure there are many different choices of unit cell. The smallest possible unit cells contain only one lattice point and are known as **primitive** unit cells. By 'contain only one lattice point' we mean that the number of unit cells in the crystal is equal to the number of lattice points.

Primitive unit cells do not always have a regular shape, and sometimes it is possible to construct a larger unit cell with a simpler geometry. This latter type of unit cell, called a **conventional** unit cell, is often employed in preference to a primitive cell in order to make calculations easier.

Whether primitive or conventional, the unit cell often takes the form of a **parallelepiped**, as shown in Fig. 1. The cell has basis vectors $\mathbf{a}$, $\mathbf{b}$ and $\mathbf{c}$ (not necessarily the same as the primitive lattice vectors $\mathbf{a}_1$, $\mathbf{a}_2$, $\mathbf{a}_3$) with angles of α, β, γ between them, as indicated. The lengths of $\mathbf{a}$, $\mathbf{b}$, $\mathbf{c}$, together with the angles α, β, γ, are known as the **cell parameters**. The cell volume is given by

$$v_0 = \mathbf{a}\cdot\mathbf{b}\times\mathbf{c} = \mathbf{b}\cdot\mathbf{c}\times\mathbf{a} = \mathbf{c}\cdot\mathbf{a}\times\mathbf{b}. \tag{2}$$

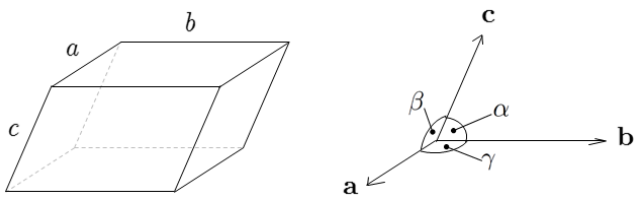


Figure 1: Geometry and cell parameters for a parallelepiped unit cell.

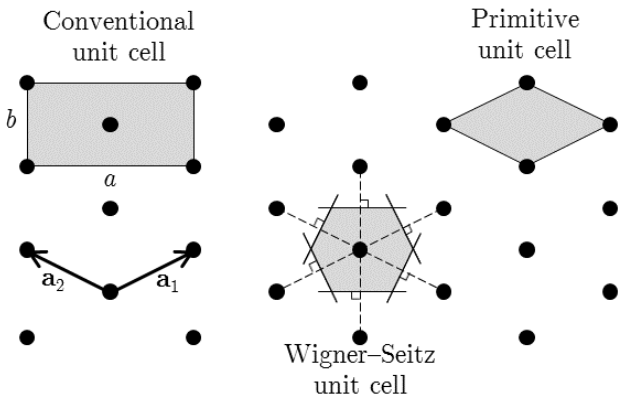


Figure 2: The two-dimensional body-centred rectangular lattice, showing two different primitive unit cells and the conventional rectangular (non-primitive) unit cell.

The use of a conventional unit cell is illustrated in Fig. 2 for the two-dimensional body-centred rectangular lattice generated by primitive lattice vectors $\mathbf{a}_1$ and $\mathbf{a}_2$. Two primitive unit cells are shown, together with the rectangular conventional unit cell of dimensions $a \times b$. The latter is seen to contain two lattice points. One of the primitive unit cells shown is the **Wigner–Seitz cell**. This cell is defined to be the area (volume in three dimensions) enclosed by the set of planes that perpendicularly bisect the vectors from the origin to the neighbouring lattice points. The Wigner–Seitz cell has the same symmetry as the lattice, and is best known in the context of wave propagation in crystals, where it is used to define the first Brillouin zone.

2.3 Crystal symmetry

In the classification of crystals we refer to two types of symmetry, *point symmetry* and *translational symmetry*. Translational symmetry is used to specify the lattice type, and point symmetry is used to classify crystals into **crystal systems**.

There are seven crystal systems in total, six of which have the same names as the corresponding Bravais lattices: *triclinic, monoclinic, orthorhombic, tetragonal, hexagonal* and *cubic*. For example, cubic crystals always have one of the three cubic lattice types: cubic P (primitive), cubic I (body-centred) or cubic F (face-centred). The seventh crystal system is the *trigonal* system. Rather confusingly, trigonal crystals can have either the rhombohedral R lattice or the hexagonal P lattice. Table 1 lists the defining point symmetry and conventional unit cell parameters for each of the seven crystal systems, together with the lattice types compatible with each crystal system.

The non-primitive conventional unit cells detailed in Table 1 are known as *centred* cells, because in addition to lattice points at the corners of the cell there are lattice points located either (i) in the centre of the cell (in the case of the I lattices), or (ii) in the centre of one or more of the faces of the cell (for A, B, C and F lattices), or (iii) in the case of the hexagonal R lattice, the R-centred cell has two lattice points along the body diagonal. The A, B and C cells are base-centred, which means they have a lattice point at the centre of two opposite faces only. The F cell is all-face-centred.

Table 2 gives, for each type of centring, the translations of these additional lattice points relative to the lattice point at the origin of the cell. Each crystal system has a primitive unit cell plus any centred cells that are compatible with the symmetry of the crystal system. Taken together, one finds 14 unique 3D lattices — these are the 14 Bravais lattices (see Supplementary Material 1).

Table 1: Point group symmetry, conventional unit cell, and lattice types for the seven crystal systems.

Crystal system	**Defining point symmetry**	**Conventional unit cell**	**Lattice types**
Triclinic	One 1 or $\bar{1}$	$a \neq b \neq c;\ \alpha \neq \beta \neq \gamma$	P
Monoclinic	One 2 or $m(\bar{2})$	$a \neq b \neq c;\ \alpha = \gamma = 90°, \beta > 90°$	P, C(A)
Orthorhombic	Three orthogonal 2 or $m(\bar{2})$	$a \neq b \neq c;\ \alpha = \beta = \gamma = 90°$	P, C(A,B), I, F
Tetragonal	One 4 or $\bar{4}$	$a = b \neq c;\ \alpha = \beta = \gamma = 90°$	P, I
Trigonal[a]	One 3 or $\bar{3}$	$a = b = c;\ \alpha = \beta = \gamma \neq 90°$	R
		$a = b \neq c;\ \alpha = \beta = 90°, \gamma = 120°$	P
Hexagonal[b]	One 6 or $\bar{6}$	$a = b \neq c;\ \alpha = \beta = 90°, \gamma = 120°$	P
Cubic	Four 3 or $\bar{3}$	$a = b = c;\ \alpha = \beta = \gamma = 90°,$	P, I, F

[a] Trigonal crystals can have either the rhombohedral R lattice or the hexagonal P lattice

[b] A rhombohedral (R) cell with $a = b = c;\ \alpha = \beta = \gamma \neq 90°$ is also used for hexagonal crystals.
For hexagonal crystals, the R cell contains 3 lattice points with fractional coordinates $0, 0, 0;\ \frac{2}{3}, \frac{1}{3}, \frac{1}{3};\ \frac{1}{3}, \frac{2}{3}, \frac{2}{3}$, whereas for trigonal systems the R cell is primitive.

2.4 Fractional coordinates, directions and planes

There are internationally agreed conventions to define the notation used to describe the geometry of crystals, and we shall adhere to them in this course.

The coordinates of an atom in the unit cell are given as fractions of the cell parameters, so x, y, z (no parentheses) represents an atom displaced from the origin by $\mathbf{r} = x\mathbf{a} + y\mathbf{b} + z\mathbf{c}$. For example, an atom right in the centre of the unit cell would have fractional coordinates $\frac{1}{2}, \frac{1}{2}, \frac{1}{2}$.

Crystallographic directions are indicated by a vector written as $[uvw]$ corresponding to $u\mathbf{a} + v\mathbf{b} + w\mathbf{c}$. Crystallographic planes are represented by their Miller indices. The Miller indices (hkl) describe a set of parallel planes such that if one of the planes passes through the origin then an adjacent plane intersects the **a**, **b** and **c** axes at a/h, b/k and c/l, respectively (see Fig. 3).

2.5 Symmetry operators of a 3D crystal

The translational symmetry of the lattice is represented by an infinite set of **translational symmetry operators**, written as column vectors in the basis of the lattice. The translation operators form a group, but unlike the point group, the translational group of a crystal is *infinite*.

Table 2: Centring translations for the different types of centred cells.

Centring type	**Description**	**Centring translation**
A	Base-centred in bc-plane	$(0, \frac{1}{2}, \frac{1}{2})$
B	Base-centred in ac-plane	$(\frac{1}{2}, 0, \frac{1}{2})$
C	Base-centred in ab-plane	$(\frac{1}{2}, \frac{1}{2}, 0)$
F	All-face-centred	$(\frac{1}{2}, \frac{1}{2}, 0)$ and $(\frac{1}{2}, 0, \frac{1}{2})$ and $(0, \frac{1}{2}, \frac{1}{2})$
I	Body-centred	$(\frac{1}{2}, \frac{1}{2}, \frac{1}{2})$
R	Rhombohedral centring	$(\frac{2}{3}, \frac{1}{3}, \frac{1}{3})$ and $(\frac{1}{3}, \frac{2}{3}, \frac{2}{3})$

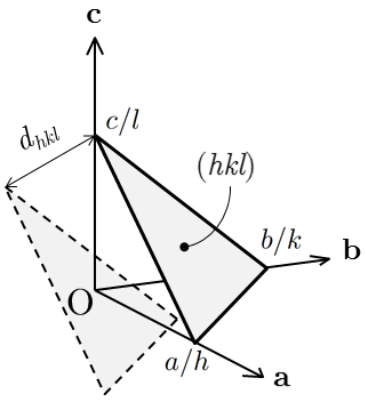


Figure 3: Representation of crystal planes by Miller indices (hkl). The inter-planar spacing is given by d_{hkl}.

We represented the symmetry operators of the molecular point groups as orthogonal matrices. As is the case for translation operators, we will now represent the rotation and rotoinversion operators as matrices in the *basis of the lattice*. For example, the symmetry operation 3_z in a Cartesian basis is:

$$\begin{pmatrix} -\frac{1}{2} & -\frac{\sqrt{3}}{2} & 0 \\ \frac{\sqrt{3}}{2} & -\frac{1}{2} & 0 \\ 0 & 0 & 1 \end{pmatrix}$$

which, in a hexagonal crystal basis with **a** and **b** 120° apart, is simplified to:

$$\begin{pmatrix} 0 & -1 & 0 \\ 1 & -1 & 0 \\ 0 & 0 & 1 \end{pmatrix}.$$

Not only does the crystal symmetry group contain an infinite set of translation operators, it will also contain an infinite set of rotations and rotoinversion operators (should they exist) related by translational symmetry. As every unit cell is identical, however, we need only consider the rotation and rotoinversion operators of a single unit cell.

Unlike in molecular point groups, the 'point' symmetry elements of a crystal do not intersect at a single point. We must therefore define the position of the rotation or rotoinversion symmetry elements within the unit cell by including a set of fractional coordinates in the notation. For example, 2 $[0, 0, z]$ is a twofold rotation about an axis which is parallel to $[0, 0, z]$ and passes through the origin.

Any **symmetry operation can be written as a rotational component plus a translational component**. Consider, for example, 2 [1/2, 0, z] operating on an atom with fractional coordinates x, y, z.

Step 1: Translate x, y, z by a vector that brings the symmetry operation to the origin:

$$\begin{pmatrix} x \\ y \\ z \end{pmatrix} - \begin{pmatrix} 1/2 \\ 0 \\ 0 \end{pmatrix}$$

Step 2: Perform rotation about the origin (2_z is in the basis of the lattice):

$$2_z \left[\begin{pmatrix} x \\ y \\ z \end{pmatrix} - \begin{pmatrix} 1/2 \\ 0 \\ 0 \end{pmatrix} \right]$$

Step 3: Translate back to arrive at the final position x', y', z':

$$\begin{pmatrix} x' \\ y' \\ z' \end{pmatrix} = 2_z \left[\begin{pmatrix} x \\ y \\ z \end{pmatrix} - \begin{pmatrix} 1/2 \\ 0 \\ 0 \end{pmatrix} \right] + \begin{pmatrix} 1/2 \\ 0 \\ 0 \end{pmatrix}$$

In general, if a symmetry operator, R, is located at x_0, y_0, z_0, the symmetry operation can be written:

$$\begin{aligned} \begin{pmatrix} x' \\ y' \\ z' \end{pmatrix} &= R \left[\begin{pmatrix} x \\ y \\ z \end{pmatrix} - \begin{pmatrix} x_0 \\ y_0 \\ z_0 \end{pmatrix} \right] + \begin{pmatrix} x_0 \\ y_0 \\ z_0 \end{pmatrix} \\ &= R \begin{pmatrix} x \\ y \\ z \end{pmatrix} + \left[\begin{pmatrix} x_0 \\ y_0 \\ z_0 \end{pmatrix} - R \begin{pmatrix} x_0 \\ y_0 \\ z_0 \end{pmatrix} \right], \end{aligned} \tag{3}$$

where, on the second line, the first term is a rotation, and the second term is a translation.

The combination of translation and point symmetry operations generates other symmetry elements. Take, for example, an atom at x, y, z and suppose the crystal has an inversion centre at 0,0,0. The inversion generates an atom at $-x, -y, -z$, which has an equivalent position at $-x+1, -y, -z$ through translation by the lattice vector **a**, i.e.,

$$\begin{aligned} \begin{pmatrix} -x+1 \\ -y \\ -z \end{pmatrix} &= \overline{1} \begin{pmatrix} x \\ y \\ z \end{pmatrix} + \begin{pmatrix} 1 \\ 0 \\ 0 \end{pmatrix} \\ &= \overline{1} \begin{pmatrix} x \\ y \\ z \end{pmatrix} + \left[\begin{pmatrix} 1/2 \\ 0 \\ 0 \end{pmatrix} - \overline{1} \begin{pmatrix} 1/2 \\ 0 \\ 0 \end{pmatrix} \right] \end{aligned} \tag{4}$$

By comparison with the general expression in eq. (3), we see that an inversion about the origin plus a translation through **a** is equivalent to an inversion through the point $1/2, 0, 0$. Extending to 3D, if a unit cell has an inversion centre at the origin, it will also have inversion centres at $1/2, 0, 0$; $0, 1/2, 0$; $0, 0, 1/2$; $1/2, 1/2, 0$; $1/2, 0, 1/2$; $0, 1/2, 1/2$ and $1/2, 1/2, 1/2$ by lattice translations to all nearest-neighbour lattice points of $0, 0, 0$.

2.6. Screw axes and glide planes

In addition to pure rotations (or rotoinversions) and pure translations, two other symmetry operations may be present in 3D crystals. These arise when the translational part of the symmetry operator is *parallel* to the rotational component, and in this case the symmetry elements are known as **roto-translations**. The following conditions must be satisfied:

a) The rotational operator is either 2, 3, 4, 6 or m, and is always applied first.
b) The translational part is equal to a lattice vector divided by the order n of the rotational part.

These two conditions ensure that application of the roto-translation n times generates a pure lattice vector, so preserving the translational symmetry of the lattice.

Roto-translations that incorporate a rotation operator (2, 3, 4, or 6) are known as **screw axes**, and roto-translation that incorporate a mirror, m, are known as **glide planes** (see Supplementary Material 2).

2.7 The 230 crystallographic space groups

Students are not expected to memorize space group notation, assign crystals to space groups, or know the symmetry elements contained in a given space group. Any space group referred to in an examination question will be defined in full. Diagrams showing the symmetry elements of all the space groups can be found at http://img.chem.ucl.ac.uk/sgp/mainmenu.htm.

A **space group** is a set of symmetry operators which satisfy the axioms of a group under composition, and which leave a 3D crystal structure (lattice + basis) invariant. There are 230 crystallographic space groups, and their properties may be perused in great detail in the International Tables for Crystallography, Volume A, published by the International Union of Crystallography (IUCr) through Wiley.

The space group notation is similar to the point group notation defined in Lecture 1. The space group symbol begins with a capital letter that denotes the lattice centring. This letter is followed by the symbols of the rotation, rotoinversion, or roto-translation operators. The order of the symbols follows the same convention as for point group notation. Take orthorhombic $Pmc2_1$ for example:

P: Primitive lattice
m: Mirror with a-axis normal
c: Glide (mirror with b-axis normal then translate along c
2_1: Two-fold screw axis parallel to c

If a space group does not include roto-translations, there will be a point in the unit cell that is invariant under all rotation or rotoinversion symmetry operations. In this case the space group is known as **symmorphic**, and the point group symbol is found explicitly in the space group symbol. E.g. space group $P2/m$ has point group $2/m$. A **non-symmorphic** space group does include roto-translations and has no invariant point in the unit cell. We still associate a point group with non-symmorphic space groups, though. It is found by neglecting the translational part of the roto-translations. E.g. space group $Pmc2_1$ has point group $mm2$.

The **origin choice** of the lattice is arbitrary, so we must decide for ourselves where to place it with respect to the symmetry elements of the space group. If inversion centres exist we normally choose the origin to coincide with one of them. There is an advantage in doing so as it simplifies structure factor calculations (see Lectures 3 and 5).

We illustrate the space group using the same symmetry element symbols defined in Lecture 1, located on planar projections of the unit cell (see Figure 4).

2.8 Wyckoff positions

General positions are *symmetry-equivalent* positions generated by individually applying all rotation, rotoinversion, roto-translation, and lattice centring symmetry operators of the space group to the *general* fractional coordinates x, y, z. Accordingly, there are as many symmetry-equivalent general positions as there are symmetry elements in the point group, times the number of centring translations [including $(0, 0, 0)$].

Special positions are positions that intersect a rotation or rotoinversion symmetry element of the space group. Atoms are often found at these 'high-symmetry' positions, which are known as **Wyckoff sites**. The number of symmetry-equivalent positions for a given Wyckoff site is known as the **site multiplicity**. We can assign a **site point group** to each Wyckoff site (not to be confused with the point group of the crystal structure), and the site multiplicity can be calculated by dividing the number of symmetry elements in the crystal point group by the number of symmetry elements in the site point group. Note that the general position is also a Wyckoff site, that with the highest possible multiplicity.

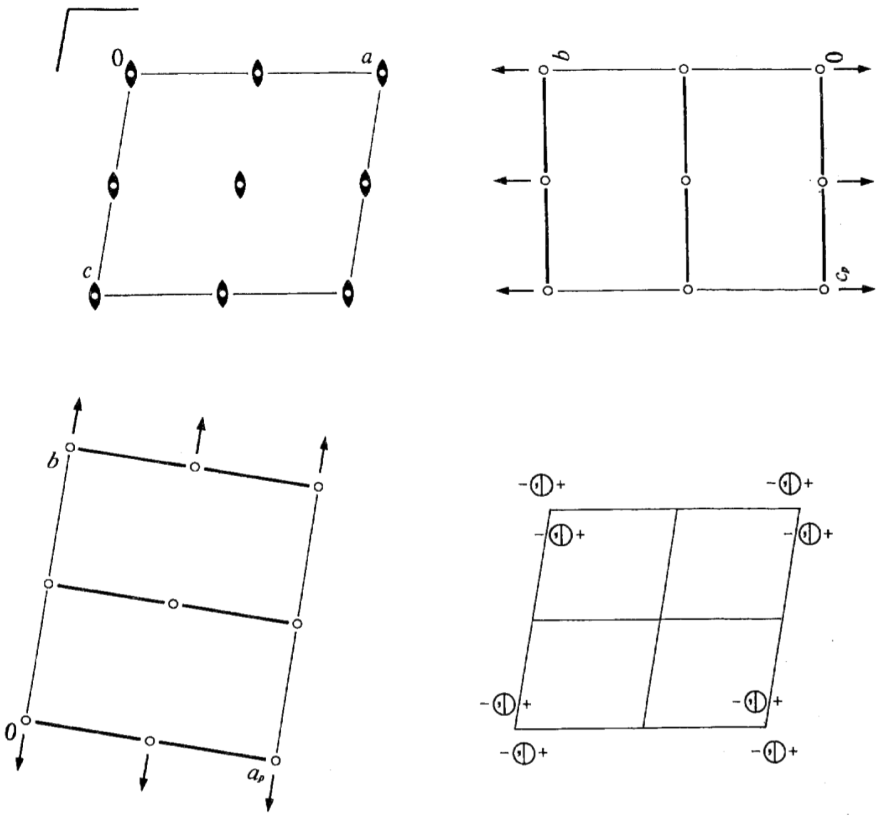
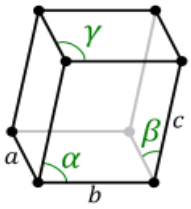


Figure 4: Space group diagram for $P2/m$. The upper and lower left diagrams show the symmetry elements of the space group in projection down the b-, a- and c-axes, respectively. The lower right diagram shows the symmetry-equivalent positions for a general point.

Supplementary Material 1: The 14 Bravais lattices

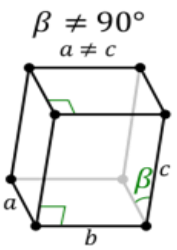
Image source: Wikipedia

Triclinic

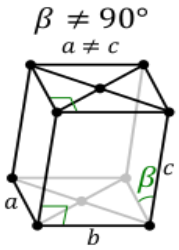


P

Monoclinic

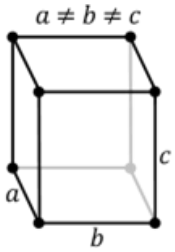


P

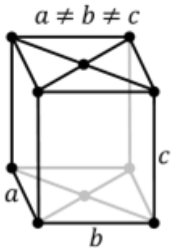


C

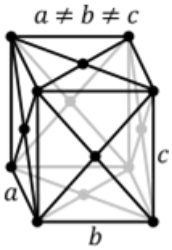
Orthorhombic



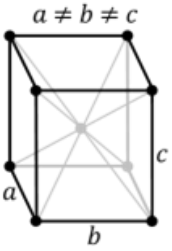
P



C

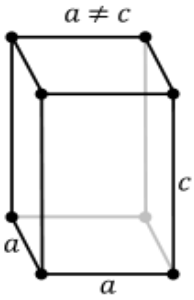


F

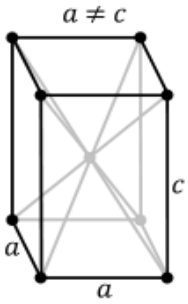


I

Tetragonal

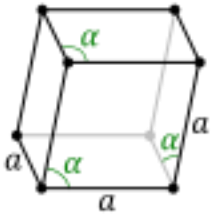


P



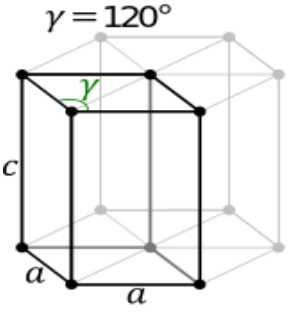
I

Rhombohedral



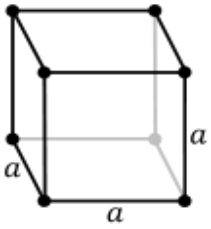
R

Hexagonal

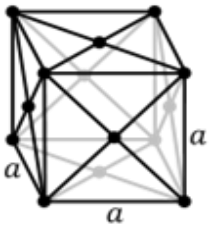


P

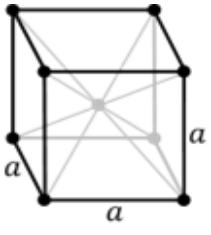
Cubic



P



F

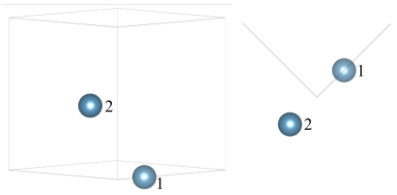
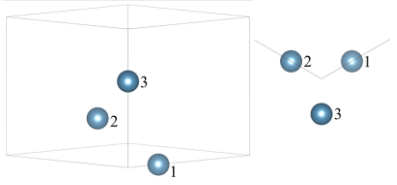
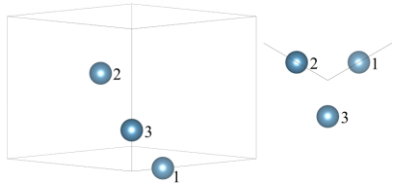
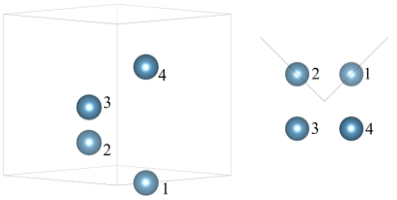
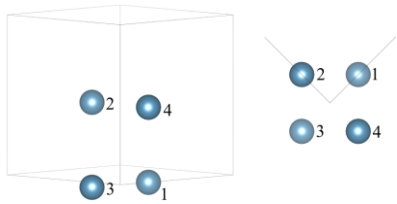
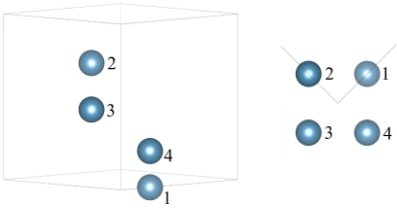


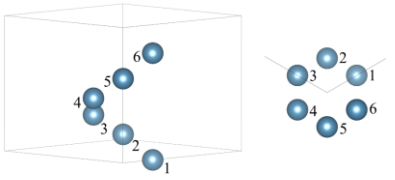
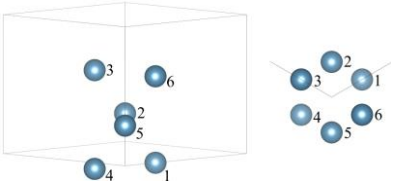
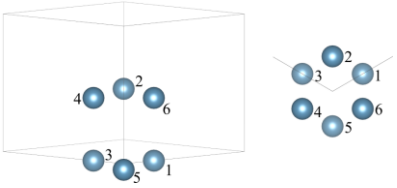
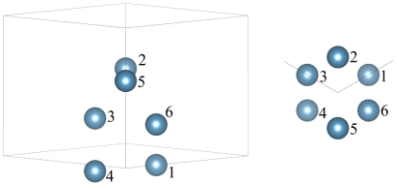
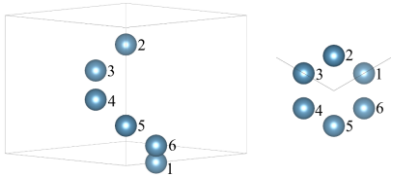
I

Supplementary Material 2: Roto-translations

(i) Screw axes [enantiomorphs (mirror images) are noted in parentheses]

First rotate about axis R, then translate along screw vector **T** = [0, 0, *t*] || R-axis

Label	R	*t*	Sketch
2_1	2^+	1/2	
3_1 (3_2)	3^+	1/3	
3_2 (3_1)	3^+	2/3	
4_1 (4_3)	4^+	1/4	
4_2	4^+	1/2	
4_3 (4_1)	4^+	3/4	

Label	R	*t*	Sketch
6_1 (6_5)	6^+	1/6	
6_2 (6_4)	6^+	1/3	
6_3	6^+	1/2	
6_4 (6_2)	6^+	2/3	
6_5 (6_1)	6^+	5/6	

(ii) Glide planes

First reflect in the mirror plane *m*, then 'glide' along **T**.

Label	*m*	**T**	Notes
a	[*x*, *y*, 0] or [*x*, 0, *z*]	(½, 0, 0)	
b	[*x*, *y*, 0] or [0, *y*, *z*] or [*x*, *x*, *z*]	(0, ½, 0)	
c	[*x*, 0, *z*] or [0, *y*, *z*]	(0, 0, ½)	
n	[*x*, *y*, 0] or [*x*, *x*, *z*]	(½, ½, 0)	Plus symmetry equivalents
d	[*x*, *y*, 0] [*x*, *x*, *z*]	(¼, ¼, 0) (¼, ¼, ¼)	Plus symmetry equivalents. Cubic and tetragonal, F and I centred lattices only.

In this lecture, we develop a formal description of the reciprocal lattice, which is an essential tool for understanding the properties of crystal vibrations and the symmetry of electronic band structure (Lecture 4), and provides important insights into the interpretation of scattering experiments used to measure the structure and dynamics of crystals (Lectures 5, 6 and 9).

3.1 The reciprocal lattice

For any real-space lattice there exists a dual lattice in wavevector space known as the *reciprocal lattice*. In the simplest terms, the reciprocal lattice is the Fourier transform of the lattice.

A lattice may be represented mathematically by

$$L(\mathbf{r}) = \sum_{\mathbf{R}} \delta(\mathbf{r} - \mathbf{R}), \tag{1}$$

where $\mathbf{R} = n_1\mathbf{a}_1 + n_2\mathbf{a}_2 + n_3\mathbf{a}_3$ is a lattice vector. The Fourier transform of $L(\mathbf{r})$ is

$$\begin{aligned} L(\mathbf{Q}) &= \int \sum_{\mathbf{R}} \delta(\mathbf{r} - \mathbf{R}) \exp(\mathrm{i}\mathbf{Q}\cdot\mathbf{r})\, \mathrm{d}^3\mathbf{r} \\ &= \sum_{\mathbf{R}} \exp(\mathrm{i}\mathbf{Q}\cdot\mathbf{R}), \end{aligned} \tag{2}$$

where $\mathbf{Q}$ is the Fourier transform conjugate variable, and is a wavevector. For a general $\mathbf{Q}$, the real and imaginary parts of $\exp(\mathrm{i}\mathbf{Q}\cdot\mathbf{R})$ will oscillate from positive to negative over the lattice, and so when the sum in (2) is performed the result is that $L(\mathbf{Q}) \simeq 0$. However, for any $\mathbf{Q}$ that satisfies

$$\exp(\mathrm{i}\mathbf{Q}\cdot\mathbf{R}) = 1 \text{ for all } \mathbf{R}, \tag{3}$$

we have that $L(\mathbf{Q}) = N$ (the total number of lattice points). A $\mathbf{Q}$ that satisfies (3) will be denoted by $\mathbf{G}$, and we see that $L(\mathbf{Q})$ consists of 'spikes' in $\mathbf{Q}$-space (or reciprocal space) located wherever $\mathbf{Q} = \mathbf{G}$.

The set of $\mathbf{G}$ vectors forms a lattice in reciprocal space called the **reciprocal lattice**. The $\mathbf{G}$ vectors are the **reciprocal lattice vectors**, and may be generated by

$$\mathbf{G} = h\mathbf{a}_1^* + k\mathbf{a}_2^* + l\mathbf{a}_3^*, \tag{4}$$

where h, k, l are integers, $\mathbf{a}_1^*$, $\mathbf{a}_2^*$, $\mathbf{a}_3^*$ are the basis vectors for the reciprocal lattice, and

$$\mathbf{a}_1^* = \frac{2\pi}{v_0}\,\mathbf{a}_2 \times \mathbf{a}_3, \quad \mathbf{a}_2^* = \frac{2\pi}{v_0}\,\mathbf{a}_3 \times \mathbf{a}_1, \quad \mathbf{a}_3^* = \frac{2\pi}{v_0}\,\mathbf{a}_1 \times \mathbf{a}_2. \tag{5}$$

Here v_0 is the volume of the real-space primitive unit cell. The basis vectors for the real-space lattice and the reciprocal lattice are related by

$$\mathbf{a}_i \cdot \mathbf{a}_j^* = 2\pi\delta_{ij} \qquad (\delta_{ij} \text{ is the Kronecker delta}).$$

The integer coefficients h, k, and l are the Miller indices, which by convention are written in round brackets, (hkl). In the B6 course, you found that $\mathbf{G}$ is the normal to the plane in real space with Miller indices h, k, l, and that $|\mathbf{G}| = 2\pi/d_{hkl}$, where d_{hkl} is the distance between adjacent (hkl) planes in real space.

3.2 Non-primitive unit cells and selection rules

The reciprocal lattice is determined uniquely from the crystal lattice by eqs. (4) and (5). It exists independently of any particular choice of crystallographic unit cell. In this section we shall explain how to construct the reciprocal lattice from the basis vectors of a non-primitive unit cell.

You will often see a set of 'reciprocal lattice' basis vectors defined similarly to those in eq. (5) but in terms of the unit cell basis vectors **a**, **b**, **c**:

$$\mathbf{a}^* = \frac{2\pi}{V_0}\,\mathbf{b}\times\mathbf{c}, \quad \mathbf{b}^* = \frac{2\pi}{V_0}\,\mathbf{c}\times\mathbf{a}, \quad \mathbf{c}^* = \frac{2\pi}{V_0}\,\mathbf{a}\times\mathbf{b}, \tag{6}$$

where $V_0 = \mathbf{a}\cdot\mathbf{b}\times\mathbf{c}$, etc, is the volume of the unit cell. A set of reciprocal space vectors can then be generated by analogy with (4):

$$\mathbf{H} = h\mathbf{a}^* + k\mathbf{b}^* + l\mathbf{c}^*. \tag{7}$$

If the unit cell is primitive, and **a**, **b**, **c** are the same as the lattice basis vectors $\mathbf{a}_1$, $\mathbf{a}_2$, $\mathbf{a}_3$, then eq. (6) reduces trivially to eq. (5), and $\mathbf{H} = \mathbf{G}$ are reciprocal lattice vectors for any integers h, k, l.

However, if we choose a **non-primitive** unit cell then $\mathbf{a}^*$, $\mathbf{b}^*$, $\mathbf{c}^*$ will not be the same as the reciprocal lattice basis vectors $\mathbf{a}_1^*$, $\mathbf{a}_2^*$, $\mathbf{a}_3^*$, and only a subset of the vectors defined by (7) will be reciprocal lattice vectors. This is because the lattice generated by $n_1\mathbf{a} + n_2\mathbf{b} + n_3\mathbf{c}$ is not the crystal lattice, but is a *sublattice* of the crystal lattice, and so (7) generates extra points in reciprocal space which are not reciprocal lattice points.

As a concrete example, consider the rectangular lattice shown in Fig. 1. The conventional cell is rectangular and C-centred, and has twice the area of the primitive cell. The reciprocal lattice is shown by the filled circles in the reciprocal space diagram, and is generated by eqs. (5) and (4) from the primitive cell. The set of **H** vectors generated by eqs. (6) and (7) from the rectangular cell includes the reciprocal lattice vectors, but also includes the vectors represented by the open circles, which are not reciprocal lattice points.

The way to determine which of the **H** vectors are reciprocal lattice vectors is to apply the **selection rule** (extinction condition) for the non-primitive unit cell. For ease of reference, the selection rules for all the standard non-primitive cells are given in Table 1. We see that for the C-centred cell the rule is $h + k = 2m$, consistent with the reciprocal lattice points shown in Fig. 1.

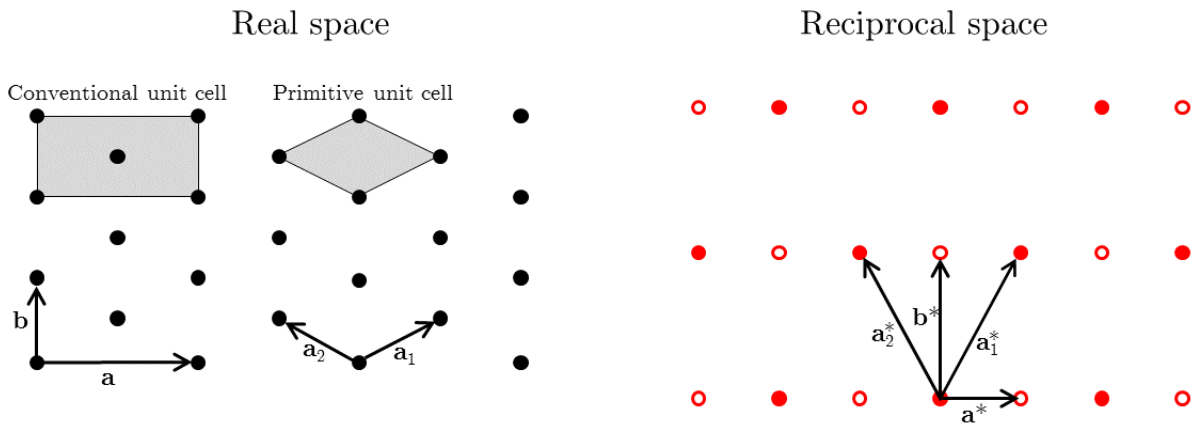


Figure 1: Left: Rectangular lattice, together with primitive and conventional (centred) unit cells and their corresponding basis vectors. Right: reciprocal lattice (filled circles) and the additional points generated by eq. (7) (open circles).

Table 1: Selection rules for allowed reciprocal lattice vectors. The first column gives the direct space lattice type, and the centring vectors in the second column give the location of lattice points in the conventional unit cell. The final column is the reciprocal lattice type.

Direct space	**Centring vectors**	h,k,l **conditions** (m integer)	**Reciprocal space**
P	None	None	P
A	$(0,\frac{1}{2},\frac{1}{2})$	$k+l=2m$	A
B	$(\frac{1}{2},0,\frac{1}{2})$	$h+l=2m$	B
C	$(\frac{1}{2},\frac{1}{2},0)$	$h+k=2m$	C
F	$(0,\frac{1}{2},\frac{1}{2}),(\frac{1}{2},0,\frac{1}{2}),(\frac{1}{2},\frac{1}{2},0)$	h,k,l all even or all odd integers	I
I	$(\frac{1}{2},\frac{1}{2},\frac{1}{2})$	$h+k+l=2m$	F
R	$(\frac{2}{3},\frac{1}{3},\frac{1}{3}),(\frac{1}{3},\frac{2}{3},\frac{2}{3})$	$-h+k+l=3m$	R

The selection rules can be obtained from the reciprocal lattice condition (3),

$$\exp(\mathrm{i}\mathbf{G}\cdot\mathbf{R}) = 1 \text{ for all } \mathbf{R}, \tag{8}$$

which implies that

$$\mathbf{G}\cdot\mathbf{R} = 2\pi m \text{ for all } \mathbf{R} \quad (m \text{ integer}). \tag{9}$$

Take, for example, the C-centred lattice again. Condition (9) is trivially satisfied by the lattice point at the origin of the unit cell ($\mathbf{R}=0$). For the lattice point in the centre of the conventional cell, $\mathbf{R}=\frac{1}{2}\mathbf{a}+\frac{1}{2}\mathbf{b}$, so that the Miller indices corresponding to reciprocal lattice vectors must satisfy

$$\begin{aligned}(h\mathbf{a}^*+k\mathbf{b}^*+l\mathbf{c}^*)\cdot(\tfrac{1}{2}\mathbf{a}+\tfrac{1}{2}\mathbf{b}) &= 2\pi m \\ \rightarrow \quad 2\pi(\tfrac{1}{2}h+\tfrac{1}{2}k) &= 2\pi m \\ \rightarrow \quad h+k &= 2m.\end{aligned} \tag{10}$$

Here we have used $\mathbf{a}^*\cdot\mathbf{a}=\mathbf{b}^*\cdot\mathbf{b}=\mathbf{c}^*\cdot\mathbf{c}=2\pi$, and $\mathbf{a}^*\cdot\mathbf{b}=0$, etc, which follow from (6).

3.3 The structure factor and roto-translations

In X-ray and neutron diffraction, the diffracted amplitude is the Fourier transform of the scattering potential:

$$\mathcal{F}(\mathbf{Q}) = \int V(\mathbf{r})\mathrm{e}^{i\mathbf{Q}\cdot\mathbf{r}}\mathrm{d}\mathbf{r}.$$

The crystal structure is the convolution of the lattice and the basis, which from the Convolution Theorem means that the Fourier transform can be written as a product

$$\mathcal{F}(\mathbf{Q}) = \left(\sum_{\mathbf{R}} \mathrm{e}^{\mathrm{i}\mathbf{Q}\cdot\mathbf{R}}\right)\left(\sum_j f_j(\mathbf{Q})\,\mathrm{e}^{\mathrm{i}\mathbf{Q}\cdot\mathbf{r}_j}\right). \tag{11}$$

The first factor is the Fourier transform of the lattice, see eq. (2), which is only non-zero when $\mathbf{Q}=\mathbf{G}$. In diffraction theory this is known as the **Laue condition**. The second factor is the **structure factor**, which we shall write

$$S(\mathbf{G}) = \sum_j f_j(\mathbf{G})\,\mathrm{e}^{\mathrm{i}\mathbf{G}\cdot\mathbf{r}_j}, \tag{12}$$

where $f_j(\mathbf{G})$ is the **atomic form factor** (X-ray diffraction) or the **nuclear scattering length** (neutron diffraction), and j sums over the atoms in the basis.

For practical calculations, we put $\mathbf{G} = h\mathbf{a}^* + k\mathbf{b}^* + l\mathbf{c}^*$ and $\mathbf{r}_j = x_j\mathbf{a} + y_j\mathbf{b} + z_j\mathbf{c}$, remembering that h, k, l must satisfy the selection rule if the cell is non-primitive, and write

$$S(hkl) = \sum_j f_j(hkl)\, \mathrm{e}^{2\pi\mathrm{i}(hx_j+ky_j+lz_j)}. \tag{13}$$

Even if the lattice selection rules are satisfied, it is still possible for the structure factor to be zero. Such extinctions occur if roto-translational symmetry elements are present. As an example, consider a c-glide involving m_y $[x, 0, z]$ and glide translation [0,0,1/2]. For every atom at x, y, z there will be an identical atom at $x, -y, z + 1/2$ related by the c-glide. Hence, the structure factor will contain the factor

$$f(hkl)[\mathrm{e}^{2\pi\mathrm{i}(hx+ky+lz)} + \mathrm{e}^{2\pi\mathrm{i}(hx-ky+l(z+\frac{1}{2}))}] = f(hkl)\mathrm{e}^{2\pi\mathrm{i}(hx+ky+lz)}[1 + \mathrm{e}^{2\pi\mathrm{i}(-2ky+l/2)}]$$

The $[\ldots]$ factor is common to every term in the structure factor, so

$$S(hkl) \propto [1 + \mathrm{e}^{2\pi\mathrm{i}(-2ky+l/2)}].$$

If $k = 0$, then

$$S(h0l) \propto 1 + \mathrm{e}^{\pi\mathrm{i}l},$$

giving the extinction condition $h0l : \; l = 2n + 1$. Extinctions due either to the lattice centring or to the presence of screw or glide symmetry elements are also known as **systematic absences**.

3.4 The phase problem

In general, the structure factor is a complex number which can be written

$$S(\mathbf{G}) = A(\mathbf{G})\, \mathrm{e}^{\mathrm{i}\phi(\mathbf{G})},$$

where the modulus A and phase ϕ are real numbers. If we could measure the modulus and phase of structure factors we could directly compute the positions of the atoms in the unit cell without any prior knowledge of the structure, simply by performing a Fourier transform on a complete set of measured structure factors. Unfortunately, this is not possible because the diffracted intensity is proportional to $|S|^2$, and

$$|S|^2 = A\mathrm{e}^{\mathrm{i}\phi} \times A\mathrm{e}^{-\mathrm{i}\phi} = A^2.$$

So all information about the phase ϕ of the structure factor is lost. This is known as the **phase problem** in crystallography.

Methods do exist to get around the phase problem. For example, one can vary the form factor at one or more sites in the structure, either by making chemical substitutions which preserve the crystal structure, or by exploiting the energy dependence of the form factor in the vicinity of an absorption resonance. However, the vast majority of crystal structures are solved by refinement of a model from an initial 'guess' at the atomic positions until the diffracted intensities calculated from the model give the best agreement with the measured intensities (see Lecture 5). Some information to constrain the initial model can be obtained from the symmetry of the observed diffraction pattern, as we shall now show.

3.5 Symmetry of diffraction patterns

In this section we obtain the following two symmetry properties of the structure factor, which are important for deducing information about the symmetry of crystal structures from their diffraction patterns:

1. $|S(\mathbf{G})|^2$ has the full point group symmetry of the crystal.
2. Friedel's law: $|S(\mathbf{G})|^2 = |S(-\mathbf{G})|^2$ whether or not the crystal structure has inversion symmetry (subject to certain conditions on the atomic form factor given below).

To prove the first of these, let us write the structure factor as an integral of the scattering potential $V(\mathbf{r})$ over the unit cell:[1]

$$S(\mathbf{G}) = \int_{\text{u.c.}} V(\mathbf{r})\, \mathrm{e}^{\mathrm{i}\mathbf{G}\cdot\mathbf{r}}\, \mathrm{d}^3\mathbf{r}. \tag{14}$$

Suppose that a crystal is invariant under a symmetry transformation $\mathbf{r}' = R\mathbf{r} + \mathbf{t}$, where R is a rotation or rotoinversion operator, and $\mathbf{t}$ is a translation. Symmetry means that $V(\mathbf{r}') = V(\mathbf{r})$. Now, the dot product $\mathbf{G}\cdot\mathbf{r}$ depends only on the angle between $\mathbf{G}$ and $\mathbf{r}$, so by applying R to both $\mathbf{r}$ and $\mathbf{G}$ we see that

$$\begin{aligned}\mathbf{G}\cdot\mathbf{r} &= R\mathbf{G}\cdot R\mathbf{r}\\ &= R\mathbf{G}\cdot(R\mathbf{r}+\mathbf{t}) - R\mathbf{G}\cdot\mathbf{t}\\ &= R\mathbf{G}\cdot\mathbf{r}' - R\mathbf{G}\cdot\mathbf{t}.\end{aligned}$$

Furthermore, as volume is preserved in rotations and translations, $\mathrm{d}^3\mathbf{r} = \mathrm{d}^3\mathbf{r}'$. Hence, we can write (14)

$$\begin{aligned}S(\mathbf{G}) &= \mathrm{e}^{-\mathrm{i}R\mathbf{G}\cdot\mathbf{t}} \int_{\text{u.c.}} V(\mathbf{r}')\, \mathrm{e}^{\mathrm{i}R\mathbf{G}\cdot\mathbf{r}'}\, \mathrm{d}^3\mathbf{r}'\\ &= \mathrm{e}^{-\mathrm{i}R\mathbf{G}\cdot\mathbf{t}} S(R\mathbf{G}),\end{aligned}$$

and so

$$|S(\mathbf{G})|^2 = |S(R\mathbf{G})|^2.$$

This shows that the squared modulus of the structure factor is invariant under any symmetry operation of the crystal point group. Note that the crystal point group includes the pure rotations and rotoinversions, and also the rotational components of any screw and glide symmetries.

Next, Friedel's law, $|S(\mathbf{G})|^2 = |S(-\mathbf{G})|^2$. This applies when either (i) the crystal has a centre of inversion symmetry, so that $S(-\mathbf{G}) = S(\mathbf{G})$, or (ii) the scattering potential is real (i.e. there is no anomalous scattering — see Lecture 5). In this latter case the atomic form factor satisfies $f(-\mathbf{G}) = f^*(\mathbf{G})$, so that

$$S(-\mathbf{G}) = \sum_j f_j(-\mathbf{G})\, \mathrm{e}^{-\mathrm{i}\mathbf{G}\cdot\mathbf{r}_j} = S^*(\mathbf{G}),$$

and therefore

$$\begin{aligned}|S(-\mathbf{G})|^2 &= S(-\mathbf{G})S^*(-\mathbf{G})\\ &= S^*(\mathbf{G})S(\mathbf{G})\\ &= |S(\mathbf{G})|^2.\end{aligned}$$

We see that when either of conditions (i) or (ii) applies the diffraction pattern is centrosymmetric (i.e. has inversion symmetry). This is known as **Friedel's law**, and it follows that the symmetry of the diffraction pattern is equal to the crystal point group augmented by an inversion centre. This symmetry is known as the **Laue Class**. For example, a crystal with space group $P2_1$ (2-fold screw symmetry and no inversion centre) has point group 2, and Laue Class $2/m$.

[1] For X-ray diffraction $V(\mathbf{r})$ is proportional to the electron density, and for neutron diffraction it is proportional to the scattering length density.

3.6. Measuring distances and angles in crystals

When dealing with crystallographic unit cells that have non-orthogonal axes (e.g. the monoclinic lattice) it can be difficult to calculate distances and angles. Both direct and reciprocal spaces are Euclidean vector spaces, and so the space can be described by a metric tensor, G (not to be confused with a reciprocal lattice vector).

Consider two vectors in the basis $\mathbf{a}$, $\mathbf{b}$, $\mathbf{c}$, such that $\mathbf{u} = u_1\mathbf{a} + u_2\mathbf{b} + u_3\mathbf{c}$ and $\mathbf{v} = v_1\mathbf{a} + v_2\mathbf{b} + v_3\mathbf{c}$. The dot product of these vectors is

$$\begin{aligned}\mathbf{u}\cdot\mathbf{v} &= (u_1\mathbf{a} + u_2\mathbf{b} + u_3\mathbf{c})\cdot(v_1\mathbf{a} + v_2\mathbf{b} + v_3\mathbf{c}) \\ &= (u_1, u_2, u_3)\, G \begin{pmatrix} v_1 \\ v_2 \\ v_3 \end{pmatrix},\end{aligned}$$

where the direct space metric tensor is

$$G = \begin{pmatrix} \mathbf{a}^2 & \mathbf{a}\cdot\mathbf{b} & \mathbf{a}\cdot\mathbf{c} \\ \mathbf{b}\cdot\mathbf{a} & \mathbf{b}^2 & \mathbf{b}\cdot\mathbf{c} \\ \mathbf{c}\cdot\mathbf{a} & \mathbf{c}\cdot\mathbf{b} & \mathbf{c}^2 \end{pmatrix} = \begin{pmatrix} a^2 & ab\cos\gamma & ac\cos\beta \\ ab\cos\gamma & b^2 & bc\cos\alpha \\ ac\cos\beta & bc\cos\alpha & c^2 \end{pmatrix}.$$

To determine the length of a vector $\mathbf{v}$:

$$v^2 = |\mathbf{v}|^2 = (v_1, v_2, v_3)\, G \begin{pmatrix} v_1 \\ v_2 \\ v_3 \end{pmatrix}.$$

To determine the angle θ between two vectors:

$$\cos\theta = \frac{\mathbf{u}\cdot\mathbf{v}}{uv} = \frac{1}{uv}(u_1, u_2, u_3)\, G \begin{pmatrix} v_1 \\ v_2 \\ v_3 \end{pmatrix}$$

Similarly, the reciprocal space metric tensor takes the form:

$$G^* = \begin{pmatrix} \mathbf{a}^{*2} & \mathbf{a}^*\cdot\mathbf{b}^* & \mathbf{a}^*\cdot\mathbf{c}^* \\ \mathbf{b}^*\cdot\mathbf{a}^* & \mathbf{b}^{*2} & \mathbf{b}^*\cdot\mathbf{c}^* \\ \mathbf{c}^*\cdot\mathbf{a}^* & \mathbf{c}^*\cdot\mathbf{b}^* & \mathbf{c}^{*2} \end{pmatrix} = (2\pi)^2 G^{-1}$$

where,

$$\mathbf{a}^{*2} = \frac{(2\pi)^2}{V_0^2} b^2c^2\sin^2\alpha, \quad \mathbf{b}^{*2} = \frac{(2\pi)^2}{V_0^2} a^2c^2\sin^2\beta, \quad \mathbf{c}^{*2} = \frac{(2\pi)^2}{V_0^2} a^2b^2\sin^2\gamma$$

and

$$\begin{aligned}\mathbf{a}^*\cdot\mathbf{b}^* &= \frac{(2\pi)^2}{V_0^2} abc^2(\cos\alpha\cos\beta - \cos\gamma), \\ \mathbf{b}^*\cdot\mathbf{c}^* &= \frac{(2\pi)^2}{V_0^2} a^2bc(\cos\beta\cos\gamma - \cos\alpha), \\ \mathbf{a}^*\cdot\mathbf{c}^* &= \frac{(2\pi)^2}{V_0^2} ab^2c(\cos\alpha\cos\gamma - \cos\beta).\end{aligned}$$

Today we consider how waves propagate in crystals, with emphasis on features imposed by the translational and rotational symmetries of the crystal. The results will be discussed with reference to phonon dispersion relations, and electron band structures.

4.1 Bloch's theorem

We begin with a reminder of the general properties of waves propagating in a periodic potential.

1. A periodic potential satisfies
$$V(\mathbf{r}) = V(\mathbf{r}+\mathbf{R}), \tag{1}$$
with $\mathbf{R} = n_1\mathbf{a}_1 + n_2\mathbf{a}_2 + n_3\mathbf{a}_3$ any lattice vector generated from the primitive lattice vectors $\mathbf{a}_1$, $\mathbf{a}_2$, $\mathbf{a}_3$.

2. Any wave propagating in such a potential satisfies Bloch's theorem (see Prof Filip's lectures):
$$\psi_{\mathbf{k}}(\mathbf{r}+\mathbf{R}) = \mathrm{e}^{\mathrm{i}\mathbf{k}\cdot\mathbf{R}}\psi_{\mathbf{k}}(\mathbf{r}), \tag{2}$$
which is equivalent to
$$\psi_{\mathbf{k}}(\mathbf{r}) = u_{\mathbf{k}}(\mathbf{r})\mathrm{e}^{\mathrm{i}\mathbf{k}\cdot\mathbf{r}}, \tag{3}$$
where $u_{\mathbf{k}}(\mathbf{r})$ is a function that is periodic in the lattice. We omit here the time dependence of $\psi_{\mathbf{k}}(\mathbf{r})$.

3. The application of periodic boundary conditions, i.e. $\psi_{\mathbf{k}}(\mathbf{r}) = \psi_{\mathbf{k}}(\mathbf{r}+N_j\mathbf{a}_j)$, $j = 1, 2, 3$, to eq. (2) implies that
$$\mathrm{e}^{\mathrm{i}\mathbf{k}\cdot\mathbf{a}_j N_j} = 1, \tag{4}$$
which constrains $\mathbf{k}$ to have the discrete set of values
$$\mathbf{k} = \frac{m_1}{N_1}\mathbf{a}_1^* + \frac{m_2}{N_2}\mathbf{a}_2^* + \frac{m_3}{N_3}\mathbf{a}_3^* \qquad (m_1, m_2, m_3 \text{ integers}), \tag{5}$$
where $\mathbf{a}_1^*$, $\mathbf{a}_2^*$, $\mathbf{a}_3^*$ are the primitive reciprocal lattice vectors [see eq. (5) of the notes for Lecture 3].

4. A Bloch function $\psi_{\mathbf{k}}(\mathbf{r}) = u_{\mathbf{k}}(\mathbf{r})\mathrm{e}^{\mathrm{i}\mathbf{k}\cdot\mathbf{r}}$ is a solution of the Schrödinger equation with energy $E(\mathbf{k})$. The function $E(\mathbf{k})$ is called the **dispersion relation**.

5. The function $\psi_{\mathbf{k}+\mathbf{G}}(\mathbf{r}) = u_{\mathbf{k}+\mathbf{G}}(\mathbf{r})\mathrm{e}^{\mathrm{i}(\mathbf{k}+\mathbf{G})\cdot\mathbf{r}}$ is also a Bloch function, where $\mathbf{G}$ is a reciprocal lattice vector. This can be seen from $\psi_{\mathbf{k}+\mathbf{G}}(\mathbf{r}) = [u_{\mathbf{k}+\mathbf{G}}(\mathbf{r})\mathrm{e}^{\mathrm{i}\mathbf{G}\cdot\mathbf{r}}]\mathrm{e}^{\mathrm{i}\mathbf{k}\cdot\mathbf{r}} = u'_{\mathbf{k}}(\mathbf{r})\mathrm{e}^{\mathrm{i}\mathbf{k}\cdot\mathbf{r}}$ and the fact that $u'_{\mathbf{k}}(\mathbf{r})$ is periodic in the lattice since $\mathrm{e}^{\mathrm{i}\mathbf{G}\cdot\mathbf{R}} = 1$ for all $\mathbf{R}$. We know that $u'_{\mathbf{k}}(\mathbf{r}) = u_{\mathbf{k}}(\mathbf{r})$ gives a solution to the Schrödinger equation. Hence, $\psi_{\mathbf{k}+\mathbf{G}} = \psi_{\mathbf{k}}$ is a solution, and for this solution $E(\mathbf{k}+\mathbf{G}) = E(\mathbf{k})$. We conclude, therefore, that **the dispersion relation is periodic in the reciprocal lattice**.

6. If there are $N = N_1N_2N_3$ lattice points, then there are N distinct wave functions, or *modes*, whose wavevectors are given by eq. (5).

7. The Wigner–Seitz cell centred on any reciprocal lattice point contains all N distinct wavevectors.

8. The Wigner–Seitz cell centred on $\mathbf{G} = 0$ is known as the **first Brillouin zone**.

4.2 Example: crystal vibrations

In the B6 course you analysed the vibrations of one-dimensional chains of atoms, assuming the **harmonic approximation**. You found that for a monatomic chain of N atoms, there are N linear equations of motion whose N solutions are the normal modes of vibration of the chain. When a single mode k is excited, the displacement d_k of an atom at position $x_n = na$ along the chain is given by

$$d_k(x_n, t) = A_k \mathrm{e}^{\mathrm{i}(kx_n - \omega t)}. \tag{6}$$

We see that eq. (6) satisfies Bloch's theorem, eq. (2), since $d_k(x_n + R, t) = \mathrm{e}^{\mathrm{i}kR} d_k(x_n, t)$, and that $d_{k+G} = d_k$, i.e. the atomic displacements in modes with wavevectors k and $k + G$ are identical, where $G = h \times 2\pi/a$ is a 1D reciprocal lattice vector (h = integer). It follows that $E(k) = E(k + G)$. For the diatomic chain, there are $2N$ equations of motion and therefore two normal modes per k which are described by the displacements $d_{1,k}(x_n, t)$ and $d_{2,k}(x_n, t)$ of the 2 atoms in the unit cell.

We can generalize these results to 3D harmonic crystals. If there are N lattice points in the crystal and p atoms per lattice point, then there are $3Np$ equations of motion, whose $3Np$ solutions are the normal modes of vibration of the crystal. As there are N allowed $\mathbf{k}$ in the first Brillouin zone, there are $3p$ modes per $\mathbf{k}$. The pattern of atomic displacements in each mode can be described by a travelling wave

$$\mathbf{d}_{j,\mathbf{k}}(\mathbf{R}, t) = \mathbf{A}_{j,\mathbf{k}} \mathrm{e}^{\mathrm{i}(\mathbf{k}\cdot\mathbf{R} - \omega t)}, \tag{7}$$

where $j = 1, \ldots, p$ labels the atoms associated with lattice vector $\mathbf{R}$. Again, we see that eq. (7) satisfies Bloch's theorem, eq. (2), as $\mathbf{d}_{j,\mathbf{k}}(\mathbf{R} + \mathbf{R}', t) = \mathrm{e}^{\mathrm{i}\mathbf{k}\cdot\mathbf{R}'} \mathbf{d}_{j,\mathbf{k}}(\mathbf{R}, t)$, and that $\mathbf{d}_{j,\mathbf{k}} = \mathbf{d}_{j,\mathbf{k}+\mathbf{G}}$. Therefore, $E(\mathbf{k}) = E(\mathbf{k} + \mathbf{G})$, i.e. the phonon dispersion relation is periodic in the reciprocal lattice.

4.3 Symmetry in reciprocal space

We recall that the reciprocal lattice is the Fourier transform of the direct (real-space) lattice. It follows that the reciprocal lattice has the same point-group symmetry as the direct lattice (note, however, that the reciprocal lattice is not necessarily the same Bravais lattice type as the direct lattice).

As mentioned earlier, the first Brillouin zone is the Wigner–Seitz cell centred on the origin of reciprocal space, $\mathbf{G} = 0$, and contains $\mathbf{k}$ points representing all the distinct wavefunctions of the system. As we shall see, the symmetry at different $\mathbf{k}$ points in the Brillouin zone is reflected in the phonon dispersion relations and electron band structure.

As an example, consider a 2D crystal with a primitive square lattice whose point group is $4mm$. Figure 1 shows the first Brillouin zone, together with the point symmetry elements which pass through the centre of the Brillouin zone. By convention, the centre of the zone is labelled Γ, and other points that lie along symmetry elements in the Brillouin zone are identified with other letters (you don't need to memorize these!): X and M are at the side and corner of the Brillouin zone, respectively, Δ is a general point along the line from Γ to X, Σ is likewise along Γ to M, and Z is likewise between X and M.

The point group of symmetries at a specific point in the Brillouin zone is called the *little group*. The points Γ and M have the full set of point symmetries of the lattice, so the little group at both these points is $4mm$. The little group at X is $2mm$, as there are mirror planes but no 4-fold symmetry axis at X. Along the lines Γ to X, Γ to M, and X to M, there is only a single mirror plane, so the little group at points Δ, Σ and Z is m. The Γ point has the full set of symmetries of the lattice point group, which for the square lattice is $4mm$, whereas other high symmetry points have a subset of the point group symmetries.

Figure 2 shows the Brillouin zone shapes and high symmetry points of some 3D Bravais lattices.

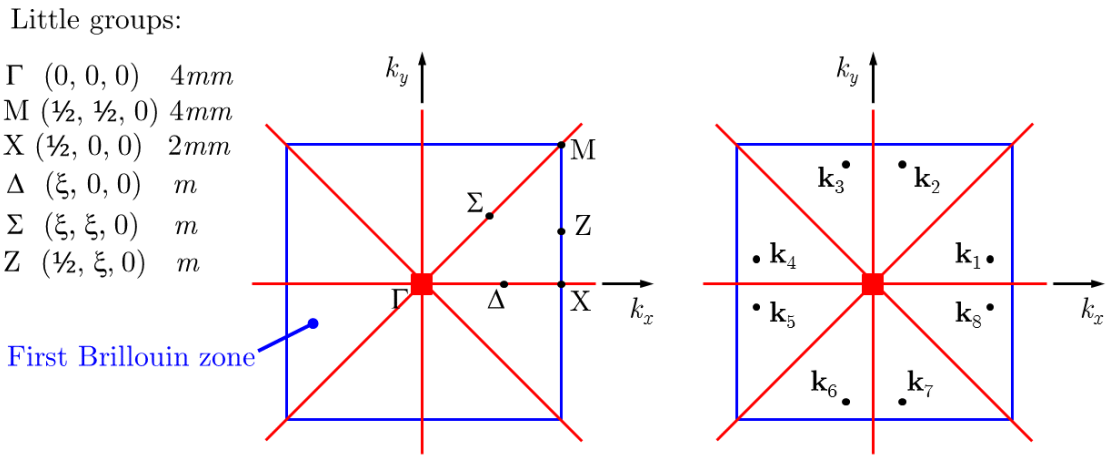


Figure 1: First Brillouin zone of the 2D square lattice, showing the point symmetry elements which pass through the Γ point. Left: high symmetry points and their little groups. Right: general point $\mathbf{k}_1$ and symmetry-related points $\mathbf{k}_2$ to $\mathbf{k}_8$.

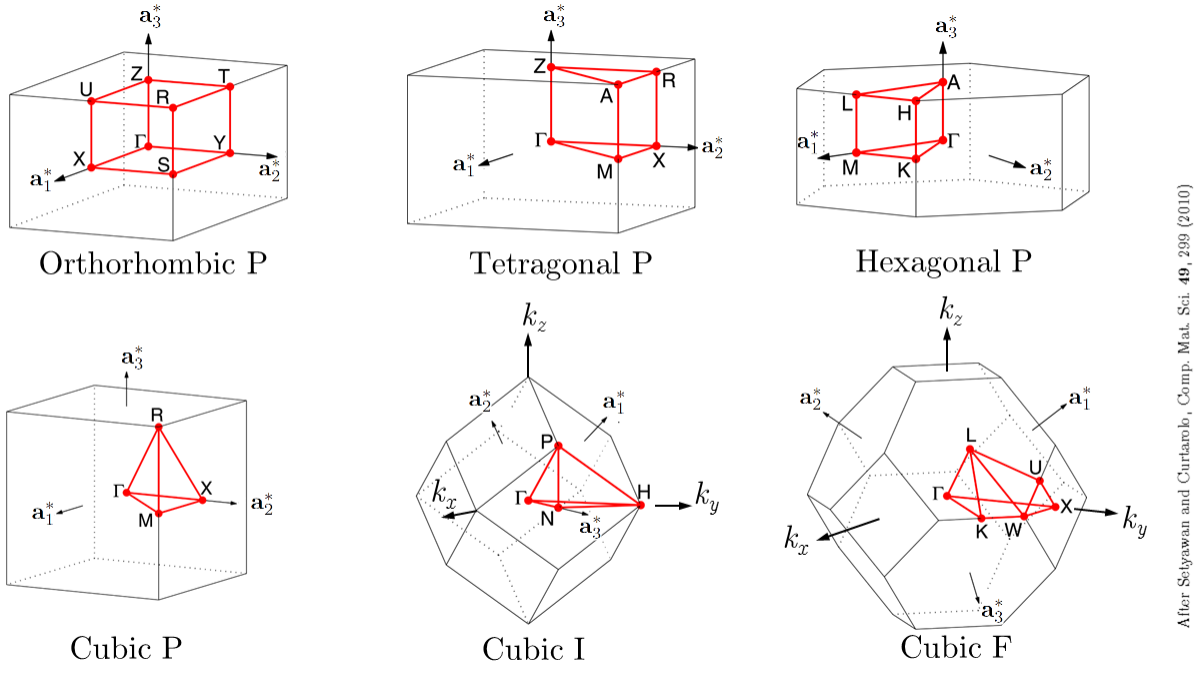


Figure 2: First Brillouin zones of six of the 3D Bravais lattice, showing the labels for the high symmetry points, and the directions of the primitive reciprocal lattice vectors $\mathbf{a}_1^*$, $\mathbf{a}_2^*$, $\mathbf{a}_3^*$. In the case of the cubic I and cubic F lattices, the standard Cartesian axes k_x, k_y, k_z are also shown.

4.4 Symmetry and degeneracy

When the arrangement of atoms in a crystal possesses a certain symmetry, or is described by a certain space group, it means that the Hamiltonian that describes the crystal dynamics or electronic energy states possesses those symmetries. The symmetry of the Hamiltonian has a profound effect on the spectrum of excitations, as we now show.

The Hamiltonian $\mathcal{H}$ determines the eigenvalues of the system through the time-independent Schrödinger equation,

$$\mathcal{H}\psi = E\psi. \tag{8}$$

Suppose that $\mathcal{H}$ is invariant under the symmetry operator T, i.e. $\mathcal{H}$ possesses the symmetry[1] described by T

$$T\mathcal{H} = \mathcal{H}. \tag{9}$$

Suppose also that T converts ψ into another function ϕ,

$$T\psi = \phi. \tag{10}$$

Let us apply T to the Schrödinger equation (8):

$$\begin{aligned} & T\{\mathcal{H}\psi\} = ET\psi \\ \rightarrow \qquad & \mathcal{H}\phi = E\phi. \end{aligned} \tag{11}$$

Now, if $\psi = c\phi$, where c is a (complex) constant, then there is nothing of interest to say as (11) is equivalent to (8). But if ψ and ϕ are distinct functions, not simply proportional to one another, then (11) implies that ψ and ϕ are both eigenstates of the Hamiltonian, and that they have the same eigenvalue. In other words, ψ and ϕ are *degenerate*.

This analysis shows that symmetry can cause degeneracies in spectra. Or, conversely, when one observes degenerate eigenstates there is usually (but not always) some symmetry which is responsible for the degeneracy. When degeneracy is caused by symmetry it is called **symmetry-protected degeneracy**. When there is no symmetry involved, it is called **accidental degeneracy**.

Let us now return to the Bloch states in a crystal. Suppose that R is one of the symmetry operations in the point group of a crystal. If we apply R to the Bloch function $\psi_{\mathbf{k}}(\mathbf{r})$ then, from (3),

$$\begin{aligned} R\psi_{\mathbf{k}}(\mathbf{r}) &= u_{\mathbf{k}}(\mathbf{r}')\mathrm{e}^{\mathrm{i}\mathbf{k}\cdot\mathbf{r}'} \qquad && (\text{where } \mathbf{r}' = R\mathbf{r}) \\ &= u_{\mathbf{k}'}(\mathbf{r})\mathrm{e}^{\mathrm{i}\mathbf{k}'\cdot\mathbf{r}} \qquad && (\text{where } \mathbf{k}' = R^{-1}\mathbf{k}) \\ &= \psi_{\mathbf{k}'}(\mathbf{r}). \end{aligned} \tag{12}$$

The second line follows because the scalar product in the exponential is the same whether we rotate $\mathbf{r}$ by an angle θ or $\mathbf{k}$ by $-\theta$. Therefore, function $\psi_{\mathbf{k}'}(\mathbf{r})$ is also a Bloch function, and as the point group contains both R and R^{-1} the Hamiltonian is invariant under R^{-1}, and so $\psi_{\mathbf{k}}$ and $\psi_{\mathbf{k}'}$ **are degenerate**.

In summary, distinct $\mathbf{k}$ states in the Brillouin zone which are related by the point symmetries of the crystal represent degenerate eigenstates.

As an example, the diagram on the right in Fig. 1 shows a general wavevector $\mathbf{k}_1$ in the Brillouin zone, together with all the other wavevectors $\mathbf{k}_2$ to $\mathbf{k}_8$ which are related to $\mathbf{k}_1$ by the symmetry operations in the point group $4mm$. As $\mathbf{k}_1$ to $\mathbf{k}_8$ are all distinct wavevectors, the normal modes and electron bands at these $\mathbf{k}$ points are all degenerate.

[1] Recall from Lecture 1 that applying a symmetry transformation to a mathematical function means transforming the coordinates, and that (9) means that the transformed Hamiltonian is the same function as the original Hamiltonian, but of the rotated coordinates.

4.5 Phonon dispersion relations of copper

Copper has a cubic F lattice (face-centred cubic). Figure 3 shows measurements of the phonon dispersion relations along the (100) direction from Γ to X, and along the (110) direction from Γ to K (see Fig. 2).

There is one atom per lattice point in copper, so there are three vibrational modes per **k**. Along the (ξ00) and (ξξ0) high symmetry lines, the atoms in each mode vibrate either parallel or perpendicular to **k**, giving one longitudinal (L) and two transverse (T_1 and T_2) modes, respectively.

The Brillouin zone has a 4-fold symmetry axis along the (ξ00) direction, which transforms the T_1 mode into the T_2 mode. Therefore, the two transverse modes are degenerate along the (ξ00) high symmetry line. Along the (ξξ0) direction, however, there is only 2-fold rotational symmetry, so the T_1 and T_2 modes are not degenerate along (ξξ0).

At (110) (which is also an X point), the L and T_1 modes are seen to become degenerate. This is because there is a 4-fold rotational symmetry axis parallel to k_z passing through the X point at (110). In the T_1 mode the atoms vibrate along the z direction, so a 90° rotation around the 4-fold axis through X converts the L mode into the T_1 mode at this point.

The degeneracy that occurs along the (ξξ0) direction where the T_2 and L branches cross is accidental.

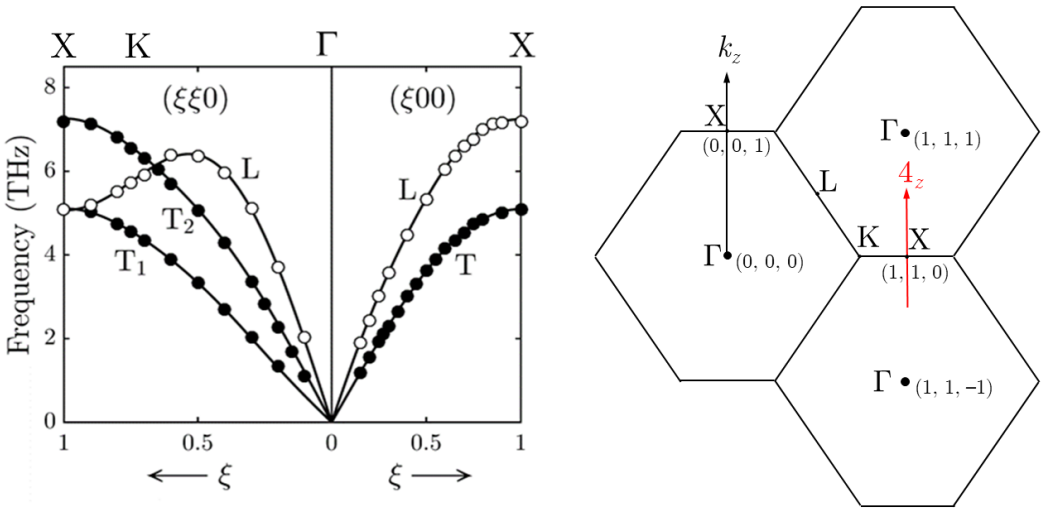


Figure 3: Left: Phonon dispersion relations of copper along two high symmetry directions. The two transverse modes T_1 and T_2 are degenerate along (ξ00). The longitudinal mode L and the transverse mode T_1 are degenerate at (110). The data were obtained by inelastic neutron scattering, Svensson *et al.*, Phys. Rev. **155**, 619 (1967). Right: Section through the Brillouin zone containing the (00ξ) and (ξξ0) directions.

4.6 Electronic structure of graphene

You were introduced to graphene earlier in the C3 course. Here we discuss some features of the electron bands which trace back to the symmetry of graphene.

Graphene is a single layer of carbon atoms bonded in hexagons by sp^2 hybridized orbitals and arranged in a honeycomb pattern (see Fig. 4). The primitive unit cell contains two carbon atoms, A and B. The first Brillouin zone is constructed in the usual way, by bisecting the vectors from Γ to the nearest-neighbour reciprocal lattice points, and is also a hexagon but rotated by 90° relative to the hexagons in real space.

The reciprocal lattice has point group symmetry $6mm$. Any pair of K (or K′) points are related by translation through a reciprocal lattice vector. For example, the two K points shown in Fig. 4 are related by translation through $\mathbf{a}_1^*$. This means the electronic wave functions at these points are the same. Points K and K′ are not related by translation through a reciprocal lattice vector, but are related by rotational symmetry. Therefore, the electronic energy is degenerate at K and K′ but the wave functions are distinct. M points on opposite sides of the Brillouin zone are equivalent as they are related by a reciprocal lattice vector, but points related to M by rotations through $\pi/3$ (M′) and $2\pi/3$ (M″) are degenerate but inequivalent.

The conduction electron bands in graphene derive from the overlap of $2p_\pi$ orbitals which point out of the plane. Figure 5 shows the electron bands obtained from the tight-binding model presented in Prof Johnston's lectures. The electronic wave function has two components representing the amplitudes on the A and B sites. There is a mirror plane along the line Γ–K. Application of a reflection twice must recover the original state, so the wave function is either symmetric or antisymmetric under reflection in this mirror (one is reminded of the acoustic and optic vibrational modes of a diatomic chain of atoms). On the lower band it is symmetric (the bonding band) and on the upper band it is antisymmetric (antibonding), as indicated on Fig. 5. As long as the two bands have different symmetry they are non-degenerate.

At the K and K′ points, however, the ratio of amplitudes becomes undefined, and we can choose the wave function to be localized completely on A or completely on B (again like the diatomic chain, in which one of the masses becomes stationary at the Brillouin zone boundary). These two choices are related by reflection

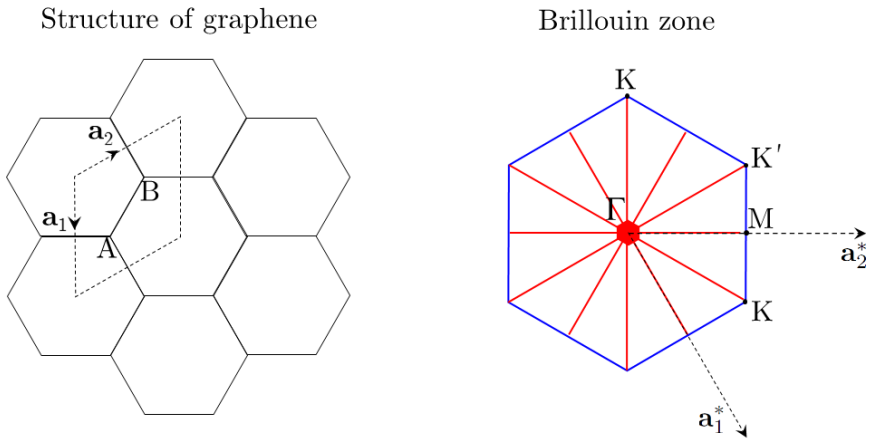


Figure 4: Left: honeycomb pattern of carbon atoms in graphene. There are two carbon atoms in the primitive unit cell, labeled A and B. Right: First Brillouin zone of graphene, showing the symmetry elements (in red), the high symmetry points, and the primitive reciprocal lattice vectors, $\mathbf{a}_1^*$ and $\mathbf{a}_2^*$.

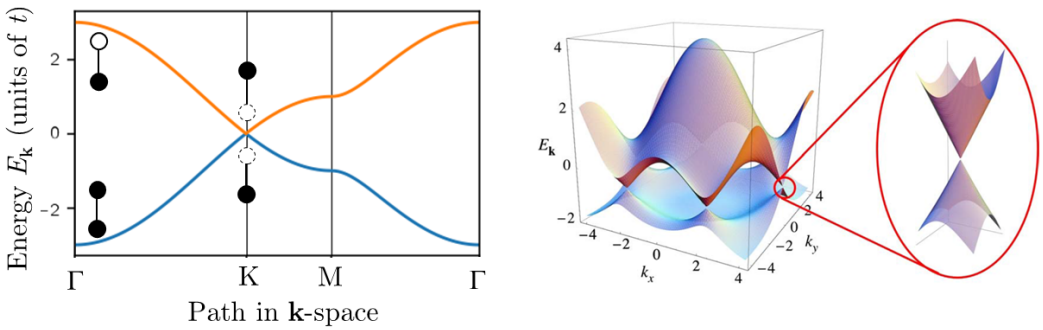


Figure 5: Left: tight-binding electron bands of graphene along the path Γ-K-M-Γ. The Fermi level is at $E_{\mathbf{k}} = 0$. The amplitudes on a pair of A and B atoms are indicated at Γ and K. Right: Dispersion surface highlighting the conical Dirac dispersion centred on the K and K' points.

in the Γ-K lines, which means they represent degenerate eigenstates. This situation does not arise anywhere else on the Brillouin zone boundary, so the two bands only touch at the K and K′ points.

The $2p_\pi$ orbitals contain one electron per atom, so the lower (bonding) band is completely filled and the upper band is completely empty. This means that the Fermi surface consists of the six isolated Dirac points, in contrast to the extended Fermi surface of a conventional metal, and that the density of states at the Fermi energy is exactly zero.

In summary: the graphene structure contains two identical sub-lattices A and B, which means that the Bloch wave functions are either symmetric or antisymmetric under reflection. The two bands only touch at the K and K′ points, and the degeneracy is symmetry-protected. This is the origin of the Dirac dispersion.

In this Lecture we build on the basic theory of X-ray and neutron diffraction which you learned in the B6 course, considering the various factors which determine the measurement of a Bragg peak intensity, and the additional effects observed when the X-ray energy is close to an atomic absorption resonance or the neutron energy close to a nuclear resonance.

5.1 Basic theory of X-ray and neutron diffraction

We first summarize some results obtained in the B6 course. The key assumption is that the interaction potential $V(\mathbf{r})$ which causes scattering is very weak. Under most conditions of interest, the scattering of X-rays and neutrons may then be calculated by time-dependent perturbation theory in the *first Born approximation*. In this approximation the scattering from an initial to a final states is given by *Fermi's Golden Rule*, and the scattering rate is proportional to

$$|\langle \mathbf{k}_\mathrm{f}|V(\mathbf{r})|\mathbf{k}_\mathrm{i}\rangle|^2. \tag{1}$$

The incident and scattered radiation can be approximated to plane waves, and $\mathbf{k}_\mathrm{i}$ and $\mathbf{k}_\mathrm{f}$ are the respective wave vectors. Here we are only considering elastic scattering, so $|\mathbf{k}_\mathrm{i}| = |\mathbf{k}_\mathrm{f}|$. For plane wave states the matrix element $\langle \mathbf{k}_\mathrm{f}|V(\mathbf{r})|\mathbf{k}_\mathrm{i}\rangle$ is simply the Fourier transform of $V(\mathbf{r})$, which may be written [see Lecture 3, eq. (11)]

$$\begin{aligned}\langle \mathbf{k}_\mathrm{f}|V(\mathbf{r})|\mathbf{k}_\mathrm{i}\rangle &= \int V(\mathbf{r})\mathrm{e}^{\mathrm{i}\mathbf{Q}\cdot\mathbf{r}}\mathrm{d}\mathbf{r} \\ &= \left(\sum_{\mathbf{R}} \mathrm{e}^{\mathrm{i}\mathbf{Q}\cdot\mathbf{R}}\right)\left(\sum_j f_j(\mathbf{Q})\,\mathrm{e}^{\mathrm{i}\mathbf{Q}\cdot\mathbf{r}_j}\right),\end{aligned} \tag{2}$$

where $\mathbf{R}$ is a lattice vector and $\mathbf{Q}$ is the **scattering vector**, given by

$$\mathbf{Q} = \mathbf{k}_\mathrm{i} - \mathbf{k}_\mathrm{f}. \tag{3}$$

The first factor in eq. (2) becomes modulus-squared in (1), and may formally be written (see Section 5.4)

$$\left|\sum_{\mathbf{R}} \mathrm{e}^{\mathrm{i}\mathbf{Q}\cdot\mathbf{R}}\right|^2 = N\frac{(2\pi)^3}{v_0}\sum_{\mathbf{G}}\delta(\mathbf{Q}-\mathbf{G}), \tag{4}$$

where v_0 is the volume of the unit cell. This expresses the **Laue condition**, that a necessary condition for constructive interference from a crystal lattice is $\mathbf{Q} = \mathbf{G}$, where $\mathbf{G}$ is a reciprocal lattice vector.

The second factor in (2) is the **structure factor**, $S(\mathbf{Q})$. The function $f_j(\mathbf{Q})$ is the **atomic form factor** in the case of X-ray diffraction, or the **nuclear scattering length** in the case of neutron diffraction.[1] The atomic form factor is the Fourier transform of the electron density in atom j and depends on $\mathbf{Q}$, whereas the nuclear scattering length is $\mathbf{Q}$-independent[2] and usually written b_j. The structure factor only needs to be evaluated for $\mathbf{Q} = \mathbf{G}$, so that

$$S_\mathrm{X}(\mathbf{G}) = \sum_j f_j(\mathbf{G})\,\mathrm{e}^{\mathrm{i}\mathbf{G}\cdot\mathbf{r}_j} \qquad \text{(X-ray)} \tag{5}$$

$$S_\mathrm{n}(\mathbf{G}) = \sum_j b_j\,\mathrm{e}^{\mathrm{i}\mathbf{G}\cdot\mathbf{r}_j} \qquad \text{(neutron)}. \tag{6}$$

The sum is over the atoms in the basis of the primitive unit cell.

[1] Neutrons can also be used to measure magnetic structures, in which case $f_j(\mathbf{Q})$ is replaced by the **magnetic form factor** and a factor which projects the magnetic moments onto the plane perpendicular to $\mathbf{Q}$.

[2] The nuclear scattering length is the Fourier transform of the nuclear potential, which acts over distances $\sim 10^{-15}$ m. Hence, interference effects within the nucleus only show up at very large $Q \sim 10^{15}\,\mathrm{m}^{-1}$, well beyond the range accessed in neutron diffraction experiments.

5.2 Factors which affect the measured intensity of a Bragg reflection

In any X-ray or neutron diffraction experiment one measures Bragg reflections from the sample. These reflections appear as peaks in intensity in well-defined directions given by the Laue condition $\mathbf{Q} = \mathbf{G}$. From the *positions* of the peaks one can learn about the symmetry of the crystal structure, and one can determine the lattice parameters (or unit cell parameters, i.e. the dimensions of the unit cell a, b, c and the inter-axial angles α, β, γ).

If one wants to go beyond the crystal symmetry and lattice parameters and determine the arrangement of atoms in the basis then it is necessary to measure the *intensities* of the Bragg peaks, and hence to determine $|S(\mathbf{G})|^2$, usually at a large set of $\mathbf{G}$ positions so as to reduce the uncertainty in the derived crystal structure. Note that owing to the *phase problem* (see Lecture 3) it might not be possible to obtain an unambiguous solution from $|S(\mathbf{G})|^2$ alone, and other information might be required.

Aside from the arrangement of atoms in the basis, there are a number of factors which control the measured intensities of Bragg peaks, depending on whether X-rays or neutrons are employed:

X-ray diffraction

- A polarization factor $P = |\hat{\boldsymbol{\epsilon}}_\mathrm{i} \cdot \hat{\boldsymbol{\epsilon}}_\mathrm{f}|^2$, where $\hat{\boldsymbol{\epsilon}}_\mathrm{i}$ and $\hat{\boldsymbol{\epsilon}}_\mathrm{f}$ are unit vectors in the direction of the electric field of the initial and final X-ray beams. This factor arises because the incident photon sets up a dipole oscillation in the atomic electrons which acts as a new source of X-rays. At distances much greater than the wavelength of the photon (the so-called far field) the amplitude of dipole radiation varies as the sine of the angle between the oscillating dipole and the direction of emission (see the A2 course), or equivalently, as the cosine of the angle between the initial and final polarization vectors (because the electric field of EM radiation is perpendicular to the direction of propagation). The dependence on P means that if the incident X-rays are horizontally polarized, and the scattered X-rays are observed in the horizontal plane at an angle ϕ to the incident beam direction, then the intensity goes as $\cos^2\phi$, which vanishes at $\phi = 90°$. If, however, the incident X-rays are vertically polarized then there is no angular dependence for scattering in the horizontal plane.
- The atomic form factor $f(\mathbf{Q})$. As mentioned before, $f(\mathbf{Q})$ is the Fourier transform of the electronic charge density in an atom. At $|\mathbf{Q}| = 0$, $f(\mathbf{Q}) = Z$, the atomic number. As $|\mathbf{Q}| \to \infty$, $f(\mathbf{Q}) \to 0$. The atomic form factors for hydrogen and neon are shown in Fig. 1 for illustration. It will be seen that the form factor of neon falls more slowly with $|\mathbf{Q}|$ than that of hydrogen. This is because as the nuclear charge $+Ze$ increases, the radius of the innermost core electrons decreases, so the electron density is more compact in neon than in hydrogen.

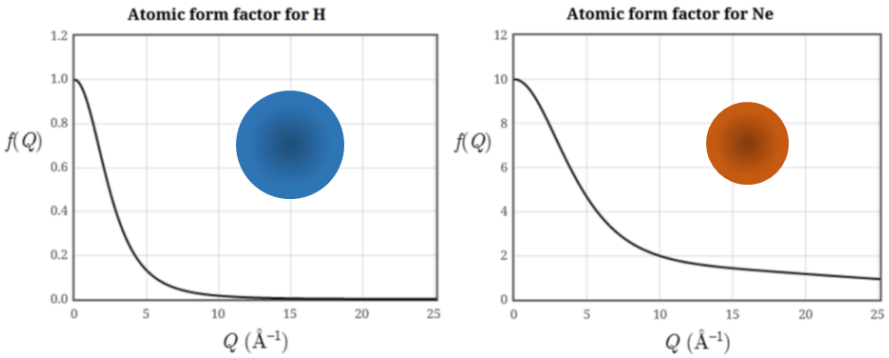


Figure 1: The atomic form factors of hydrogen and neon.

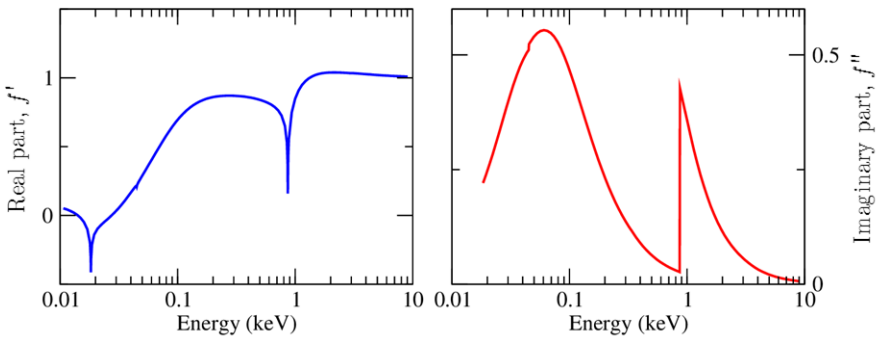


Figure 2: Anomalous terms in the atomic form factor of neon.

When the incident X-ray energy is near to an atomic transition (i.e. an excitation of a core electron into an empty valence state, followed by a near-instantaneous decay back to the core state) we see a departure from energy-independent Thomson scattering considered up to now.[3] Such resonant effects in the scattering process can be accounted for by including energy-dependent, complex terms in the atomic form factor, known as anomalous terms:

$$f(\mathbf{Q}) = f^0(\mathbf{Q}) + f'(\hbar\omega) + \mathrm{i}f''(\hbar\omega). \tag{7}$$

The $f^0(\mathbf{Q})$ term is the energy-independent Thomson scattering. The anomalous terms f' and f'' are independent of $\mathbf{Q}$, but strongly dependent on the X-ray energy $\hbar\omega$ in the vicinity of atomic transitions. Below an atomic transition the core electrons are tightly bound, whereas above the transition energy they become essentially free. Their ability to respond to the driving force of the incident X-ray's electric field is therefore reduced below the resonance, and increased above it. This behaviour is captured by $f'(\hbar\omega)$. Atomic resonances coincide with X-ray absorption, which is contained in the imaginary part $f''(\hbar\omega)$. Both anomalous terms are plotted as a function of energy for neon in Figure 3. An application of anomalous scattering is described below, in Section 5.3.

- The Debye–waller factor, $D(\mathbf{Q}, T)$. The atoms in crystals are never stationary. Even at absolute zero the atoms have zero-point energy, and with increasing temperature the amplitude of vibration increases as more phonons are thermally excited. The vibrational motion of the atoms spreads out the average electron distribution compared with a stationary atom, and reduces the Bragg peak intensity by a factor D^2, where in the case of an atom in an isotropic potential,

$$D(\mathbf{Q}, T) = \exp(-\tfrac{1}{2}Q^2\langle u^2\rangle).$$

$\langle u^2\rangle$ is the mean squared amplitude of vibration, which increases with temperature. The Debye–Waller has a similar effect to the atomic form factor, except that D is temperature-dependent. At small Q and low temperatures $D \simeq 1$, and can often be ignored.

- The Lorentz factor L. The intensity of a Bragg peak contains the factor $\delta(\mathbf{Q} - \mathbf{G})$ which comes from the Fourier transform of the lattice, see eq. (4). To obtain $|S(\mathbf{G})|^2$, therefore, one would ideally perform measurements in such a way that one could integrate the peak over $\mathbf{Q}$. However, this is not what is usually done in practice. Instead, the quantity that is obtained in an experiment is the integrated intensity of the peak measured in a scan in which the intensity is measured as (usually) an angle is

[3]The energy-independent scattering theory is called Thomson scattering, after J. J. Thomson who discovered the electron.

varied (e.g. the angle of diffraction, or a crystal rotation angle). Therefore, one needs the conversion between the integral over $\mathbf{Q}$ and the integral over the scan variable. The conversion factor is known as the Lorentz factor, L, and is an example of a *Jacobian*.

- Absorption and extinction, A. These are distinct processes, but they both have a similar effect of attenuating the X-ray beam as it passes through the sample. X-rays interact with the electrons in matter through a number of different processes, all of which remove X-rays from the incident or diffracted beam causing diffracted intensity to be attenuated. Extinction is a process where X-rays diffracted from one part of the crystal are diffracted a second time from another part of the crystal. Absorption and extinction depend on the X-ray path length, which depends on the shape and size of the sample, and on other factors such as the X-ray wavelength and the size of the crystallites.

Neutron diffraction

- There is no polarization factor in the scattering of neutrons from atomic nuclei.
- The nuclear scattering length b is independent of Q in the range of Q used for diffraction experiments, but as with the atomic form factor, b can be complex:

$$b = b' + \mathrm{i}b''.$$

  The imaginary part is non-negligible when the neutron energy is close to a nuclear resonance. For the typical neutron energies used in diffraction experiments, strong absorption occurs for a relatively small number of nuclides, such as ^{3}He, ^{6}Li, ^{10}B, ^{113}Cd, and a few others.

- The Lorentz and Debye–Waller factors are the same as for X-rays.
- Absorption and extinction also occur for neutrons, but the attenuation of a neutron beam in matter is usually much less than that of an X-ray beam. X-rays penetrate typically between 10 and 1000 μm, depending on wavelength and atomic number, whereas neutrons penetrate typically between 1 and 10 mm.

In summary, the diffracted intensity in a scan through a Bragg peak at $\mathbf{Q} = \mathbf{G}$ measured with X-rays (X) and neutrons (n) may be written

$$\begin{aligned} I_{\mathrm{X}} &\propto PLA|S_{\mathrm{X}}(\mathbf{G})|^2 \\ I_{\mathrm{n}} &\propto LA|S_{\mathrm{n}}(\mathbf{G})|^2, \end{aligned} \tag{8}$$

where

$$\begin{aligned} S_{\mathrm{X}}(\mathbf{G}) &= \sum_j D_j f_j(\mathbf{G})\, \mathrm{e}^{\mathrm{i}\mathbf{G}\cdot\mathbf{r}_j} \\ S_{\mathrm{n}}(\mathbf{G}) &= \sum_j D_j b_j\, \mathrm{e}^{\mathrm{i}\mathbf{G}\cdot\mathbf{r}_j}. \end{aligned} \tag{9}$$

Calculations of the L, A and D factors are beyond the syllabus of the C3 course.

5.3 Anomalous scattering

We now consider a case where anomalous scattering can be particularly informative. That is, for non-centrosymmetric crystals where Friedel's Law is violated (see Lecture 3, Section 3.5). We shall show how, by measuring $|S(hkl)|^2$ and $|S(\bar{h}\bar{k}\bar{l})|^2$ pairs, one can determine whether or not a crystal has an inversion centre. Furthermore, one can find the absolute direction of the atomic displacements away from the inversion centre.

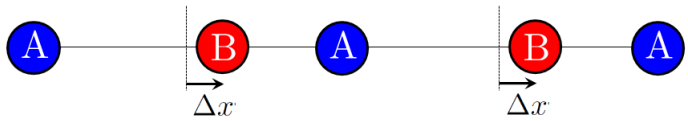
Consider, for example, a diatomic 1D crystal (see figure below). Atom A has fractional coordinate $x_{\mathrm{A}} = 0$,

and atom B has fractional coordinate $x_{\rm B} = 0.5 + \Delta x$. If $\Delta x = 0$ the crystal has an inversion centre at every atomic position, figure (a). If $\Delta x \neq 0$, all inversion symmetry elements are broken, and the crystal becomes non-centrosymmetric, figure (b).

(a) Centrosymmetric:



(b) Non-centrosymmetric:



We proceed by calculating the X-ray structure factor for the crystal, where $f = f^0 + f'$ is the real part of the atomic form factor, and f'' is the imaginary part, see eq. (7). The structure factor is then given by

$$S(h) = \sum_j f_j(h) \mathrm{e}^{2\pi \mathrm{i} h x_j} = (f_{\rm A} + \mathrm{i}f''_{\rm A}) + (f_{\rm B} + \mathrm{i}f''_{\rm B}) \exp\{2\pi\mathrm{i}(\tfrac{1}{2} + \Delta x)h\}$$

where h is the Miller index of the 1D reciprocal lattice. The diffracted intensity is proportional to

$$I(h) = |S(h)|^2 = f_{\rm A}^2 + f''^2_{\rm A} + f_{\rm B}^2 + f''^2_{\rm B} + 2(f_{\rm A}f_{\rm B} + f''_{\rm A}f''_{\rm B}) \cos\{2\pi(\tfrac{1}{2} + \Delta x)h\} + 2(f''_{\rm A}f_{\rm B} - f_{\rm A}f''_{\rm B}) \sin\{2\pi(\tfrac{1}{2} + \Delta x)h\}$$

so

$$I(h) - I(-h) = 4(f''_{\rm A}f_{\rm B} - f_{\rm A}f''_{\rm B})\ \cos(\pi h)\ \sin(2\pi\Delta x h) \tag{10}$$

Consider the following three cases:

(1) If the **anomalous terms of the atomic form factors are zero**, $f''_{\rm A} = f''_{\rm B} = 0$ (the incident X-ray energy does not correspond to an atomic absorption edge), then

$$I(h) = f_{\rm A}^2 + f_{\rm B}^2 - 2f_{\rm A}f_{\rm B}\cos(2\pi\Delta x h), \tag{11}$$

and

$$I(h) - I(-h) = 0.$$

Hence, Friedel's law holds and we are not directly sensitive to the breaking of inversion symmetry. A model would be needed to determine the crystal structure, and there are cases when alternative centrosymmetric and non-centrosymmetric structures give equally good descriptions of the diffraction pattern.

(2) If the **anomalous terms of the form factor are non-zero and $(f''_{\rm A}f_{\rm B} - f_{\rm A}f''_{\rm B}) \neq 0$, but $\Delta x = 0$** (the crystal is centrosymmetric), then eq. (10) becomes

$$I(h) - I(-h) = 4(f''_{\rm A}f_{\rm B} - f_{\rm A}f''_{\rm B})\cos(\pi h)\sin(0) = 0, \tag{12}$$

and Friedel's law holds.

(3) If the **anomalous terms of the form factor are non-zero and $\Delta x \neq 0$** (inversion symmetry is broken):

$$I(h) - I(-h) = 4(f''_{\rm A}f_{\rm B} - f_{\rm A}f''_{\rm B})\cos(\pi h)\sin(2\pi\Delta x h) \tag{13}$$

therefore Friedel's law is broken. We can then directly determine directly whether or not the structure is centrosymmetric. Furthermore, we can determine the absolute direction of the atomic displacement. If $I(h) - I(-h) > 0$ for even h reflections (and therefore $I(h) - I(-h) < 0$ for odd h) then $\sin(2\pi\Delta x h)$ has the same sign as the factor $(f''_{\rm A}f_{\rm B} - f_{\rm A}f''_{\rm B})$, and *vice-versa*.

5.4 Appendix: Proof of a lattice summation identity

General arguments suggest that the lattice sum (4) is sharply peaked at the reciprocal lattice vectors. Here we prove this result. First, note that

$$\Big|\sum_{\mathbf{R}} \exp(\mathrm{i}\mathbf{Q}\cdot\mathbf{R})\Big|^2 = \sum_{\mathbf{R}}\sum_{\mathbf{R}'} \exp\{\mathrm{i}\mathbf{Q}\cdot(\mathbf{R}-\mathbf{R}')\}$$
$$= N\sum_{\mathbf{R}} \exp(\mathrm{i}\mathbf{Q}\cdot\mathbf{R}). \tag{14}$$

The last line follows because $\mathbf{R}-\mathbf{R}'$ is a lattice vector, and for very large numbers of lattice points N the sum over $\mathbf{R}$ is the same for any $\mathbf{R}'$. One can then simply choose $\mathbf{R}'=0$ and replace the sum over $\mathbf{R}'$ by N.

Our assertion is that

$$\sum_{\mathbf{R}} \exp(\mathrm{i}\mathbf{Q}\cdot\mathbf{R}) = c\sum_{\mathbf{G}} \delta(\mathbf{Q}-\mathbf{G}). \tag{15}$$

To determine the constant c, integrate both sides of (15) over a Brillouin zone (a unit cell of the reciprocal lattice). A Brillouin zone contains one reciprocal lattice point, and the integral of a δ function is 1, so the integral of the right-hand side of (15) is simply c. On the left-hand side, the $\mathbf{R}=0$ term in the sum is equal to 1, so its contribution to the integral is simply the volume of the Brillouin zone, which is $(2\pi)^3/v_0$. For the terms with $\mathbf{R}\neq 0$ we can write $\mathbf{Q} = q_1\mathbf{a}_1^* + q_2\mathbf{a}_2^* + q_3\mathbf{a}_3^*$, and use the definition of the direct space and reciprocal lattice basis vectors to obtain

$$\mathbf{Q}\cdot\mathbf{R} = 2\pi(q_1n_1 + q_2n_2 + q_3n_3), \qquad n_1, n_2, n_3 \text{ integers.} \tag{16}$$

The lattice sum in (15) then factors into the product of three geometric series of the form $\sum_n \exp(2\pi\mathrm{i}qn)$, each of which integrates to zero as may be seen by the following:[4]

$$\int_{-\frac{1}{2}}^{\frac{1}{2}} \exp(2\pi\mathrm{i}qn)\,\mathrm{d}q = \frac{1}{2\pi\mathrm{i}n}\Big[\exp(2\pi\mathrm{i}qn)\Big]_{-\frac{1}{2}}^{\frac{1}{2}} = 0.$$

Hence,

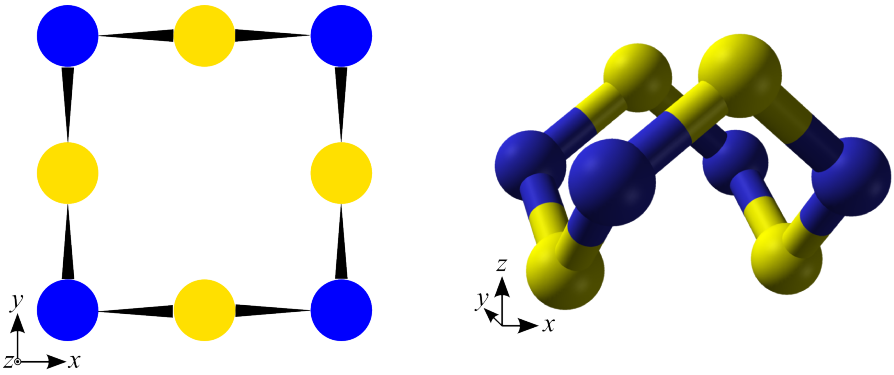
$$\sum_{\mathbf{R}} \exp(\mathrm{i}\mathbf{Q}\cdot\mathbf{R}) = \frac{(2\pi)^3}{v_0}\sum_{\mathbf{G}} \delta(\mathbf{Q}-\mathbf{G}). \tag{17}$$

[4]Without loss of generality, we choose to integrate over the first Brillouin zone, for which $-\frac{1}{2} \le q_j \le \frac{1}{2}$.

Problem Sheet 1
Michaelmas Term 2021

1. **Point symmetry**

Consider the molecule in the figure below, comprising four nitrogen atoms (blue) and four sulphur atoms (yellow).



(a) Identify the highest-order rotation or rotoinversion symmetry element and mark it on the left hand figure with the appropriate symbol.

(b) Draw any lower order rotation axes on the left hand figure with the appropriate symbols.

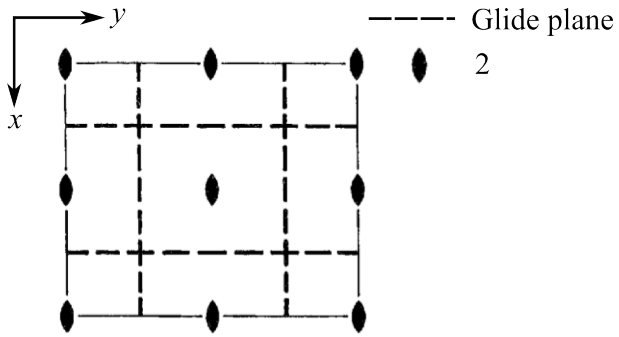
(c) Draw any mirror planes on the left hand figure with the appropriate symbol.

(d) Using the decision tree provided in the notes to accompany Lecture 1, or otherwise, identify the point group of the molecule.

(e) List all symmetry operators of the point group, divided into classes (n.b. a class can contain a single symmetry operation, for example {1}).

2. **Space group symmetry**

Consider the orthorhombic space group *Pba*2.



(a) Explain the meaning of all symbols in the space group notation.

(b) Derive the point group and explain your reasoning.

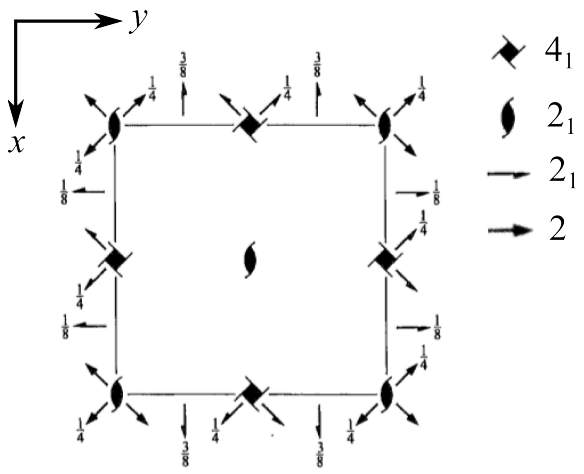
(c) Derive the multiplicity of a general site x, y, z in this space group. What would change in your derivation if the lattice was I-centred (e.g. space group $Iba2$)?

(d) A special Wyckoff position in space group $Pba2$ is $0, 0, z$ with site point symmetry 2. Derive the multiplicity of this Wyckoff position by comparing the number of symmetry operators in the crystal point group with the number of operators in the site point group.

(e) Write the symmetry operators 2 $[0, 0, z]$, a $[x, \frac{1}{4}, z]$, and b $[\frac{1}{4}, y, z]$ as a rotation or rotoinversion matrix about the origin *followed* by a translation. Separately transform $0, 0, z$ by all three symmetry operations. Hence, show that this Wyckoff position is invariant under the 2-fold symmetry with which it coincides, and that both a and b generate the same line of points, consistent with the site multiplicity found in part (d).

3. **Wyckoff positions**

The diagram represents the tetragonal space group $P4_12_12$, looking down the 4_1 axis.



(a) Explain the meaning of all symbols in the space group notation, $P4_12_12$.

The coordinates of the general equivalent positions of $P4_12_12$ are:

(1) x, y, z	(2) $-x, -y, z + \frac{1}{2}$
(3) $-y + \frac{1}{2}, x + \frac{1}{2}, z + \frac{1}{4}$	(4) $y + \frac{1}{2}, -x + \frac{1}{2}, z + \frac{3}{4}$
(5) $-x + \frac{1}{2}, y + \frac{1}{2}, -z + \frac{1}{4}$	(6) $x + \frac{1}{2}, -y + \frac{1}{2}, -z + \frac{3}{4}$
(7) $y, x, -z$	(8) $-y, -x, -z + \frac{1}{2}$

(b) Suppose an atom is located directly on a 2-fold axis of symmetry. Write out its equivalent positions.

(c) Starting with the general position x, y, z, derive a list of positions in a single unit cell that are equivalent by the 4_1 screw axis at $\frac{1}{2}, 0, z$. Hence, calculate systematic absences (extinction conditions) in the structure factor for $00l$ reflections due to the 4_1 symmetry.

4. **Crystal geometry**

   A monoclinic crystal has cell parameters $a = 0.6\,\mathrm{nm}$, $b = 0.7\,\mathrm{nm}$, $c = 0.8\,\mathrm{nm}$, $\beta = 110°$.

   (a) Find the magnitude of the direct space vector $[31\overline{2}]$.

   (b) Find the magnitude of the reciprocal lattice vector $(31\overline{2})$.

   (c) Find the angle between the $[31\overline{2}]$ direction and the normal to the plane $(31\overline{2})$.

   (d) The crystal has space group $C2/m$ ($2 \parallel \mathbf{b}$). Determine the extinction condition (in terms of h, k, and l) for the reciprocal lattice due to the C-centring of the direct lattice.

   (e) Draw to scale the $(hk0)$ and $(h0l)$ reciprocal space planes for $-2 \leq h \leq 2$, $-2 \leq k \leq 2$, and $-2 \leq l \leq 2$. What is the centring type of the reciprocal lattice?

5. **Friedel's Law**

   A crystal contains two atoms, one at $0, 0, 0$ and the other at a general position x, y, z in the unit cell. Suppose the first atom has a real atomic form factor f_1, while the second has atomic form factor $f_2 = f' + \mathrm{i}f''$ with real and imaginary components. Write down the structure factor for the hkl and $\overline{h}\overline{k}\overline{l}$ reflections, showing that in this case Friedel's law does not hold, i.e. show that $I(hkl) \neq I(\overline{h}\overline{k}\overline{l})$. Illustrate your answer on an Argand diagram.

Problem Sheet 2
Michaelmas Term 2021

1. **Powder diffraction crystal structure solution**

   USi crystallises in an orthorhombic space group with lattice parameters $a = 0.565\,\text{nm}$, $b = 0.765\,\text{nm}$, $c = 0.390\,\text{nm}$. There are four USi 'formula units' per crystallographic unit cell ($Z = 4$). The general equivalent positions of the space group are

$$\begin{array}{llll} x,y,z & x,y,\frac{1}{2}-z & \frac{1}{2}+x,\frac{1}{2}-y,\overline{z} & \frac{1}{2}+x,\frac{1}{2}-y,\frac{1}{2}+z \\ \overline{x},\overline{y},\overline{z} & \overline{x},\overline{y},\frac{1}{2}+z & \frac{1}{2}-x,\frac{1}{2}+y,z & \frac{1}{2}-x,\frac{1}{2}+y,\frac{1}{2}-z \end{array}$$

   Given that all four U atoms have $z = \pm\frac{1}{4}$, show that the four U atoms lie at the positions

$$\pm\left[x, y, \tfrac{1}{4}\right] \quad \text{and} \quad \pm\left[\tfrac{1}{2}-x, \tfrac{1}{2}+y, \tfrac{1}{4}\right]$$

   (a) Show that the structure factor for the U atoms alone (fractional coordinates x, y, z) and for a general hkl is given by

$$F_{hkl} = 4f_{\text{U}} \cos 2\pi\left[hx - \tfrac{1}{4}(h+k)\right] \cos 2\pi\left[ky + \tfrac{1}{4}(h+k+l)\right],$$

   where f_{U} is the atomic form factor of uranium.

   (b) We are now interested in using diffraction data to determine the exact location of the U atoms. Because the choice of origin is arbitrary, it is sufficient to limit our search to the range $0 \le x < \frac{1}{4}$ and $0 \le y < \frac{1}{4}$. Given that the (200) and (040) reflections have zero intensities, would measuring the intensities of the (111) and (231) reflections be sufficient to determine x and y uniquely?

   (c) An X-ray powder diffraction experiment is performed on USi with copper K_α radiation ($\lambda = 0.1542\,\text{nm}$). Determine the multiplicity of the reflections (111), (200), (211), (040), and (231). From the measured intensity data below (which have been corrected for Lorentz, polarisation, and attenuation factors), determine approximate values for the positions x and y (the Si contributions can be neglected — why is this?). In the table, f_{U} is the uranium form factor at the appropriate value of $|\mathbf{Q}|$.

hkl	111	200	211	040	231
I	457	$\sim$0	221	$\sim$0	630
2θ (deg.)	30.12	31.6	40.09	47.41	53.70
$f_{\text{U}}(\lvert\mathbf{Q}\rvert)$	81	79	75	71	69

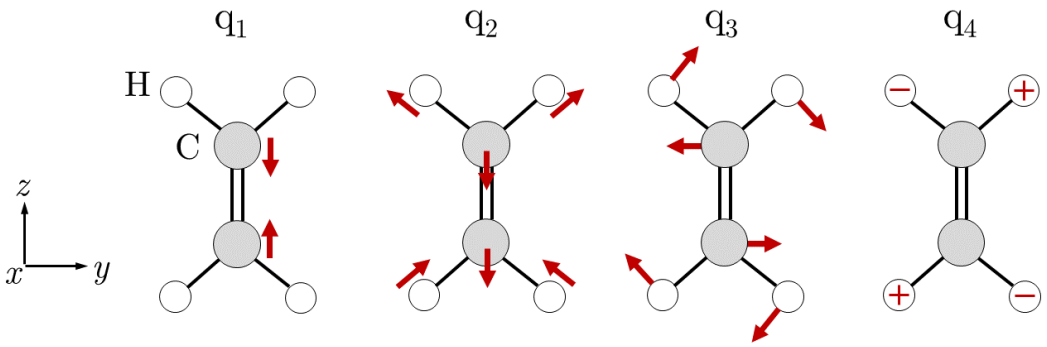
   (d) Draw to scale the positions of the U atoms in the unit cell projected on (001). Calculate and mark on your diagram the shortest U–U distance in nm.

2. **Crystal symmetry and macroscopic properties**

   (a) Sketch an object which exhibits the orthorhombic point group symmetry 222 (three, mutually perpendicular, 2-fold rotation axes), and illustrate on a stereogram (or otherwise) all the directions which are equivalent to a general direction $[xyz]$ in this point group. Show that the tensor representing any second-rank physical property of a crystal with point group 222 is diagonal, with three independent principal coefficients.

   (b) An orthorhombic crystal with unit cell dimensions $a = 0.451\,\text{nm}$, $b = 0.455\,\text{nm}$ and $c = 0.764\,\text{nm}$, is cut into a thin plate of area $2.5 \times 10^{-3}\,\text{m}^2$ and thickness 1 mm. The large faces are parallel to the (211) planes and are maintained at temperatures that differ by 10 K. The principal coefficients of thermal conductivity κ_{11}, κ_{22} and κ_{33} are 40.8, 88.3 and $16.0\,\text{Wm}^{-1}\,\text{K}^{-1}$, respectively. Determine how much heat would flow through the crystal in 1 minute.

3. **Molecular vibrations**



Ethene (C_2H_4) is a planar molecule whose static structure is described by the point group mmm. The symmetry operations in mmm are E, 2_x, 2_y, 2_z, $\overline{1}$, m_x, m_y and m_z.

(a) How many vibrational normal modes do you expect for an ethene molecule?

(b) The figure shows four of the vibrational normal modes of ethene. Determine the characters of each of the modes under the symmetry operations 2_x, 2_y, 2_z and $\overline{1}$ (the other symmetry operations in mmm do not provide any distinct information because $m = \overline{1} \circ 2$).

(c) Determine the characters of each component of the dipole moment vector $\mathbf{p} = (p_x, p_y, p_z)$ and polarizability tensor α_{ij} under 2_x, 2_y, 2_z and $\overline{1}$. Hence, determine which of the four modes are (i) infra-red active, and (ii) Raman active.

(d) If a molecule has a centre of inversion symmetry (as does ethene) what can you say about the selection rules for infra-red and Raman spectroscopy?

4. **Measurements of phonons by triple-axis neutron scattering**

The phonon dispersion relations of a primitive tetragonal crystal with cell parameters $a = 0.387\,\text{nm}$ and $c = 0.949\,\text{nm}$ are measured by inelastic scattering of neutrons of incident energy $E_\text{i} = 25\,\text{meV}$ with a triple-axis spectrometer. The crystal is aligned with the c-axis normal to the horizontal scattering plane of the instrument, and can be rotated around the c-axis. One of the optical phonon modes has energy $E = 12\,\text{meV}$ at the zone-boundary point X $(\frac{1}{2}, 0, 0)$.

(a) Draw a diagram of the a^*b^* reciprocal space plane of the crystal and indicate all points equivalent by symmetry to X in the 1st Brillouin zone, and also the X points in the next set of Wigner–Seitz unit cells further out.

(b) Consider processes in which neutrons scatter inelastically by exciting a phonon (energy-loss scattering). Show that such processes cannot occur with the 12 meV phonon mode when the scattering vector is $\mathbf{Q} = (\frac{1}{2}, 0, 0)$. Show, however, that the 12 meV phonon can be observed when $\mathbf{Q} = (1, \frac{1}{2}, 0)$, an X point in a further out Wigner–Seitz cell. In this case, find the total scattering angle ϕ, and the angle between the incident neutron beam and the crystal a-axis.
[Hint: consider the conservation of energy and momentum, and use the convention for the scattering vector $\mathbf{Q} = \mathbf{k}_\text{i} - \mathbf{k}_\text{f} = \mathbf{k}_\text{ph} + \mathbf{G}$].

(c) Could the phonon mode be observed with $\mathbf{Q} = (\frac{1}{2}, 0, 0)$ by energy-gain scattering, i.e. when neutrons scatter by absorbing energy from the phonon? What should the temperature of the crystal be for this scattering process to have sizeable intensity?

5. **Ferroelectric phase transitions**

Barium titanate ($BaTiO_3$) becomes ferroelectric below $T_\text{C} = 395\,\text{K}$, and undergoes the following sequence of structural phase transitions on cooling:

$$\text{Cubic } (Pm\bar{3}m) \xrightarrow{395\text{K}} \text{Tetragonal } (P4mm) \xrightarrow{270\text{K}} \text{Orthorhombic } (Cm2m)$$

The different phases are related by small distortions of the lattice. The table below gives the directions of the unit cell axes for the above ferroelectric phases in terms of the Cartesian axes of the cubic phase.

$P4mm$	[100]	[010]	[001]
$Cm2m$	[110]	[$\bar{1}$10]	[001]

(a) Explain what is meant by *ferroelectricity*. State the symmetry requirement for a crystal to be ferroelectric.

(b) For each of the two ferroelectric phases,

(i) explain the meaning of the space group symbol, identify the point group, and draw a stereographic projection showing the point group symmetries;

(ii) deduce the direction of the ferroelectric polarization relative to the cubic axes, explaining your reasoning;

(iii) determine how many distinct ferroelectric domains can exist
[Hint: consider all the symmetry-equivalent directions of the polarization axis with respect to the original cubic axes].

(c) Explain how you might detect the structural change from cubic to tetragonal symmetry using X-ray powder diffraction data. Explain why no net ferroelectric polarization is observed when a single crystal of $BaTiO_3$ is cooled through T_C?